Geological Survey of Sweden

Bedrock investigation of the Skrickerum area, Southern Bergslagen



Dick Claeson & Virginie Leroux

www.sgu.se

SGU-rapport 2026:20

Authors: Dick Claeson & Virginie Leroux
Reviewed by: Stefan Bergman & Johan Jönberger
Responsible head of unit**:** Ildikó Antal Lundin
Editor: Lina Rönnåsen

Cover image: Old pit in sulphide mine at Häradsgruvor.
Photo: Dick Claeson.

November 2026

Geological Survey of Sweden
Box 670, 751 28 Uppsala
phone: 018-17 90 00
e-mail: sgu@sgu.se
www.sgu.se

Innehåll

Sammanfattning 5

Abstract 7

Introduction 8

Methods 8

- Lithogeochemical analyses 8
- Geophysics: methods and data collected 9

Geological setting 10

Geophysics: results and some comments 12

- Petrophysics 12
- Gamma-ray spectrometry measured on outcrops 13
- Gravimetry 15
- Magnetometry 16
- VLF 18
- Spectrometry 20
- Ground magnetometry 26
  - Profiles in the northern part of the Skrickerum area 26
  - Profiles and area covered in the southern part of the Skrickerum area 27

Volcanic rocks 29

Intrusive rocks 37

- Older generation of acid intrusive rocks 37
- Younger generation of acid intrusive rocks 39
- Basic to intermediate intrusive rocks 42

Iron mineralisations 47

- Oltorps gruvor 47
- Knappekulla gruva 48
- Skårsjö Gruvfält 49
- Norrby gruvor 51
- Lillgöl prospect 52

Sulphide mineralisations 55

- Häradsgruvor and Snarkullegruvan 55

Spångdalen 57
Åläng gruva 58
Skrickerums gruva 59
Sjögerums gruva, Silvermossens gruva 61
Karlsmåla prospect 62
Rumhult prospect 63
Fåfalla prospect 63
Structural measurements 66
References 68

Sammanfattning

Sveriges geologiska undersökning (SGU) har sedan 2023 bedrivit ett stort kartläggningsprojekt i nordöstra Småland och sydöstra Östergötland. Det övergripande målet med projektet är att uppgradera SGU:s kartdatabas till en mer detaljerad skala, samt att ta prover på bergarter från områdets mineralfyndigheter med särskilt fokus på så kallade kritiska och strategiska råvaror. Denna rapport sammanfattar resultaten av de geofysiska och geologiska mätningar och observationer som samlats in under 2023 och 2024 i projektområdet Skrickerum, som är ett delområde inom denna satsning.

Det övergripande målet för delprojektet var att förfina kartorna över Skrickerumsområdet och producera nya data. Arbetet är relaterat till det regeringsuppdrag SGU fick under 2024 som syftar till att förstärka kartläggningen av malmpotentiella områden i Sverige. Särskild uppmärksamhet ägnades därför åt mineraliseringar i området.

I delområdet Skrickerum finns kända mineraliseringar med till exempel järn, koppar och selen, vilka nu också har undersökts med avseende på kritiska eller strategiska råvaror. Under 2024 utfördes 534 markmätningar av tyngdkraften. Gammastrålning uppmättes på 21 hällar. Sammanlagt sex profiler och sex yttäckande mindre områden uppmättes med magnetometer. Längs två av profilerna insamlades även VLF data. Totalt utfördes 83 berggrundsobservationer under 2023 och 2024, data som nu finns lagrade i SGU:s databas Berggrundsobservationer. 35 prover har samlats in från varphögar och hällar för litogeokemisk analys. Petrofysiska mätningar, det vill säga mätning av bergarternas fysikaliska egenskaper såsom densitet, magnetisk susceptibilitet och elektrisk ledningsförmåga, utfördes på 78 insamlade prover. För mikroskopiarbete framställdes 35 polerade tunnslip.

Berggrunden i Skrickerumsområdet ligger i den sydligaste delen av Bergslagen och tillhör den svekokarelska bergskedjebildningen. Den är nära på lika fördelad mellan vulkaniska och intrusiva bergarter och närmast samtliga har genomgått minst en metamorf episod av deformation och omvandlingar. Duktila deformationsmönster påverkar hela området och manifesteras av olika grader av foliation, veckning och skjuvzoner.

I rapporten visas resultaten av de geofysiska mätningarna från luften och på marken på tematiska kartor med provtagningsplatser. De petrofysiska mätningarna representeras i klassiska diagram. De metoder som användes inkluderade gravimetri, magnetometri, gammastrålningsspektrometri och VLF-mätningar med varierande upplösning och de övergripande resultaten kommenteras kortfattat.

Efter en kort genomgång av de geologiska förhållandena beskrivs, illustreras och diskuteras de viktigaste bergartsgrupperna successivt, följt av de viktigaste, kända järnoxid- och sulfid-mineraliseringarna i området. I Skrickerumsområdet utvanns koppar och järn från ett antal lokala gruvor mellan slutet av 1700-talet och slutet av 1800-talet och selen utvanns vid Skrickerums-gruvan. Litogeokemisk analys utfördes för varje bergartsgrupp och för de besökta mineraliseringarna. Resultaten presenteras i olika diagram och diskuteras i relation till petrologi och petrofysiska egenskaper.

De vulkaniska bergarterna domineras av 1,91–1,86 miljarder år gamla basaltoider och andesitoider, ofta observerade som alternerande lager. De är generellt överpräglade av metamorfos vid hög temperatur och relativt högt tryck. Granater observeras ofta och en granatförande migmatit av andesitiskt ursprung hittades. Dacitoid och ryolit förekommer underordnat.

Två generationer kan urskiljas bland de sura, intrusiva bergarterna: äldre bergarter vars sammansättning sträcker sig från tonalit till granodiorit och inkluderar även några graniter. Samtliga är deformerade, starkt folierade och kraftigt omvandlade. Den yngre generationen består troligen av graniter av TIB1-ålder och anatektisk granit av ungefär samma ålder. De uppträder som intrusioner, gångar och ådror vilka penetrerar samtliga äldre bergarter, särskilt vulkaniter, vilka i sin tur ibland observeras som xenoliter. De yngre sura bergarterna är i allmänhet svagt folierade och ibland massiva.

Gabbroiska bergarter med kraftigt varierande grad av deformation och metamorf överprägling förekommer och tolkas därför som att de är av olika åldrar. De äldre är deformerade och framträder som konforma gångar i de äldre vulkaniska bergarterna. De yngre gabbro intrusionerna tolkas vara samtida med den förmodade TIB1-generationen. Två prover av ultramafiska bergarter samlades in, där den positiva Bouguer-anomalin under Storsjön antyder att de skulle kunna utgöra delar av en lagrad intrusion på djupet.

Järnoxidmineraliseringarna visade sig innehålla mycket lite sulfider. En hade förhöjda halter av mangan och förhöjda halter av tunga sällsynta jordartsmetaller hittades i skarn. Sulfid-mineraliseringarna befanns vara av typen Cu, Ni-Cu-Au eller Zn.

Efter observationerna utförts och med hjälp av de geofysiska mätningarna från luften gjordes ändringar i den geologiska kartan. Alla resultat görs kontinuerligt tillgängliga via SGU:s databaser. Insamlade data och information kan tjäna som underlag för vidare undersökningar och modellering.

Abstract

This report summarises the results of geophysical and geological measurements and observations collected during 2023 and 2024 in the project area Skrickerum. The overall aim was to refine the maps of this area and produce new data. All this work is related to the governmental assignment to re-inforce the mapping of ore-potential areas in Sweden that SGU received in 2024. Special attention was therefore given to mineralisations.

The bedrock in the Skrickerum area is situated in the southernmost part of the Bergslagen province that belongs to the Svecokarelian orogen. It is almost equally divided between volcanic and intrusive rocks and nearly all of them have undergone at least one deformation and metamorphic episode. Ductile deformation patterns affect the whole area and are manifested by different grades of foliation, sheath folds, and shear zones.

The results of airborne and ground-based geophysical measurements are shown on thematic maps with the location of sampling. Petrophysical measurements are represented in classical diagrams. The methods used include gravimetry, magnetometry, gamma-ray spectrometry, and VLF measurements of varying resolution and the overall results are briefly commented.

After a short recall of the geological settings the main rock groups are successively described, illustrated and discussed, followed by the main known iron-oxide and sulphide mineralisations in the area. In the Skrickerum area copper and iron were extracted from a number of local mines between the end of the eighteenth and the end of the nineteenth century and selenium was extracted at the Skrickerum mine. Lithogeochemical analyses were made for each group of rock and for all visited mineralisations. The results are given as spider diagrams and succinctly discussed in relation to petrology and petrophysical properties.

The volcanic rocks are dominated by 1.91–1.86 Ga old basaltoids and andesitoids often observed as alternating layers. They are generally affected by high-temperature and relatively high-pressure metamorphism. Garnets are often observed and a garnet-bearing migmatite of andesitoid origin was found. Dacitoid and rhyolite are subordinate.

Two generations can be distinguished among the acid intrusive rocks: older rocks ranging from tonalite to granodiorite and even including some granite, all deformed, strongly foliated and metamorphosed. The younger generation consists of presumably TIB1 age granites and anatectic granite of about the same age. They appear as intrusions, dykes and veins penetrating all the older rocks, particularly the volcanics, which in turn are sometimes observed as xenoliths. The younger acid rocks are in general weakly foliated and sometimes massive.

Gabbros with varying grades of deformation and metamorphic overprinting occur and are therefore interpreted as being of different ages. The older ones are deformed and appear as conform dykes in the older volcanics. The younger gabbros are thought contemporary of the presumably TIB1 generation. Two samples of ultramafic rocks were collected, where the positive Bouguer anomaly below the lake Storsjön suggests they could make up parts of a layered intrusion at depth.

The iron-oxide mineralisations were found to contain very little sulphides. One had elevated manganese and elevated heavy rare earth elements content was found in skarn. The sulphide mineralisations were found to be of Cu, Ni-Cu-Au, or Zn types.

Following the observations and using the airborne geophysical measurements changes were made to the geological map. All results are made available through SGU:s databases. The collected data and information can serve as a basis for further investigations and modelling.

Introduction

SGU has been conducting a major mapping project since 2023 in northeastern Småland and southeastern Östergötland. The overall aim of the project is to upgrade SGU's map data to a more detailed scale, as well as to sample rock types from the area's mineral deposits with a particular focus on so-called critical and strategic raw materials. The project area Skrickerum is a sub-area of this effort, along with sub-areas Västervik (start 2024) and Åtvidaberg. Collected geological, lithogeochemical, and geophysical data are continuously made available in SGU's databases.

In the Skrickerum sub-area there are known mineralisations with, for example iron, copper, and selenium, which have now also been investigated with regard to critical or strategic raw materials. Field work in the Skrickerum sub-area began in 2023 and was completed in 2024. During 2024, 534 gravity measurements on the ground were acquired. Gamma-ray spectrometry was measured on 21 outcrops. Six profiles and six small areas were covered by ground measurements with a magnetometer. Along two of these profiles, also VLF data were collected. A total of 83 bedrock observations were made during 2023 and 2024, data that are now stored in SGU's database Bedrock Observations. 35 samples have been collected from waste-rock heaps and outcrops for lithogeochemical analysis. For petrophysical measurements, i.e., measurement of the physical properties of the rocks such as density, magnetic susceptibility, and electrical conductivity, 78 samples were collected. For microscopy work 35 polished thin sections were prepared.

The mapping is linked to the assignment from the government to strengthen the mapping of ore potential areas that SGU received in early 2024 and is part of promoting mineral extraction in Sweden. The aim is to contribute to a secure supply of minerals and metals that are critical and strategically important for the functioning of society and to contribute to the transition to green energy and technical development. Metals and minerals are needed in, for example, electric vehicles and solar panels, in the arms industry, and healthcare.

Almost all rocks described in this publication have been through one or several metamorphic events, but for simplicity the prefix meta is left out. The coordinates are reported in SWEREF99 TM. All measurements of planes are according to the right-hand rule in this publication.

Methods

Lithogeochemical analyses

In the field, samples for geochemical analyses were collected by hammer or sledgehammer from outcrops, abandoned mine workings and waste-rock heaps. A total of 2 to 4 kg of fresh material consisting of several smaller rock fragments and chips were collected at the location for each sample.

All lithogeochemical analyses were performed by ALS using the analytical packages CCP-PKG01, ME-MS41 and PGM-ICP23 (ALS 2023). Three internal rock standards were used for quality control of each sample batch. Data can be accessed through SGU's map viewer "Rock Chemistry" which is available at the SGU website: https://apps.sgu.se/kartvisare/kartvisare-bergartskemi.html. The full dataset can be obtained by using SGU's download service or by contacting SGU's customer service. The download service is described at the following link: https://resource.sgu.se/dokument/produkter/lithogeochemistry-description.pdf.

Plotting of geochemical data was done using the GCD-kit package (Janoušek *et al.* 2006).

Geophysics: methods and data collected

Within and in relation to the Skrickerum project new geophysical data were collected.

New airborne data were collected during the summer of 2023 by SGU, which covered a larger area over parts of eastern Småland and Östergötland and included the Skrickerum area. These data consist of the total magnetic field, VLF signal using two transmitters, and gamma spectrometry data regarding potassium, uranium, and thorium concentrations in the ground (specifications and data available from www.sgu.se). The flight height was 60 m, the distance between flight lines was about 200 m and they were flown in north–south direction. The data collection was done with better precision and consistency over the area compared to data that previously had been collected by several and independent airborne campaigns (1986, 1998, and 1999). The new data cover all the area, except for small easternmost parts where data from 1998 and 1999 were used. Except for a few valleys the soil cover is generally thin over the Skrickerum area, thus the gamma spectrometry (radiometrics) response is probably mostly representative of the bedrock.

The location of the geophysical data collected on the ground can be seen in Figure 1. During 2024, 534 gravity measurements were added to the previously 123 existing in the area that were collected from 1983 to 2001, but mostly in 2001. With some variation related to ease of access the typical distance between neighbouring gravimetry data points is now in average about 1 to 1.2 km.

Within this project 78 rock samples were collected and analysed for petrophysical properties at SGU's petrophysical laboratory, adding to the 53 already existing. Density and magnetic susceptibility as well as the natural remanent magnetisation were measured on all new samples. Resistivity could be estimated on 28 of them. The rock samples were divided into seven large groups (Fig. 3). Eighteen of the samples were collected from iron-oxide or sulphide mineralisations.

Magnetic susceptibility was measured on nearly all the visited outcrops, and their locations are shown in Figure 6. Eight measurements were generally performed with a hand-held magnetic susceptibility meter (SM20 from GF Instruments) on each rock type where observations were performed.

Magnetometric profiles were measured on the ground, either individually or covering small areas. VLF data were collected along two of these profiles. Both types of data were measured with GSM-19 Overhauser magnetometers from GEM Solutions equipped with VLF receivers.

Gamma-ray spectrometry has been measured on 83 outcrops in the area (21 within this project) using a handheld RS-230 gamma-ray spectrometer from Radiation Solutions. Usually, and when possible, three measurements are made on each rock type at an outcrop, which provide information of radioactive activity and of the concentrations in potassium (K), uranium (U), and thorium (Th) centred on a surface of about 1 m^2 and down to about 0.2 m at most. Reliable measurements are obtained if the outcrop is reasonably flat over about 5 m^2 and there are no protruding or dipping surfaces nearby.

Simple processing was applied to aeromagnetic and gravimetric data in order to enhance anomalies. Processed data is shown on several maps together with results from ground and petrophysical measurements.

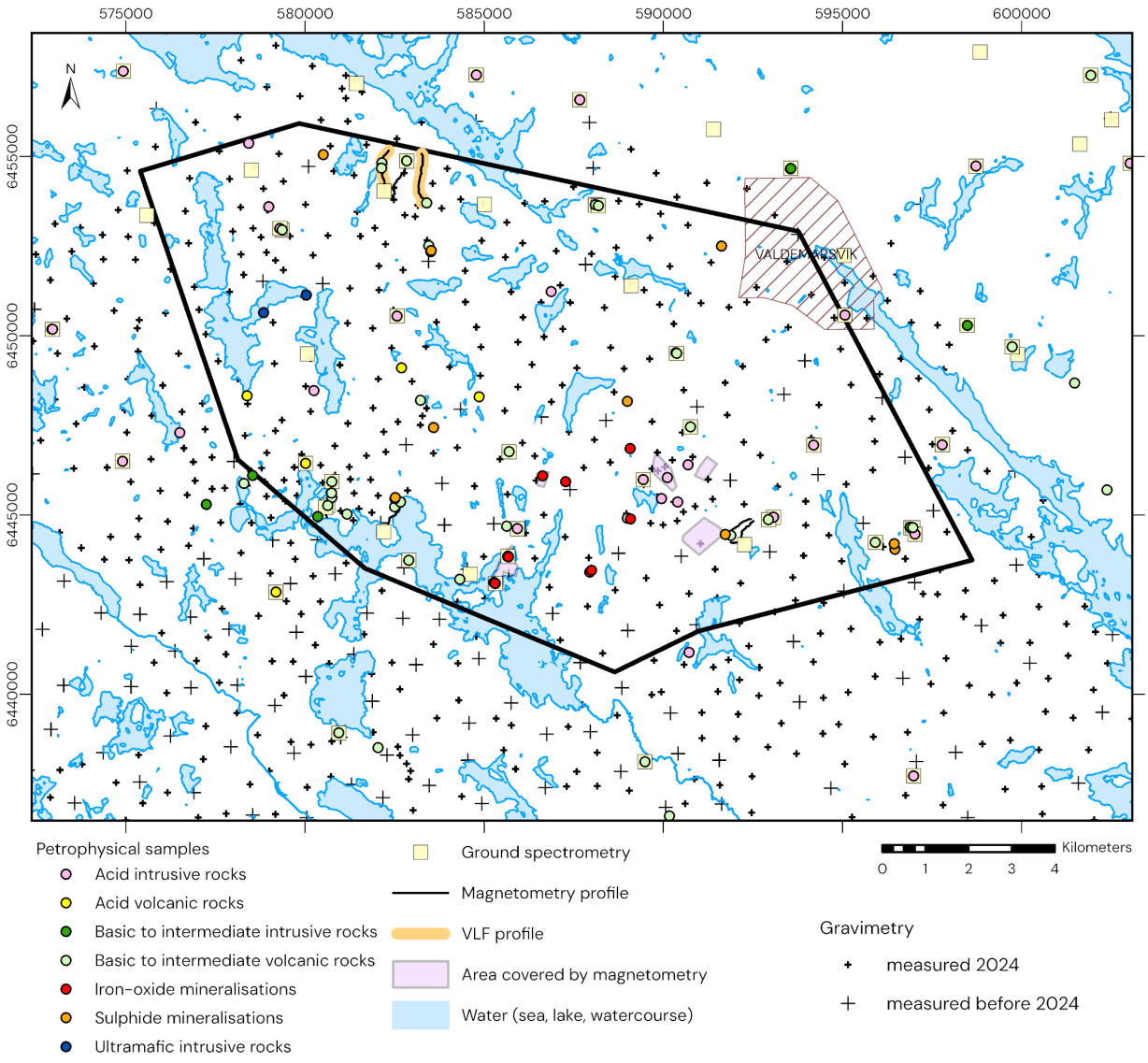

Figure 1. Map over all available geophysical data measured on the ground in the Skrickerum area.

Geological setting

The bedrock within the project area forms a small part of the extensive Svecokarelian orogen, which includes parts of eastern Sweden and western Finland (Fig. 2; Lundqvist *et al.* 2011, Stephens & Bergman 2020). The project area and surroundings are considered one of the southernmost parts of the Bergslagen, with similar rocks, deformation history as well as metamorphic overprinting, and historically important economic deposits of the same types. The volcanic formations are about 1.91–1.86 Ga old in this area and have been metamorphosed under high temperature and relatively high pressure. They have thereby been converted into veined gneisses, which means that granitic and pegmatitic veins, sheaths, and segments have formed in the rock. The older granitoids and associated basic rocks are also of early Svecokarelian age. They intruded into the supracrustal rocks, and their age is about 1.90–1.85 Ga. Deformation and metamorphism have affected the rocks to varying degrees. In connection with the metamorphism, aluminium-rich index-minerals were formed, e.g., sillimanite, andalusite, cordierite, and garnet. Formation of late orogenic migmatite granite occurred about 1.85–1.80 Ga ago. Coarse porphyritic granite to quartz monzonite and more even-grained granitoids intruded during the

same time in the Transscandinavian Igneous Belt (TIB) and few TIB-related intrusions are found within the project area. In eastern Sweden, older dykes of basic rocks are usually decimetre to metre wide, deformed, and converted to amphibolite. An extension of the bedrock about 1.55–1.47 Ga ago led to intrusion of lots of dolerite dykes in large parts of eastern Sweden, mainly in a west-northwest and north-west direction in the area now investigated.

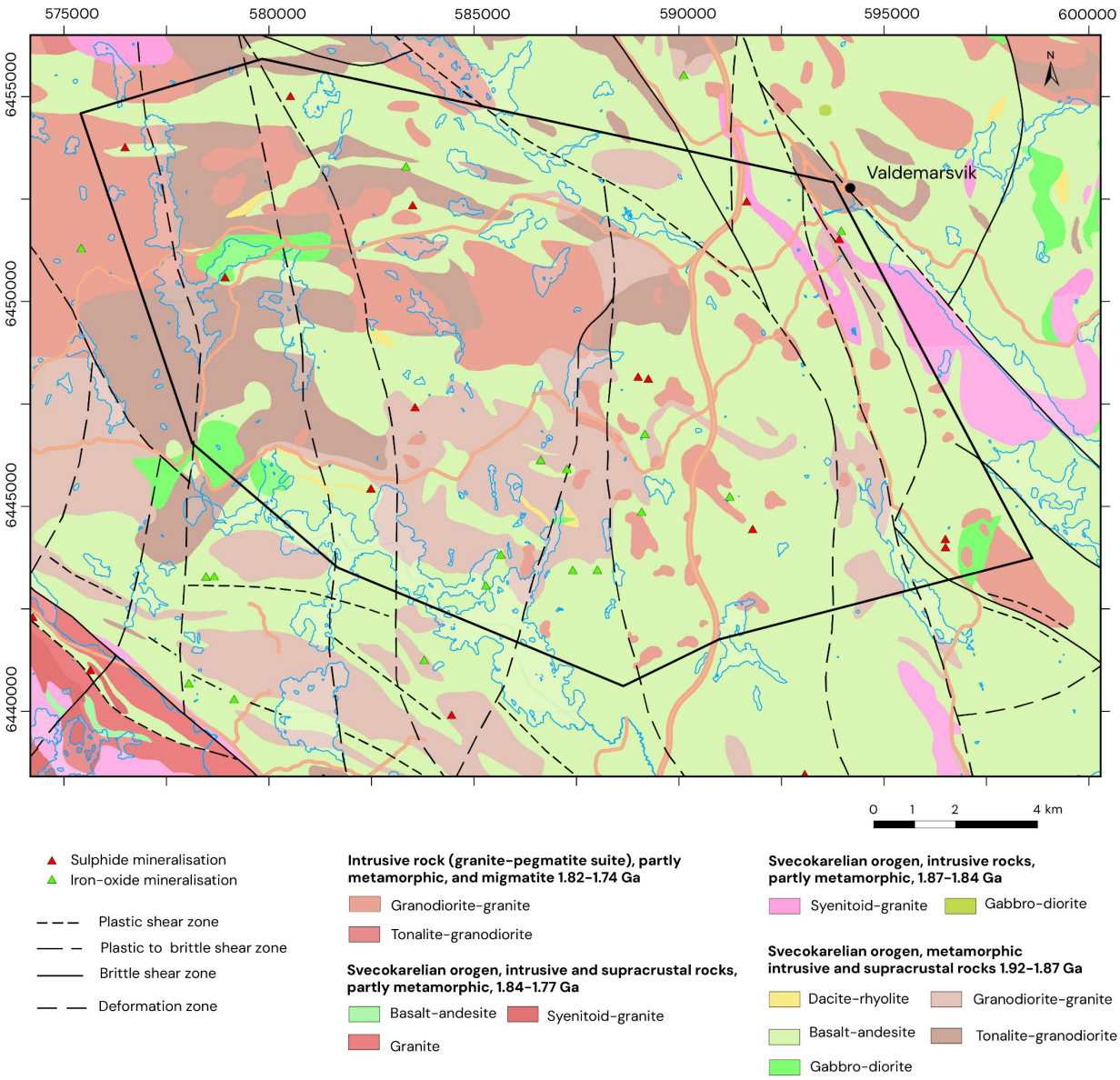

Figure 2. Bedrock map of the Skrickerum project area and surroundings. Blue lines outline water bodies and orange lines represent larger roads.

Geophysics: results and some comments

Petrophysics

After the completion of this mapping project, there are 131 samples available in the studied area. They have been grouped into seven large categories: acid intrusive rocks, acid volcanic rocks, basic to intermediate intrusive rocks, basic to intermediate volcanic rocks, ultramafic intrusive rocks, sulphide mineralisations, and iron-oxide mineralisations (Fig. 3). The categories "acid intrusive rocks" and "basic to intermediate volcanic rocks" dominate largely with 45 and 49 samples respectively and they are also the most frequently observed rocks at outcrops (see Fig. 3D). 13 sulphide mineralisations and 11 iron-oxide mineralisations occur in the area, and petrophysical properties were measured on eight samples of each category. The mineralised samples were also analysed.

Acid rocks have the lowest densities as expected, followed by denser rocks of intermediate to basic composition (Fig. 3A). Except for one sample, sulphide mineralisations have densities comparable to those of the most dense of the basic to intermediate rocks. The two ultramafic samples have a density equivalent to that of the less dense basic to intermediate rocks. It could be due to a higher content of hydrous minerals. The magnetic susceptibility of these two samples is about 10 000 μSI. The density of samples collected from iron-oxide mineralisations is clearly higher, above 3 500 kg/m^3. They also have clearly higher magnetic susceptibility, above 1 SI. The magnetic susceptibility of the other groups of rocks varies in a large range, from a few hundreds of μSI to a few hundreds of thousands of μSI. One sample within the group basic to intermediate volcanic rocks has a magnetic susceptibility as high as the iron-oxide samples and one sample of sulphide mineralisation has almost as high magnetic susceptibility. The latter comes from the Karlsmåla prospect. Some acid rocks have distinctly lower magnetic susceptibility, below 200 μSI.

In Figure 3, 54 samples have a Koenigsberger ratio greater than 1, which means that for these samples the remanent magnetisation dominates over the induced magnetisation. This is the case for about half of the samples from iron-oxide mineralisations, nearly all samples from sulphide mineralisations, about half of the samples from acid intrusive rocks, and half of the samples from basic to intermediate volcanic and intrusive rocks. The Koenigsberger ratio also gives indications about the type of iron-oxide and/or the type of iron sulfide contained in the rock (see e.g. Henkel 1994, Dentith & Mudge 2014 about possible interpretation of these diagrams)

The electrical resistivity could only be measured inductively on 28 conductive enough samples, which included all of the samples from mineralisations. The results can only give general estimations and are not presented here but indicate a large variation for the resistivity of sulphide-mineralised samples from a few Ωm to over 10 000 Ωm.

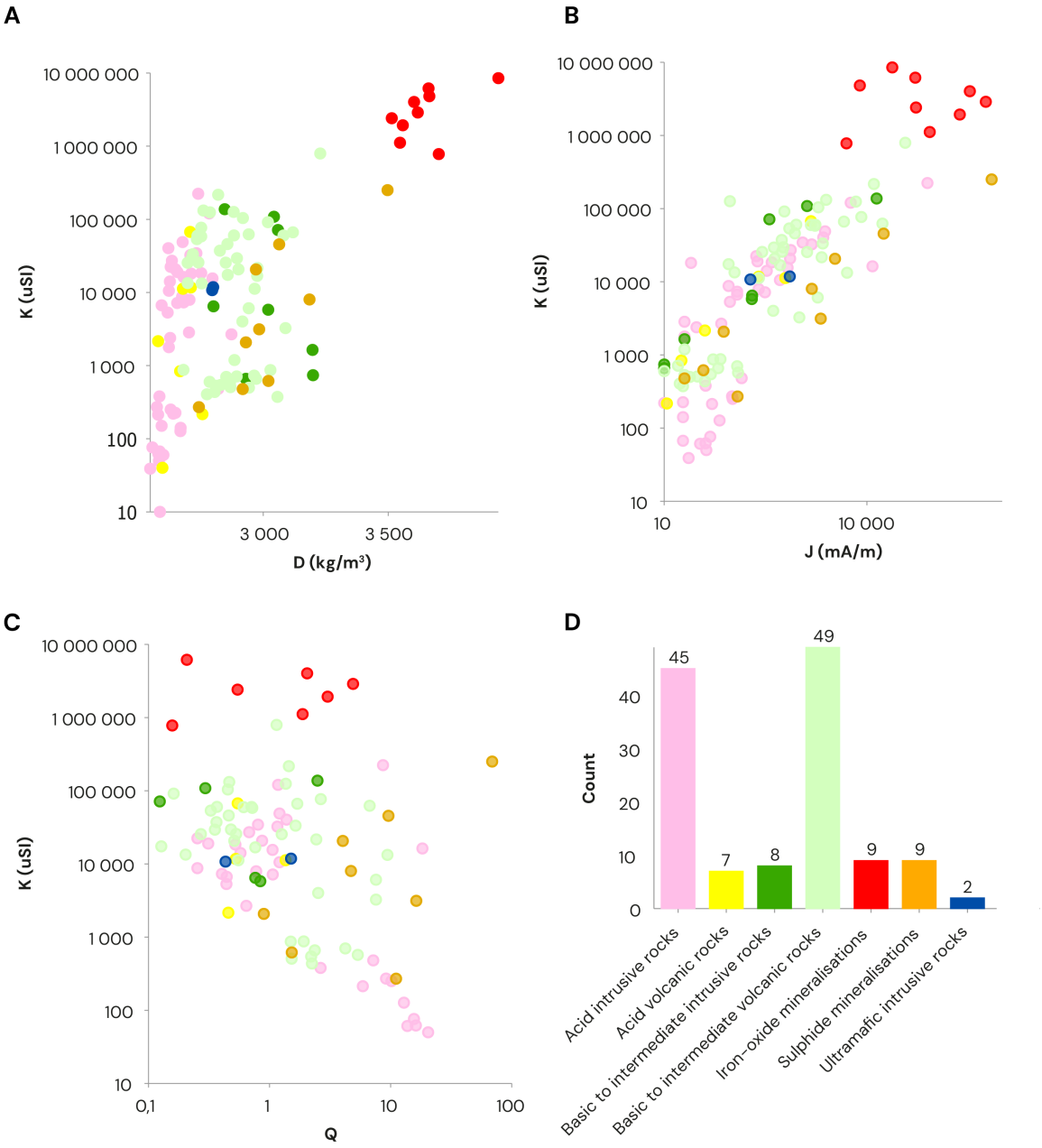

Figure 3. Petrophysical measurements on rock samples, summary over all available results. **A.** Magnetic susceptibility against density. **B.** Magnetic susceptibility against remanent magnetisation. **C.** Magnetic susceptibility against Koenigsberger ratio. **D.** Number of samples of each class. The same colour legend is applied to all parts of the figure.

Gamma-ray spectrometry measured on outcrops

From the project area there are 83 measurements on outcrop available, most of them done on acid intrusive rocks, the second most represented group is the basic to intermediate volcanic rocks (Fig. 4). Acid intrusive rocks have generally higher K, U, and Th content but the values vary over a relatively large range that overlap those measured for the other groups, in particular for the basic to intermediate volcanic rocks. One pegmatite has a measured K concentration above 8%, but relatively moderate concentrations of U and Th. Basic to intermediate intrusive rocks are not well represented, but the measured concentrations vary as much as for the larger group basic to intermediate volcanic rocks. The concentrations in the latter group vary to a lesser extent compared to the acid intrusive rocks.

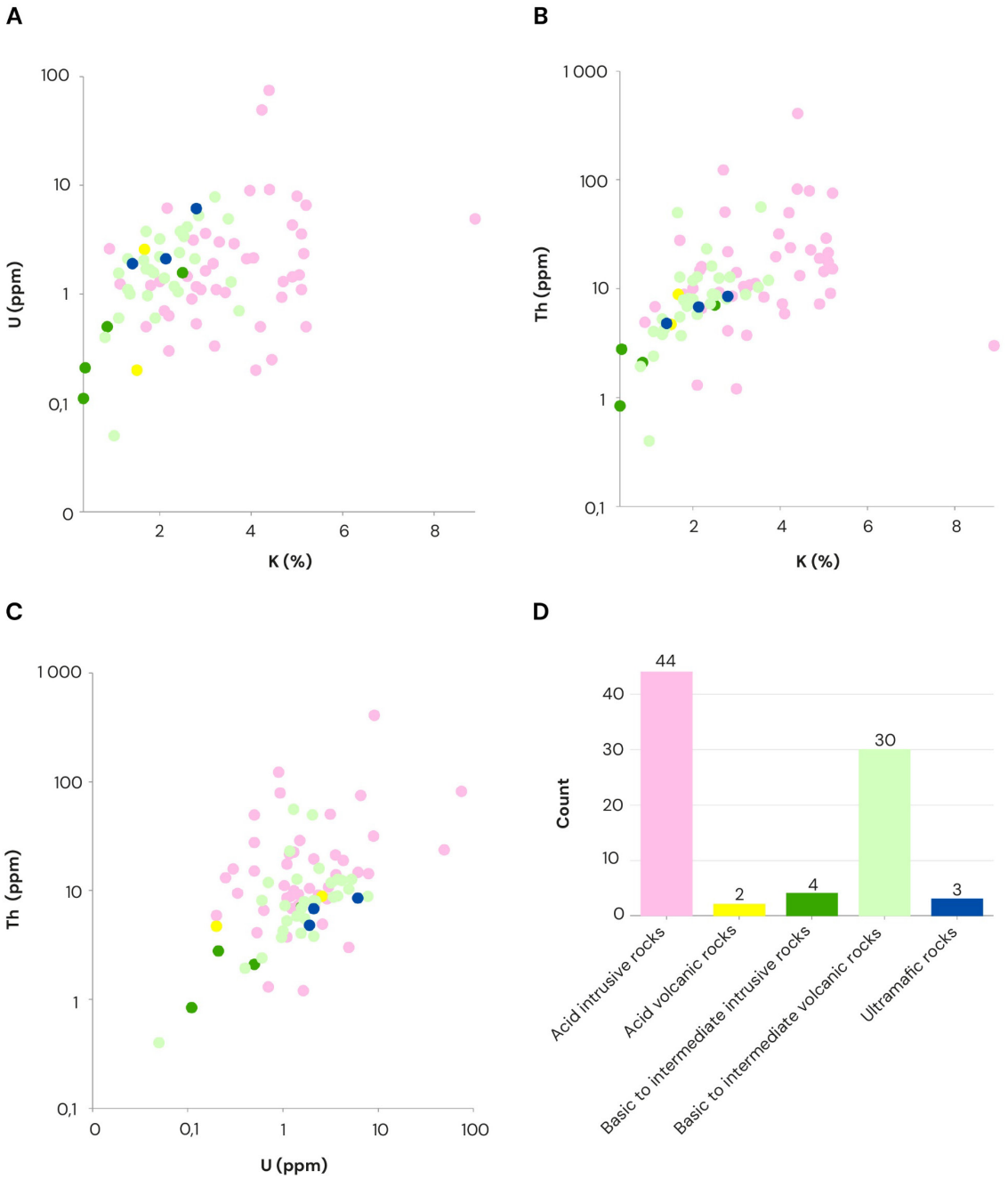

Figure 4. Gamma-ray spectrometry on outcrops, summary over all available results. **A.** Measured uranium concentration against potassium concentration. **B.** Measured thorium concentration against potassium concentration. **C.** Measured thorium concentration against uranium concentration. **D.** Number of outcrops of each class considered. The same colour legend is applied to all parts of the figure.

Gravimetry

The gravity map is presented in Figure 5 as the residuals from the (terrain-corrected) Bouguer anomaly after subtraction of a 3 000 m upward continuation, in order to enhance more shallow-seated mass distribution in the bedrock. The density measured on the 131 rock samples is also shown on the map. In general, the amplitude of the residuals is moderate, 3.4 mGal at most. Negative gravity anomalies in the eastern part of the Skrickerum area and southwest of it, are correlated to large known deformation zones. Positive anomalies suggest the presence of bodies with higher density, most probably mafic rocks. Rock samples with densities larger than 2 750 kg/m^3 were collected from outcrops that coincide with these anomalies and among them the two samples of ultramafic rocks. Rock samples with densities greater than 3 000 kg/m^3 were collected from outcrops at their edges. High-density iron-oxide mineralisations are also found at these edges or in areas with negative gravity anomaly. Low-density acid rocks were found in areas with negative gravity anomaly. The detail in the interpretation is limited by the mean distance between adjacent gravity measurement points (about 1 km) and the spatial distribution of the rock samples.

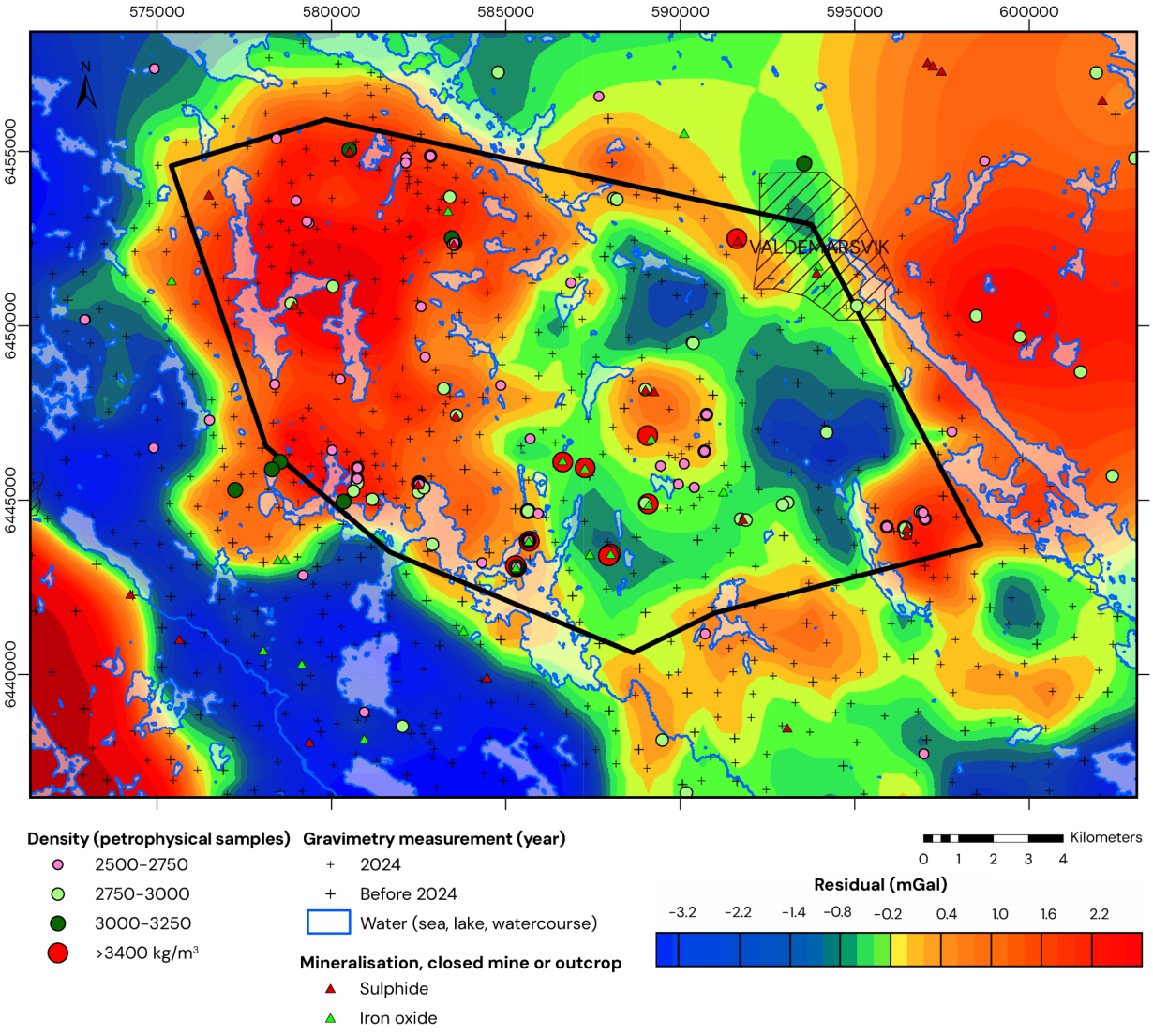

Figure 5. Gravity map: residuals of (terrain-corrected) Bouguer anomaly after subtraction of a 3 000 m upward continuation, together with density measured on rock samples.

Magnetometry

The results of the airborne measurements of the total magnetic field are presented as the residuals obtained after subtraction of a 1 000 m upward continuation of the reduced-to-pole total magnetic field. Shading is added to the colour scale representation in order to enhance the residual anomalies. This processing was applied in order to focus on the more shallow-seated anomalies from the bedrock. In Figure 6, the magnetic residual field is shown together with the average magnetic susceptibility measured on outcrops and in Figure 7 it is shown together with the magnetic susceptibility measured on rock samples.

In the Skrickerum area, in general, the magnetic pattern reflects structures resulting from ductile deformations (folds and shear zones, especially in the southern half). Two large and distinct negative anomalies are visible in the north-northwest–south-southeast direction in the northeastern corner of the area. They coincide with previously mapped ductile shear zones, which are visible in the topography. Some elongated, curvy, positive anomalies in a more or less east–west direction are visible and they are more curved and discontinuous in the southern half of the area, perhaps related to folding. In general, the area is dominated by large negative anomaly zones around the usually narrower positive anomalies. Several narrow and straight discontinuities in the north-northwest–south-southeast direction are also visible that seem to cross most of the previously named features. They could correspond to partly ductile and at least partly brittle deformation. They are partly visible in the topography, often coinciding with lakes. South of the Skrickerum area the Loftahammar-Linköping Deformation Zone (LLDZ) is seen as a low magnetic zone in a northwest–southeast direction and it is marked in the topography.

Low values of magnetic susceptibilities are often measured on outcrops that coincide with negative magnetic anomalies. Likewise, high magnetic susceptibilities are mostly observed on outcrops that are located at positive magnetic anomalies. However, large variation can be observed between neighbouring measurements, suggesting even smaller scale anomalies.

The known iron-oxide mineralisations are found on positive magnetic anomalies. Except for the Skårsjö Gruvfält, they are not found on the strongest and largest anomalies, but instead on anomalies appearing small in the airborne data. The known sulphide mineralisations are found in the middle (like Larum or Häradsgruvorna) or at the edges of negative magnetic anomalies (like Skrickerum gruva or Sjögerums gruva).

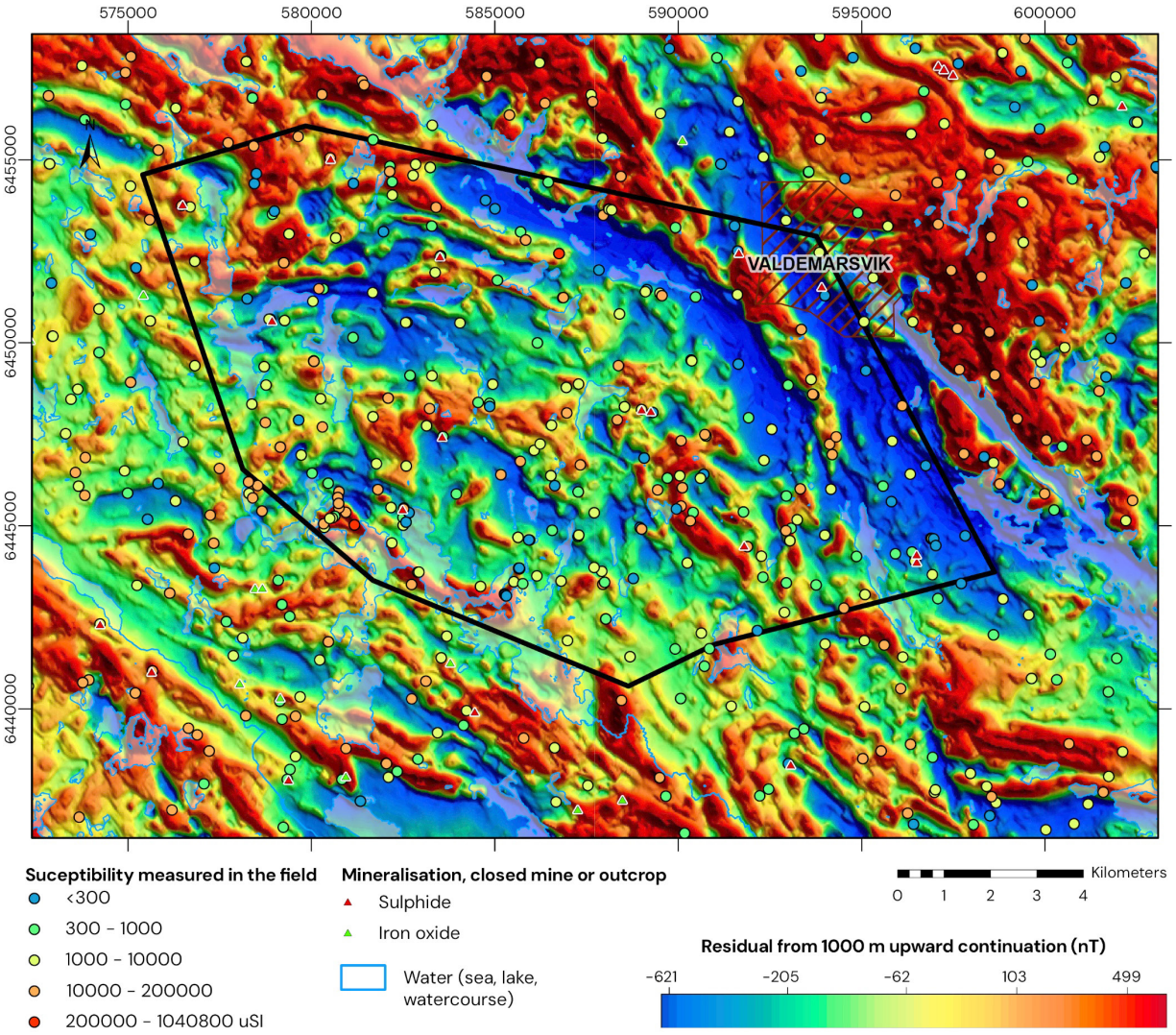

Figure 6. Aeromagnetic map: residuals of the total magnetic field after reduction to magnetic pole and subtraction of a 1 000 m upward continuation, together with magnetic susceptibility values measured on outcrops. The magnetic susceptibility is the average of (generally) eight measured values on each reported outcropping rock.

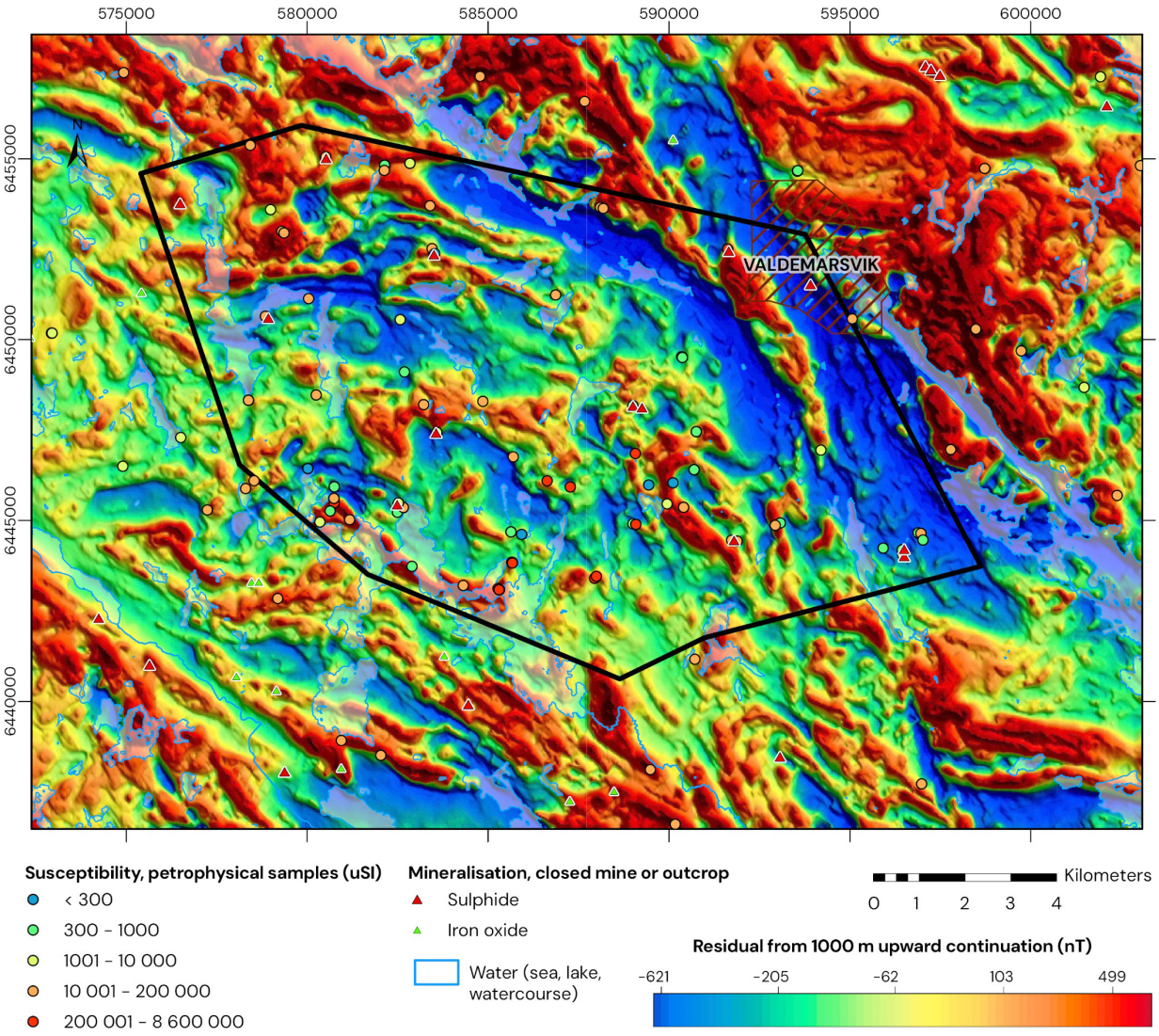

Figure 7. Aeromagnetic map: residuals of the total magnetic field after reduction to magnetic pole and subtraction of a 1 000 m upward continuation, together with magnetic susceptibility of petrophysical samples.

VLF

The result of the airborne VLF measurements is presented as a map over the calculated current density (Fig. 8). Higher current density corresponds to lower electrical resistivity and usually reveals zones of weakness in the bedrock that are often related to the presence of water. They can also reveal conducting mineralised bodies. But high current density anomalies can also be caused by man-made infrastructure such as power lines and cables, for instance along roads. For that reason, the main infrastructure is also plotted in Figure 8. There could be low resistivity zones caused by geological features, which coincide with infrastructure, but their interpretation is ambiguous.

The overall picture of the VLF response appears related to the topography and different from the pattern of the magnetic anomalies but some features are common to both. Localised high-current density zones in the northwest–southeast direction are visible in the northeastern most corner that coincide with the low magnetic bands from Figures 6 and 7. Most of the north–south oriented features are also visible, and they are also stressed in the topography. West of Valdemarsvik the high-current density anomaly crossing the area from north to south is explained by a power line.

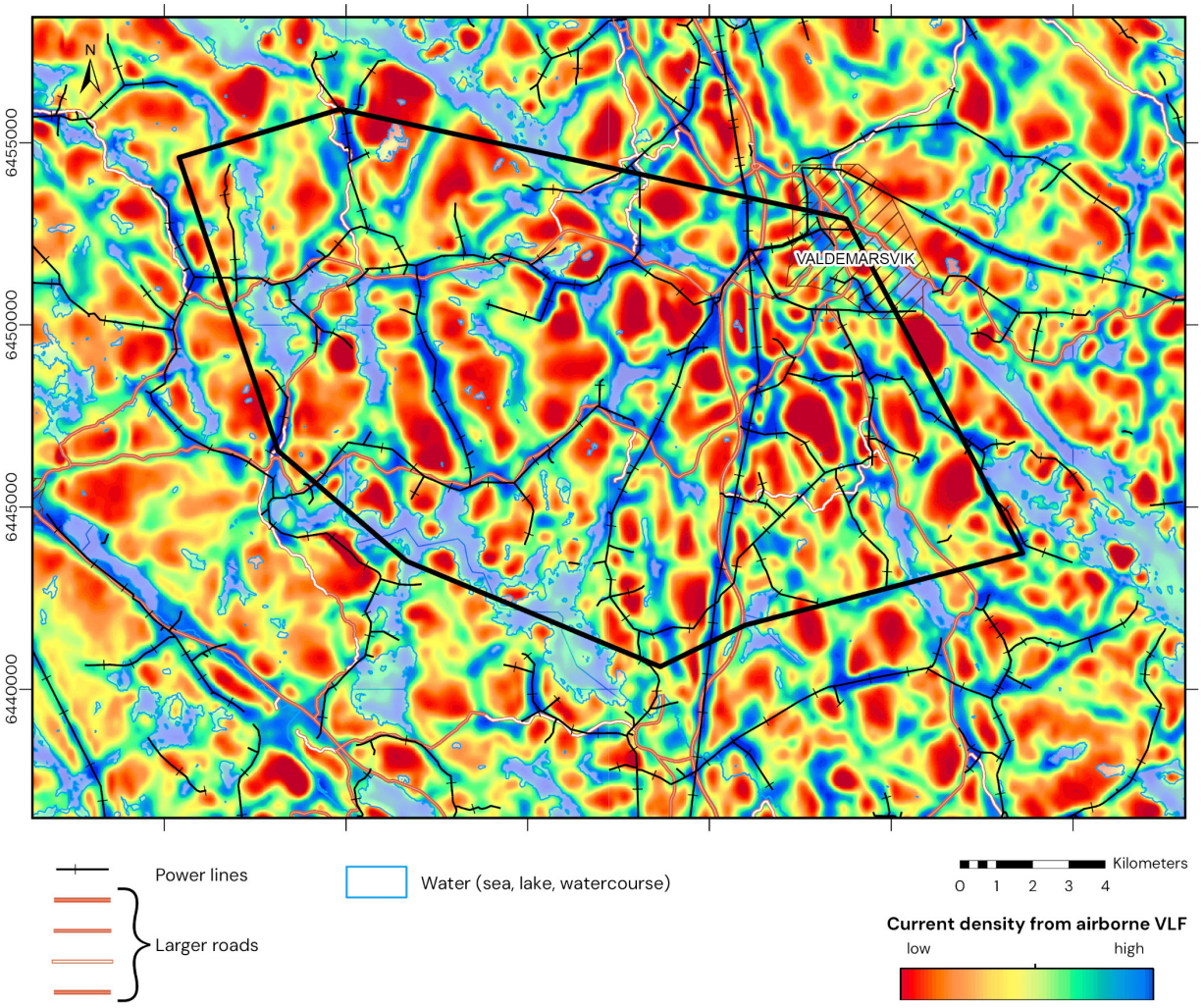

Figure 8. Map of the current density calculated from airborne VLF measurements. The main and possibly interfering infrastructures are also represented (source: Lantmäteriet).

Spectrometry

The results of the airborne gamma spectrometry measurements are shown in five different but related maps. In the Skrickerum area the soil cover is generally thin, except in a few valleys, and many, often relatively large outcrops can be found. Consequently, the result of these measurements can be expected to be closely related to the composition of the bedrock in most places. It is important to remember that the footprint of airborne measurements on the ground is large, and that they represent an average of the material's properties only to a few decimetres' depth at most. The airborne spectrometry data were complemented by measurements on outcrops, which are also presented. However, spectrometry cannot give information on the areas covered by water or by marshlands, which cover significant surfaces in the Skrickerum area.Where the bedrock is altered or eroded the radiation can originate from the quaternary cover or from local outcrops of small dimensions.

The first map shows the radiometric activity index (AI) (Fig. 9).

It is calculated in the following way:

$AI = C_K/3000 + C_{Ra}/300 + C_{Th}/200$

Where C_{Th} are the activity concentration of potassium-40, radium-226 and thorium-232. These can be estimated way from the measured concentrations of potassium, thorium, and uranium in Bq/kg since 1 % K corresponds to 313 Bq/kg, 1 ppm U to 12.35 Bq/kg and 1 ppm Th to 4.06 Bq/kg.

Larger index numbers (sometimes above one) are found in several areas, notably in the northwest corner and in the southeast corner of the project area. In the western and southwestern part of the area they are often found in zones that are topographically lower. Activity indexes larger than two were measured on two granitoid outcrops in the southeastern corner of the project area. Such a level was also measured on an outcrop close to the Skårsjö Gruvfält, within an area appearing small from the airborne measurements. When the activity index from the airborne measurements is close to or larger than one it can be recommended to control the level of radiation on the ground prior to the extraction of building materials (see general considerations in Jelinek & Eliasson 2015). The Skrickerum area is in general identified as situated in a region with elevated levels of radiation (see for example Wik *et al.* 2005) but some outcrops show very low levels, especially in the western part, north of lake Vindommen.

On the second map (Fig. 10) a ternary representation of the relative concentrations of potassium, uranium, and thorium is shown.

The geographic distributions of the measured concentrations in potassium, thorium, and uranium are presented in Figures 11, 12, and 13 respectively and show the overall range of variation for the respective element.

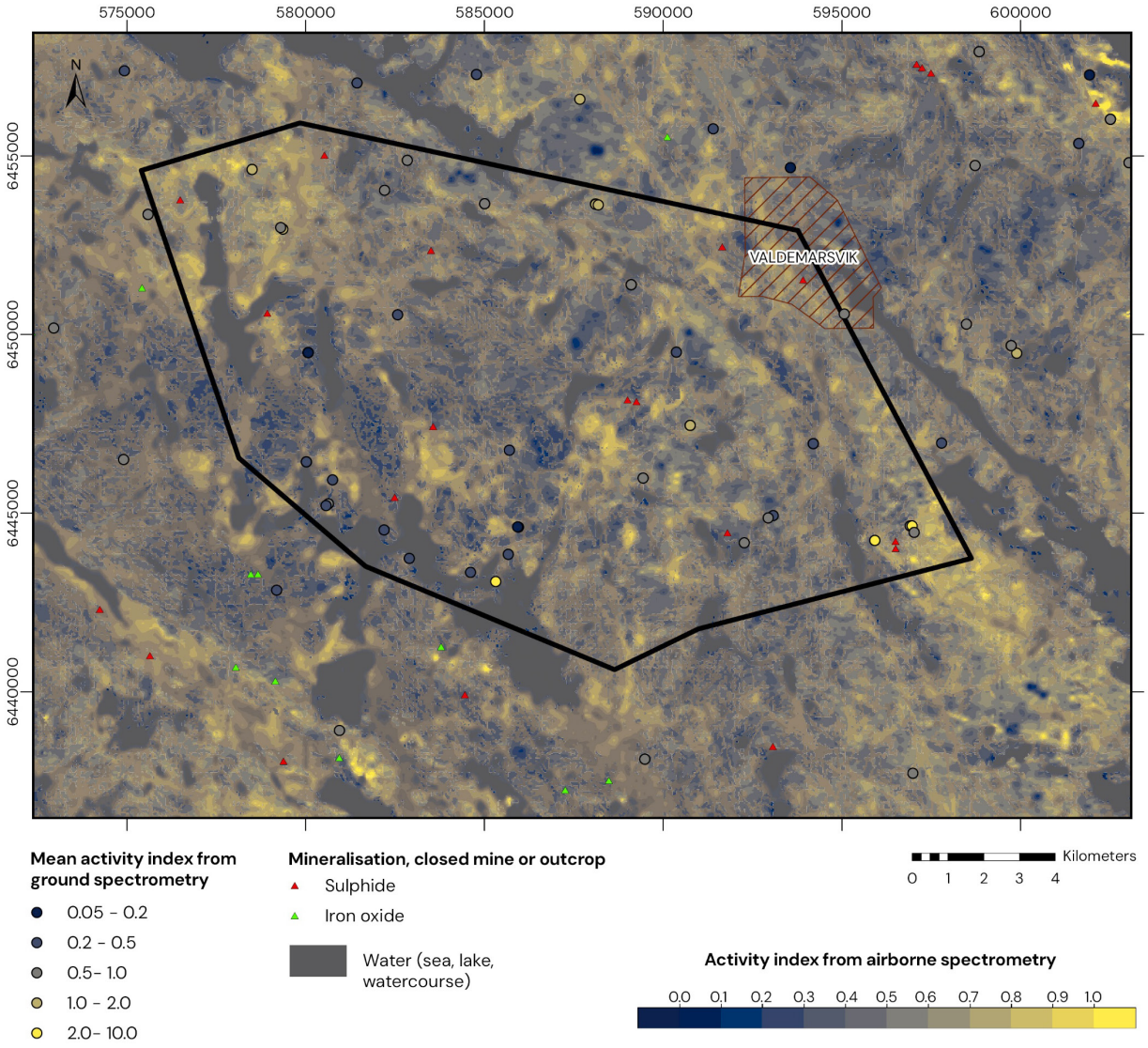

Figure 9. Map of radioactive activity index retrieved from airborne gamma spectrometry. The values reflect averaged material properties over large surfaces and down to a few decimetres' depth. Complementary measurements on the ground are necessary for accurate estimations. Results from measurements on the ground are also represented.

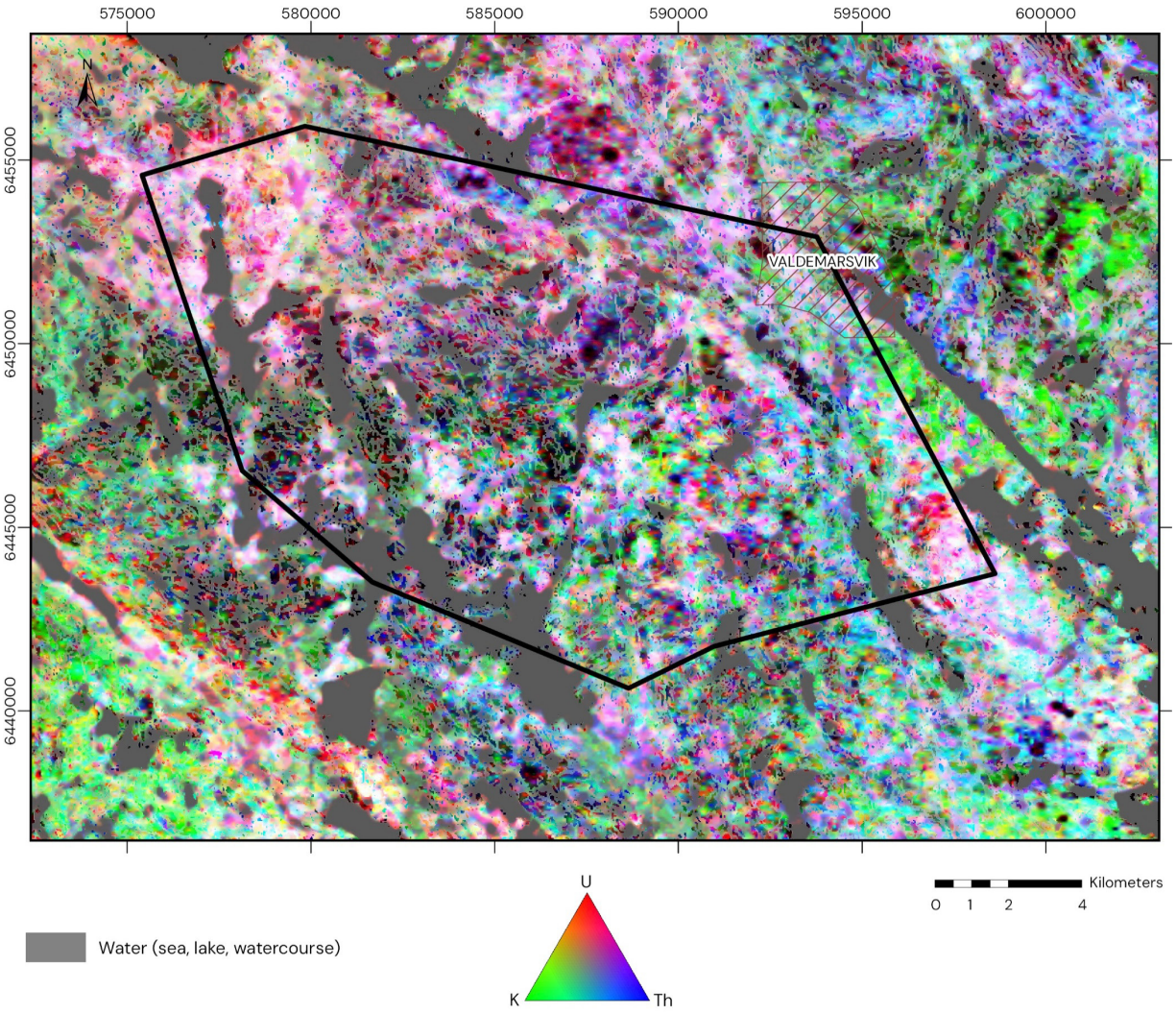

Figure 10. Map of measured concentrations in potassium, thorium, and uranium in ternary colour scale retrieved from airborne gamma spectrometry. The values reflect averaged material properties over large surfaces and down to a few decimetres' depth. Complementary measurements on the ground are necessary for accurate estimations.

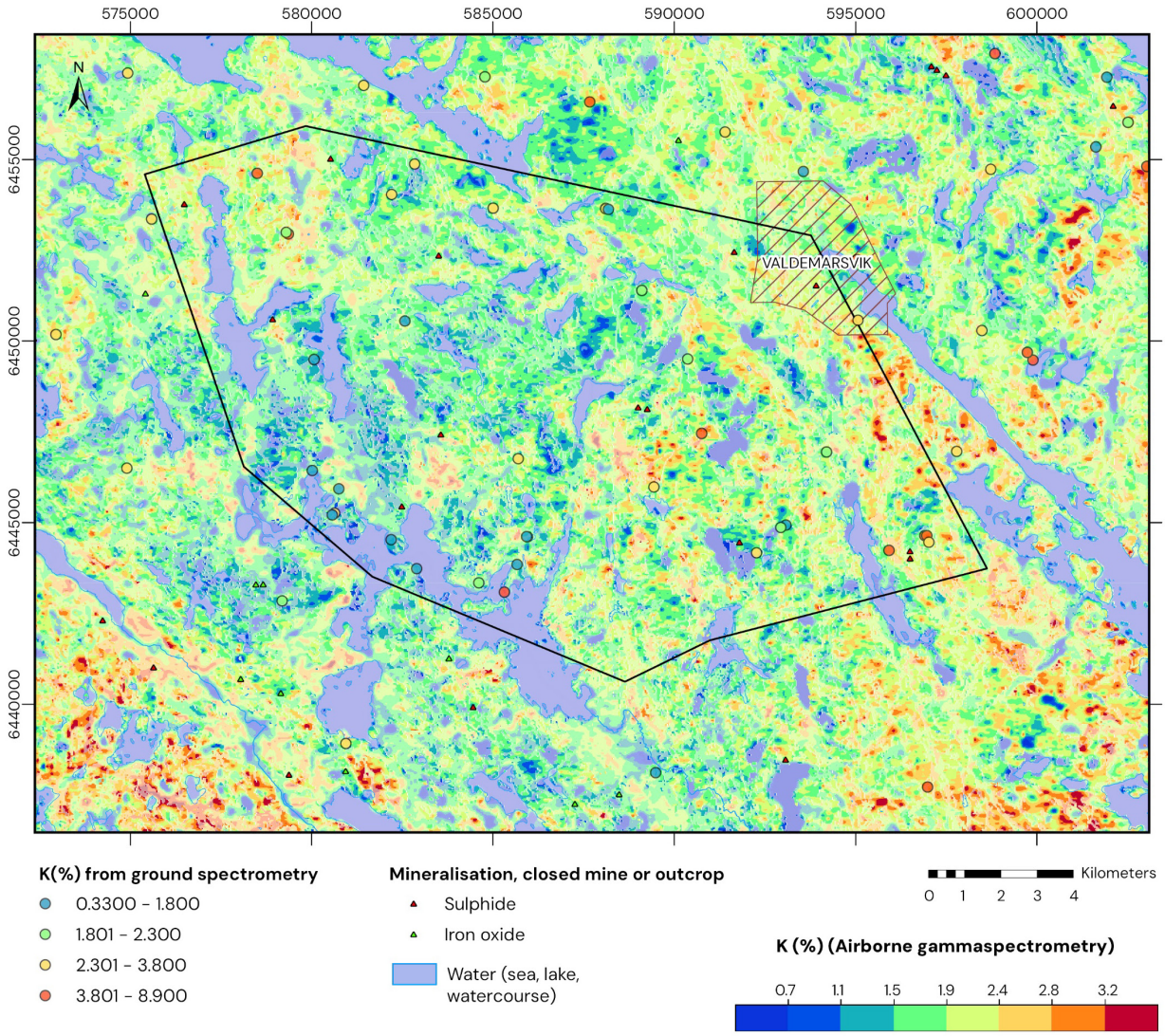

Figure 11. Map of measured concentrations in potassium retrieved from airborne gamma spectrometry. The values reflect averaged material properties over large surfaces and down to a few decimetres' depth. Complementary measurements on the ground are necessary for accurate estimations. Results from measurements made on the ground are also represented.

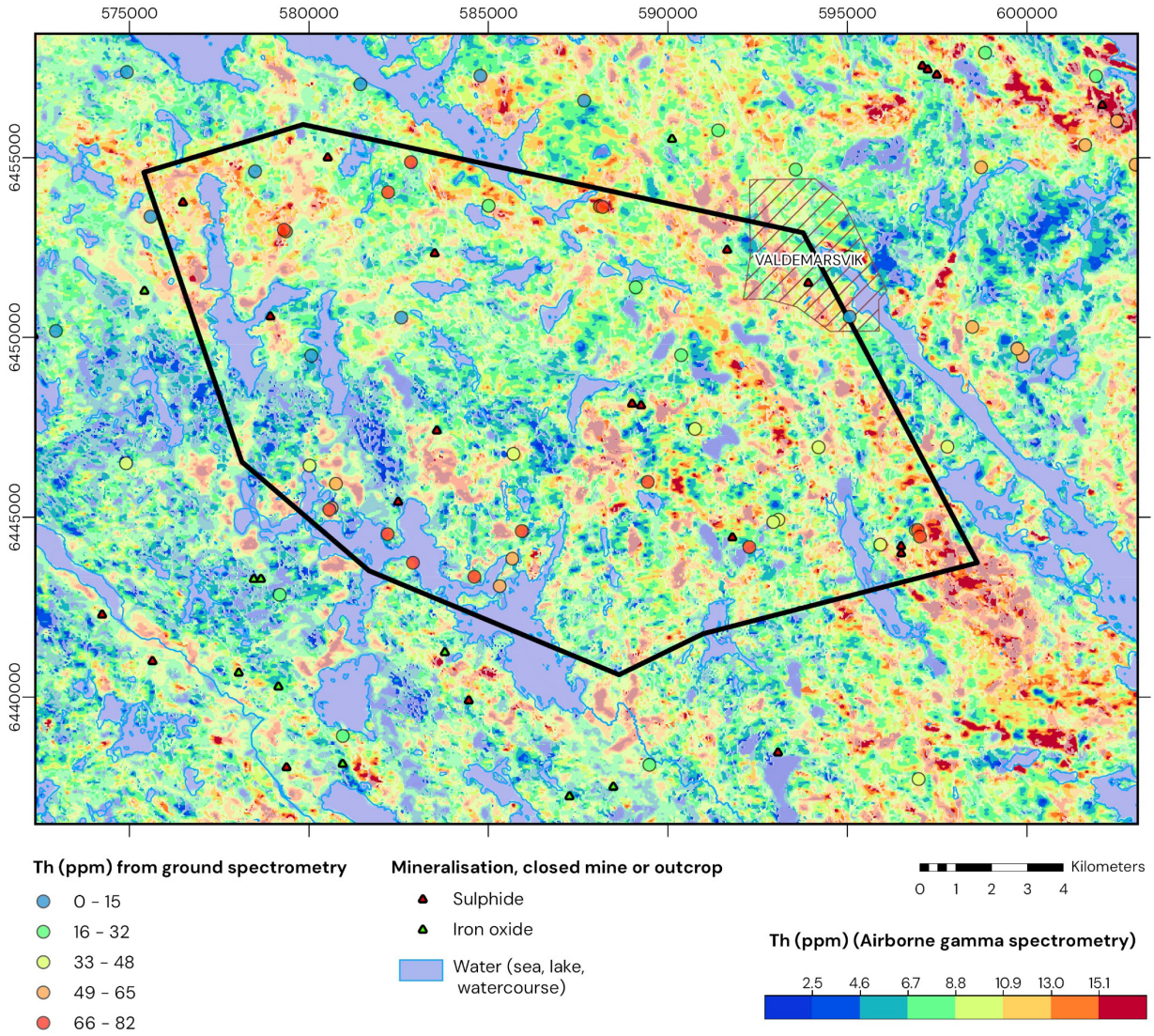

Figure 12. Map of measured concentrations in thorium retrieved from airborne gamma spectrometry. The values reflect averaged material properties over large surfaces and down to a few decimetres' depth. Complementary measurements on the ground are necessary for accurate estimations. Results from measurements made on the ground are also represented.

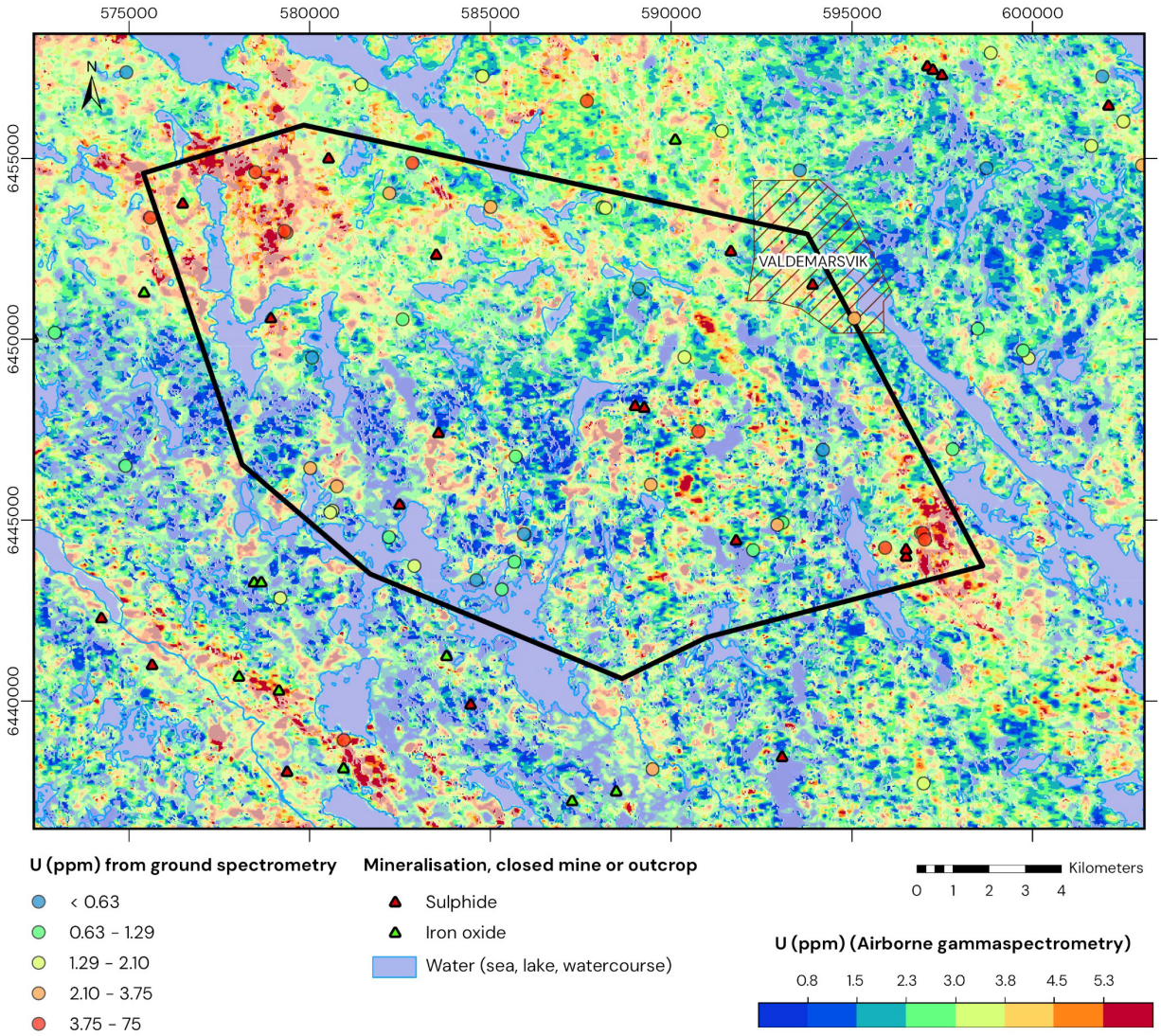

Figure 13. Map of measured concentrations in uranium retrieved from airborne gamma spectrometry. The values reflect averaged material properties over large surfaces and down to a few decimetres' depth. Complementary measurements on the ground are necessary for accurate estimations. Results from measurements made on the ground are also represented.

Ground magnetometry

The total magnetic field was measured on the ground using a GSM-19 magnetometer (GEM systems Inc.) with differential GPS positioning.

Profiles in the northern part of the Skrickerum area

Three magnetometry profiles were measured on the ground in the northern part of the project area. Their position and the field intensity measured are represented on the map below (Fig. 14). The average distance between measurement points is about 1 m. The measurements indicate very locally increased magnetite content in generally steeply dipping layers.

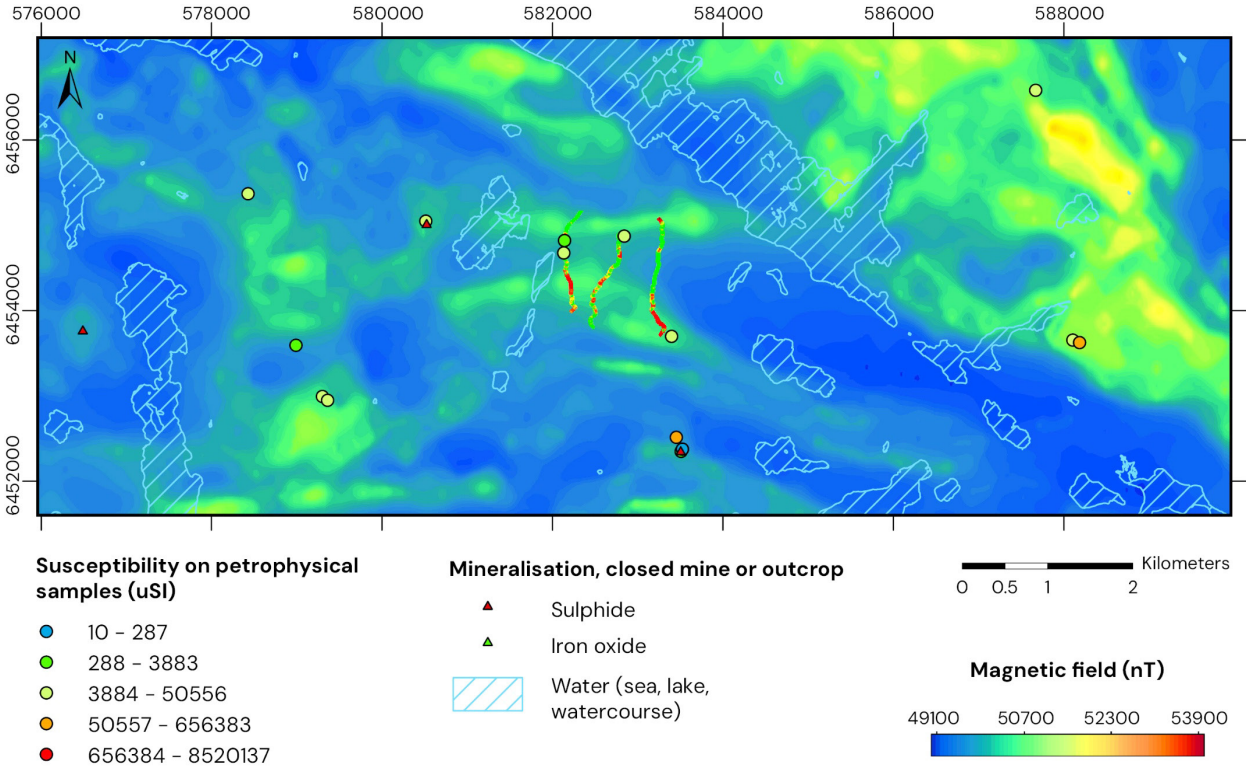

Figure 14. Location of the measured ground magnetometric profiles in the northern part of the Skrickerum area together with magnetic susceptibility of petrophysical samples. Magnetic data from airborne measurements are represented in the background using the same linear colour scale as the magnetic data along the profiles.

Profiles and area covered in the southern part of the Skrickerum area

Three profiles and six small areas were covered by magnetometry measurements. Their geographical positions and the intensity of the field measured are represented in Figure 15. A more detailed view of the small areas can be seen in Figure 16.

Here too the positive magnetic anomalies appear localised and mostly due to steeply dipping layers. From Figure 16 parallel bands can be seen or inferred on almost all small areas, but they are discontinuous, and the directions even seem to change in Figures 16B and 16D.

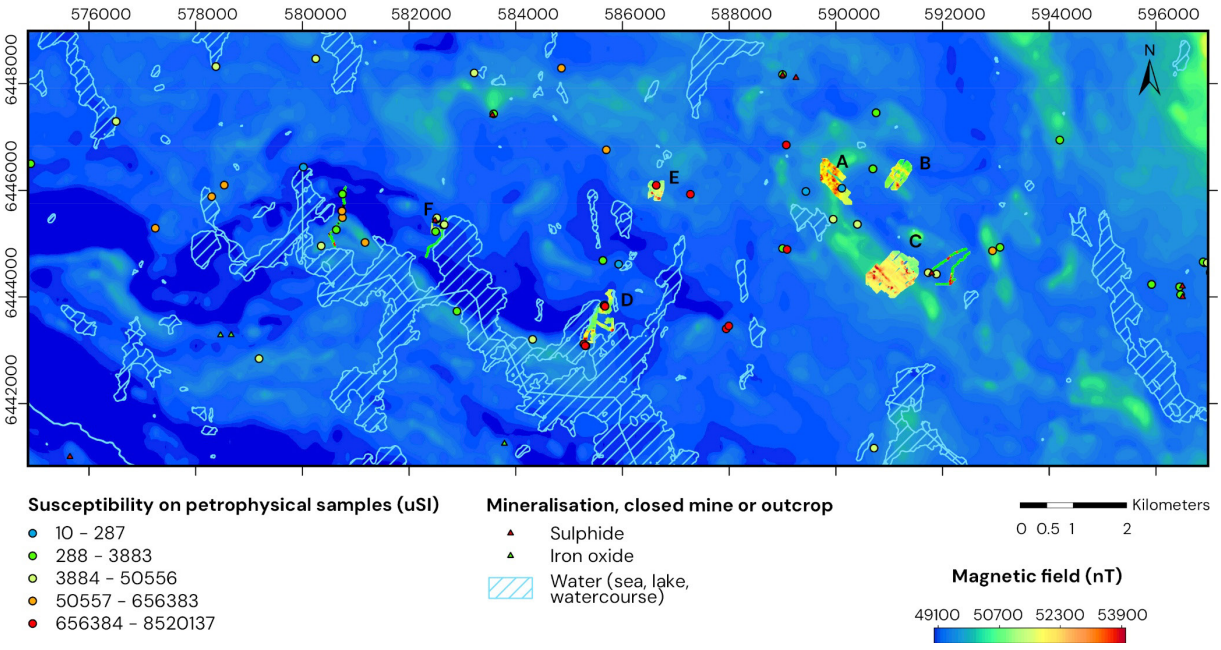

Figure 15. Location of the ground magnetometric profiles in the southern part of the Skrickerum area together with magnetic susceptibility of petrophysical samples. Magnetic data from airborne measurements are represented in the background using the same linear colour scale as the magnetic data along the profiles.The areas with ground magnetometry are labeled with letters from A to F and relate to the close-ups on Figure 16.

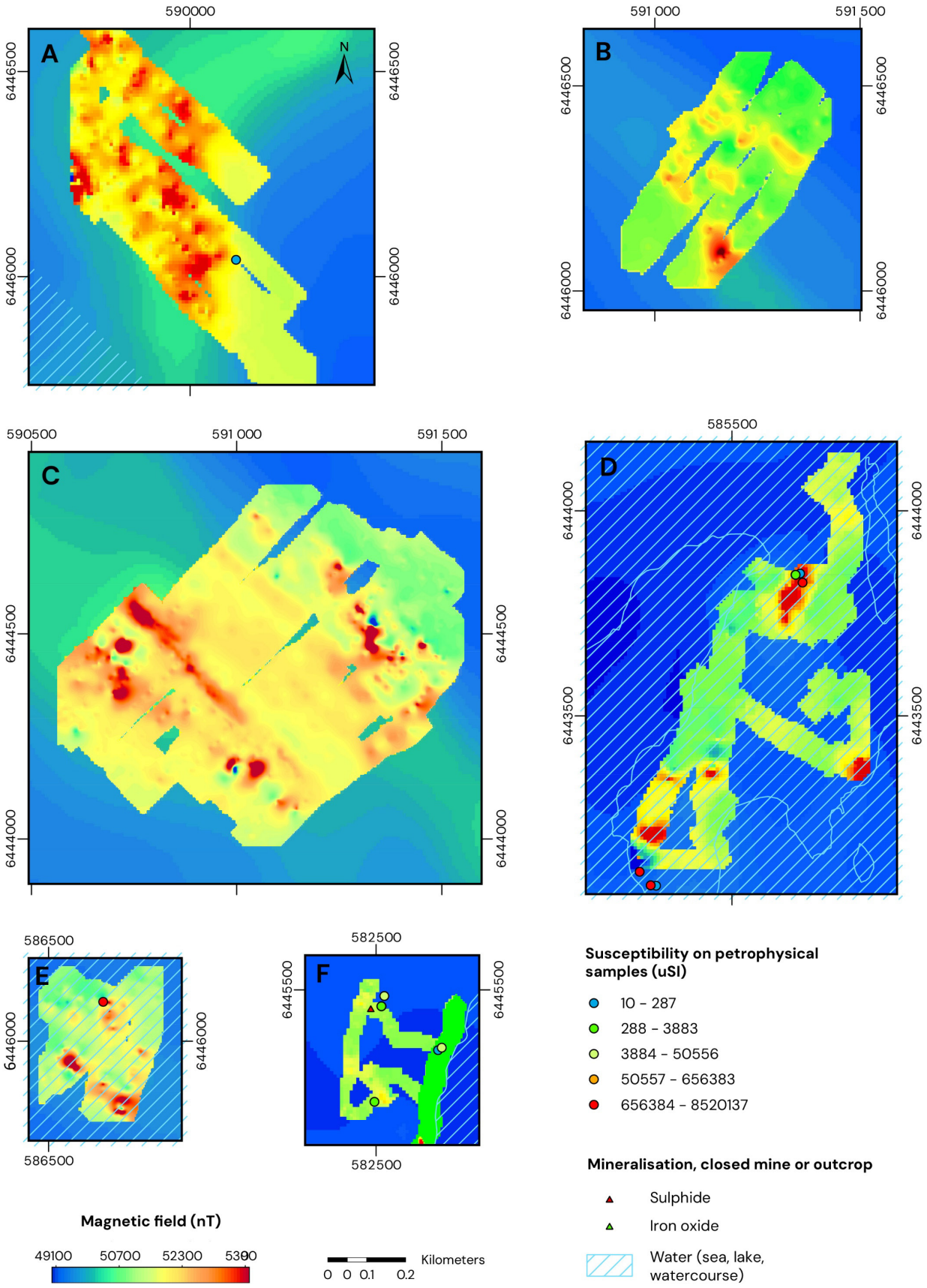

Figure 16. Close-up on the surfaces covered by ground magnetometric profiles in the southern part of the Skrickerum area together with magnetic susceptibility of petrophysical samples. Magnetic data from airborne measurements are represented in the background using the same linear colour scale as the magnetic data along the profiles. **A.** Area A. **B.** Area B. **C.** Area C. **D.** Area D. **E.** Area E. **F.** Area F (areas as defined in Fig. 15).

Volcanic rocks

The volcanic rocks of the Skrickerum project area are dominated by basaltoid and andesitoid. Dacitoid to rhyolite is also present but subordinate for the most part.

Feldspar porphyritic volcanic rocks are rare among the visited outcrops. A relatively homogenous plagioclase porphyritic andesitoid to dacitoid volcanic rock is an example of this type of rock and occurs in a gravel pit with good, clean, well-exposed outcrops (Fig. 17A). Small sections of basaltoid are present as long bands, often broken off along the foliation plane (Fig. 17B). Granite to pegmatite occurs as dykes. All rocks are severely deformed and exhibit S-folds and foliation.

Andesitoid and basaltoid often occur as alternating layers in outcrops. Occasionally granodiorite is observed cutting the layering of volcanic rocks (Fig. 17C). The granodiorite there is foliated and folded, the latter probably related to the contact with the volcanic rocks. All these rocks are cut by younger granite to pegmatite dykes, which are mostly massive and lack deformation. This generation of granite-pegmatite is also seen as conformable dykes with the layering of the volcanic rocks (Fig. 17D).

Rather flat outcrops with mostly basaltoid to andesitoid volcanic rocks and veins of granite to pegmatite can exhibit a chaotic pattern of deformation and metamorphic overprinting (Fig. 17E–F). All rocks are deformed, foliated, and folded at this outcrop. A foliation is present with a main direction, but parts of the outcrop are in completely different directions, in principle any can be measured.

In a local rock quarry, 50 × 30 metres and bench height c. 15 metres, basalt with a relatively primitive composition of MgO 12.2%, Cr 896 ppm, and Ni 203 ppm is interlayered with a basaltic andesite with MgO 3.05%, Cr 14 ppm, and Ni 15 ppm. Dacitoid and granitic gneiss are also present in the quarry, along with a few pegmatite dykes (Fig. 18A–B). Sulphide minerals are seen primarily in the andesitoid rocks but also in the acid volcanics, where they occur primarily as up to a couple of centimetres wide fracture fillings rich in sulphide minerals, probably primarily pyrite. Some of these fracture fillings run perpendicular to the foliation in the acid volcanics. The measured petrophysical values of the primitive basalt (Fig. 18C) are a density of 3 057 kg/m^3, a magnetic susceptibility of 37 × 10^{-5} SI, a natural remanent magnetisation of 18.7 mA/m, a resistivity of 372 Ωm, and the basaltic andesite (Fig. 18D) values are a density of 2 850 kg/m^3, a magnetic susceptibility of 2 559 × 10^{-5} SI, a natural remanent magnetisation of 282 mA/m, and Q-value 0.27.

Some outcrops have strongly deformed volcanic sequencies with alternating andesitoid and basaltoid layers, where ductile deformation resulted in a strong foliation (Fig. 18E–F) In the foliation planes streaks and veins of granitic composition occur and sometimes younger generations of granite dykes have intruded along the foliation. Granite and pegmatite dykes also cut the strong foliation at high angles.



Figure 17. A. Plagioclase porphyritic andesitoid to dacitoid with granite to pegmatite S-folded dykes. **B.** Bands of elongate basaltoid in the plagioclase porphyritic andesitoid to dacitoid, often torn apart along the foliation. Granite to pegmatite dykes are deformed and all rocks have been folded, and S-folds are common (6451287/589557). **C.** Andesitoid and basaltoid layering cut in the centre of image by granodiorite to the right. **D.** All rocks are cut by granite to pegmatite dykes which are mostly massive. This generation of granite-pegmatite is also seen as dykes conformable with the layering of the volcanic rocks (6448251/588536). **E.** and **F.** Flat outcrops showing deformation of layering in basaltoid and andesitoid, which is also present in granite to pegmatite dykes. In both images the hammer rests on a metre-wide dyke. Folding of all rocks means all direction of foliation can be seen in E. and F. and the photos were taken at roughly 45 degrees angle to each other (6449099/583287). Photo: Dick Claeson.

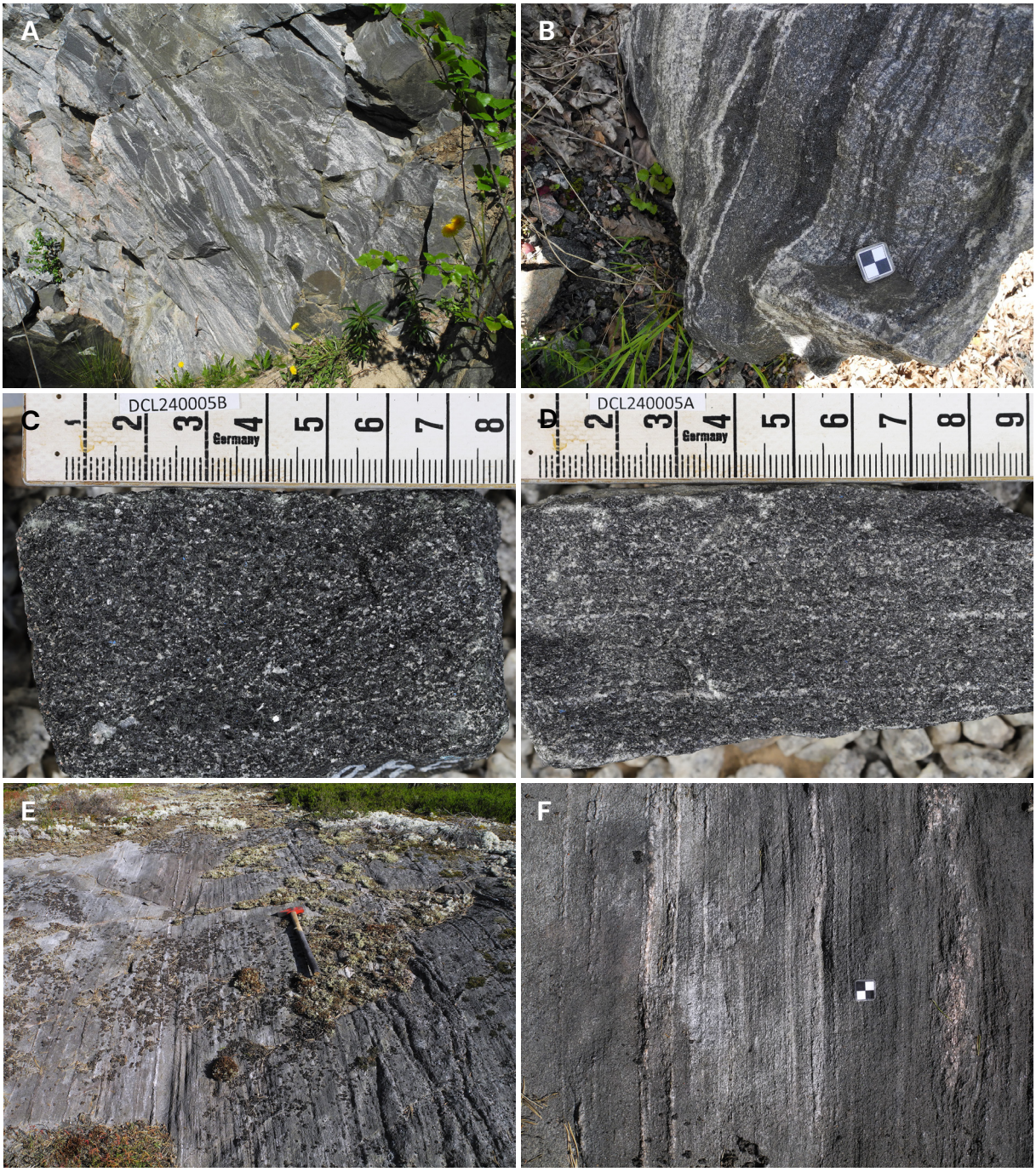

Figure 18. A. Primitive basalt interlayered with dacitoid, and granitic gneiss at a small quarry. **B.** Close-up of the interlayered primitive basalt, basaltic andesite, and dacitoid (6444685/585633). Photos: Dick Claeson. **C.** and **D.** Samples used for petrophysical lab measurements, primitive basalt and basaltic andesite, respectively. Photos: Peter Hedin. **E.** Predominantly andesitoid interlayered with minor basaltoid, and granitic veins and dykes in a strongly foliated volcanic sequence. **F.** Close-up of the interlayered volcanic rocks, and granite in the foliation plane (6445500/582170). Photos: Dick Claeson.

Close to the Åläng gruva a new forest road has been made and uncovered new exposures of rock. Strongly deformed and metamorphically overprinted volcanic rocks are often interlayered with bands of granitic gneiss (Fig. 19). These units are partially strongly folded, and both S- and Z-folds are commonly observed (Fig. 19). Among the volcanic rocks basaltoid and andesitoid dominate the outcrops but dacitoid is also present as layers or bands. All rocks in these exposures are garnet-bearing, most garnets are reddish brown to red and 0.5 to 5 mm large. The outcrops next to the road, closest to the Åläng gruva has minor sulphide mineralised layers that strike 310 and dip 82 degrees. The garnets are reddish brown and the largest are up to 30 mm in the basaltoid and andesitoid, whereas the dacitoid has the highest abundance of garnets here (Fig. 19). The garnet-bearing dacite has SiO_2 67.7%, Al_2O_3 17.5%, Fe_2O_3 4.93%, CaO 5.12%, MgO 1.26%, Na_2O 3.40%, K_2O 1.00%, TiO_2 0.30%, MnO 0.08%, and P_2O_5 0.11%. The garnet-bearing dacite has a density of 2 757 kg/m^3, a magnetic susceptibility of 22 × 10^{-5} SI, a natural remanent magnetisation of 10.6 mA/m, and a resistivity of 940 Ωm (Fig. 19G).

At several outcrops basaltoid was transformed to garnet amphibolite, e.g., at Sjögerum (Fig. 20A–B). The outcrop consists of andesitoid and basaltoid metavolcanic rocks with veins and streaks of light-coloured pegmatite. All rocks at the outcrop are strongly deformed, foliated, and are garnet-bearing to varying degrees. The garnets are 1 to 10 mm in size, mostly brown but in places with a reddish hue. The garnet amphibolite has a density of 2 966 kg/m^3, a magnetic susceptibility of 1 123 × 10^{-5} SI, and a natural remanent magnetisation of 252 mA/m.

Basaltoid and andesitoid are in some areas intimately associated with gabbroid rocks (Fig. 20C–F). The gabbroid is conformable with the volcanic rocks and the foliation plane of both rocks for the most part. There are some gabbroic rocks that can be interpreted as sills, conformable to layering, from ½ to several metres wide, and continues throughout the outcrop. Both the volcanic rocks and the gabbroid are strongly deformed and metamorphically overprinted, sometimes even veined, and when folded their relation as conformable rocks is still evident.

A rare occurrence of garnet-bearing migmatite, probably originally an andesitoid to basaltoid volcanic sequence that is consistent with the high measured density, occurs not far from the sulphide mineralisation at Fåfalla. The migmatite is heavily veined with granite, which formed by partial melting of the andesitoid to basaltoid (Fig. 21). In most of the outcrop, the migmatite lacks a consistent orientation of any kind and is heterogeneously folded, but at the western edge there is a strongly deformed portion that has a steep, mainly east-dipping foliation. Garnets are seen as possibly two generations, a brown and a brownish-red to reddish-brown, 1 to 20 mm in size, with garnet aggregates up to 20 mm wide and 60 mm long. The garnet-bearing migmatite signifies a high-grade metamorphism event that happens at the upper amphibolite to granulite transition. Loss of ignition registered by the whole rock lithogeochemical analysis was only 0.13%, the lowest value of all analysed silicate rocks in the project area, indicating no major presence of hydrous minerals like biotite or amphibole in the garnet-bearing migmatite and a dehydration reaction is plausible during the migmatitisation. The garnet-bearing migmatite has similar patterns in the REE-spidergram and N-MORB normalised spidergram as the mafic to intermediate volcanic rocks (Fig. 22). However, the relative abundance of garnet, which preferably incorporates heavy REE in its structure when forming, is evident in those spidergrams as the highest REE concentrations compared to all volcanic rocks.

The garnet-bearing migmatite has a density of 2 894 kg/m^3, a magnetic susceptibility of 71 × 10^{-5}SI, and a natural remanent magnetisation of 16.2 mA/m (Fig. 21E).

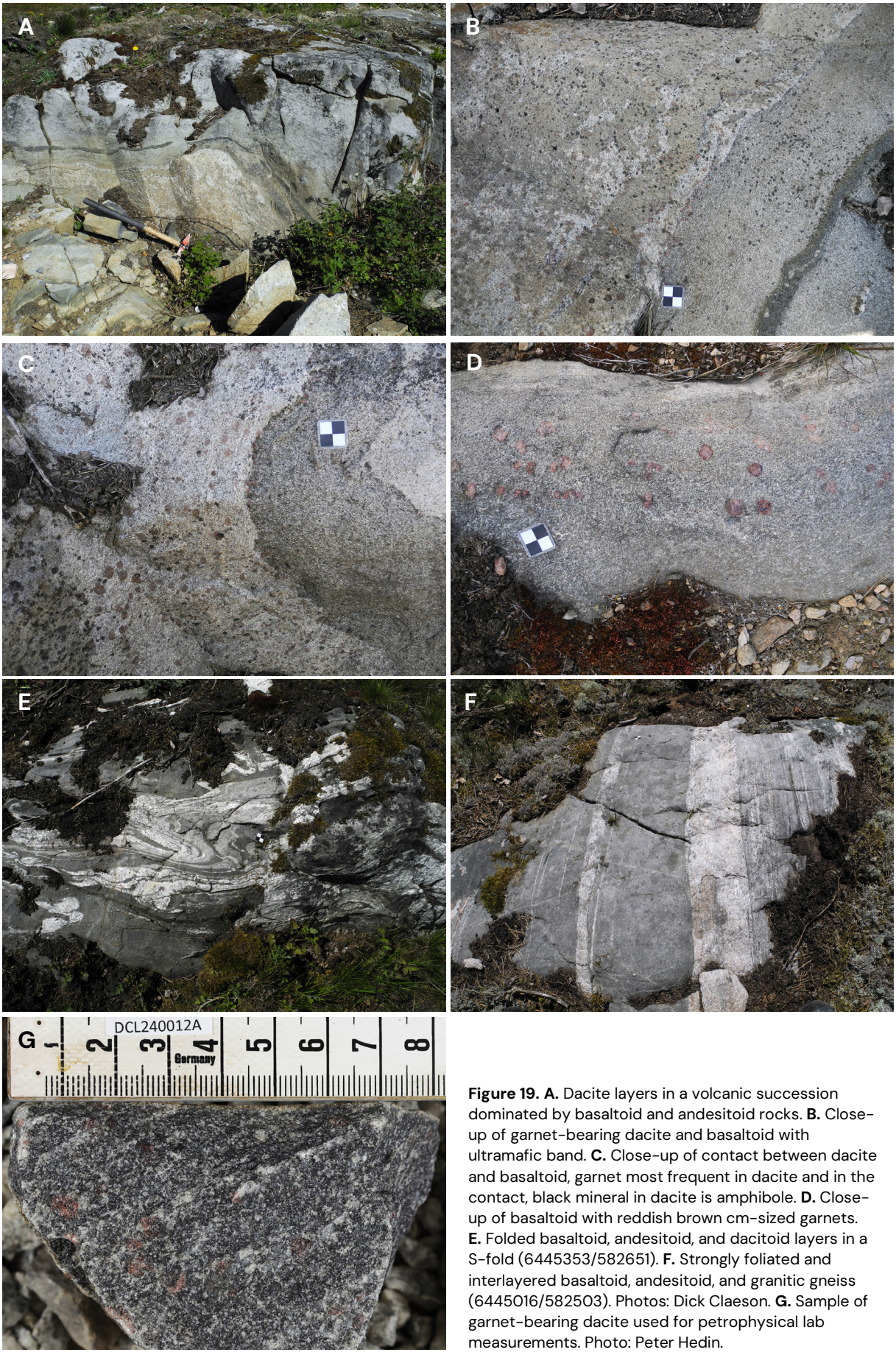

Figure 19. A. Dacite layers in a volcanic succession dominated by basaltoid and andesitoid rocks. **B.** Close-up of garnet-bearing dacite and basaltoid with ultramafic band. **C.** Close-up of contact between dacite and basaltoid, garnet most frequent in dacite and in the contact, black mineral in dacite is amphibole. **D.** Close-up of basaltoid with reddish brown cm-sized garnets. **E.** Folded basaltoid, andesitoid, and dacitoid layers in a S-fold (6445353/582651). **F.** Strongly foliated and interlayered basaltoid, andesitoid, and granitic gneiss (6445016/582503). Photos: Dick Claeson. **G.** Sample of garnet-bearing dacite used for petrophysical lab measurements. Photo: Peter Hedin.



Figure 20. A. Basaltoid, andesitoid, garnet amphibolite, and pegmatite veins at Sjögerum. **B.** Close-up of garnet amphibolite (6444430/591886). **C.** Contact between basaltoid and gabbroid, the latter interpreted as a larger conformable dyke, both rocks are strongly deformed and have light-coloured veins. **D.** Basaltoid volcanic rock with layers of andesitoid (6444958/580352). **E.** Contact between basaltoid and ½ meter wide conformable gabbroid dyke. **F.** Z-folded granitic dyke in basaltoid (6446162/580458). Photo: Dick Claeson.

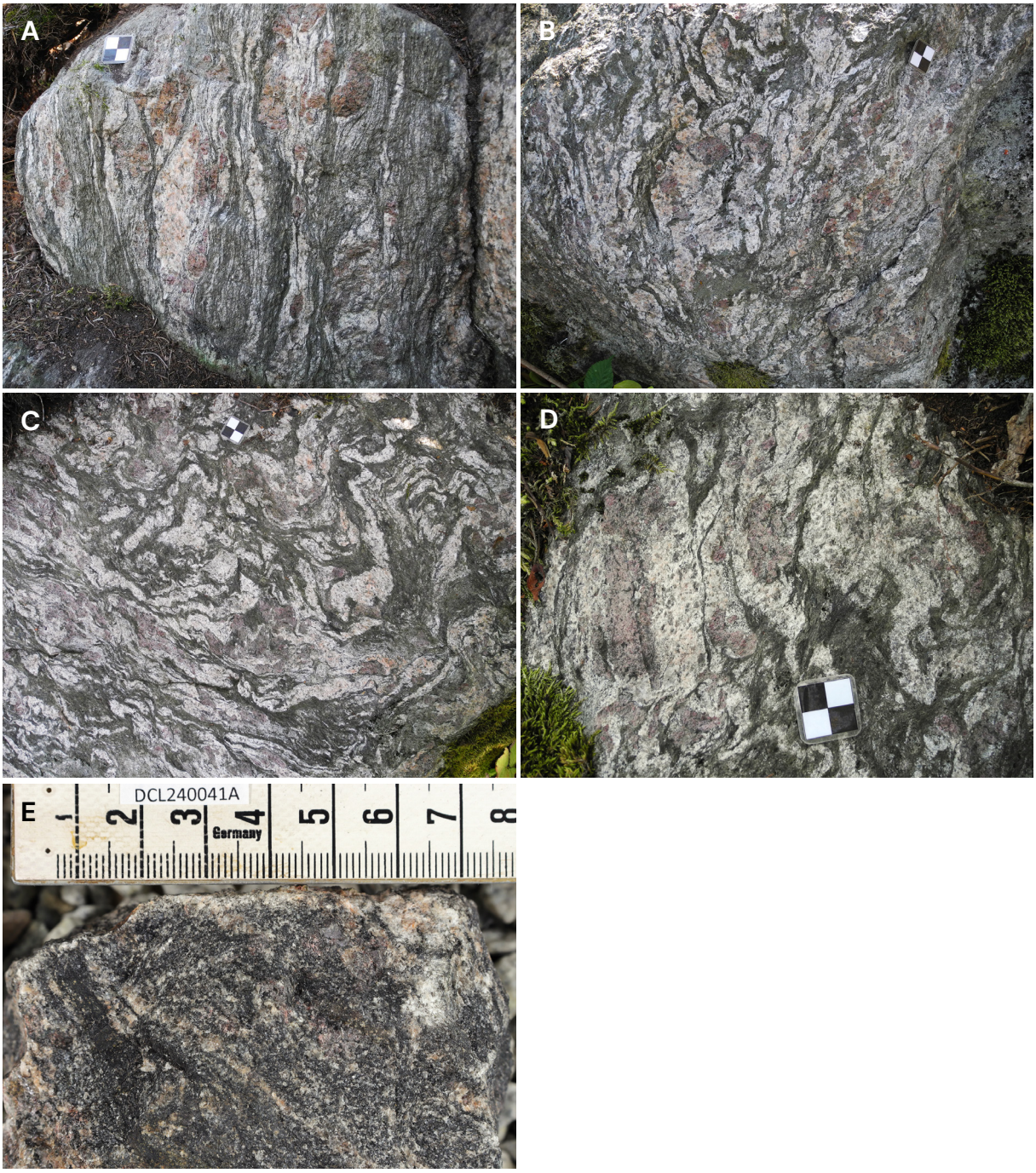

Figure 21. A. Strongly deformed garnet-bearing migmatite of probable andesitoid to basaltoid origin with veins of granite, note brown colour of garnet. **B.** Close-up of folded garnet-bearing andesitoid to basaltoid migmatite. **C.** Close-up of garnet-bearing andesitoid to basaltoid migmatite with granite veins, foliation seen in the lower left and the rest is irregularly folded. **D.** Close-up of andesitoid to basaltoid migmatite with brownish red garnet aggregates 2 cm wide and 6 cm long and lots of granite veins (6452350/583509). Photos: Dick Claeson. **E.** Sample of garnet-bearing migmatite used for petrophysical lab measurements. Photo: Peter Hedin.

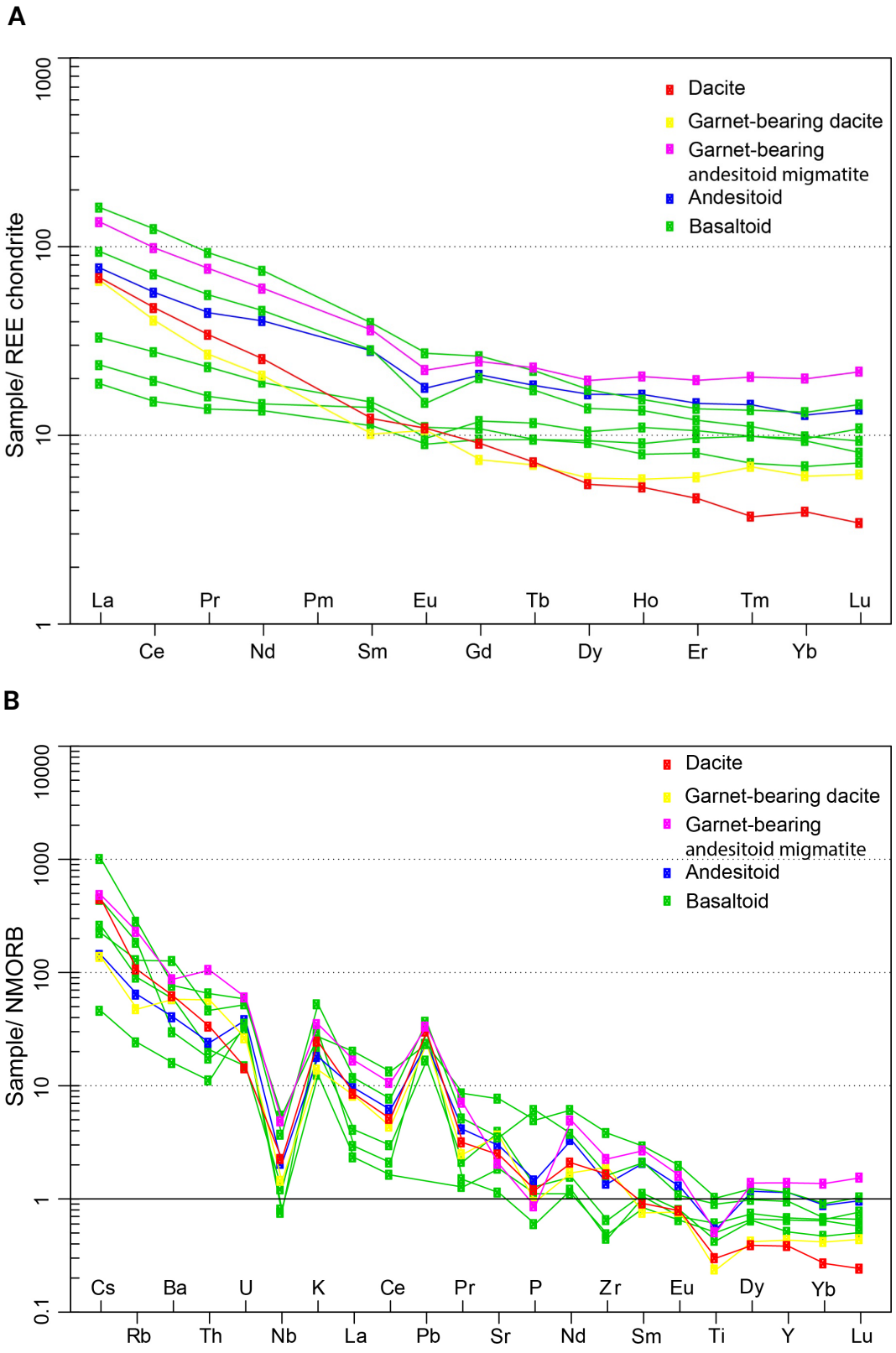

Figure 22. A. REE-spidergram of metavolcanic rocks from the Skrickerum project area. Normalisation values for chondrite Boynton (1984). **B.** N-MORB normalised spidergram of same rocks, values Sun & McDonough (1989).

Intrusive rocks

Older generation of acid intrusive rocks

Tonalite to granodiorite of Svecokarelian age occurs in large parts of the Skrickerum project area. The colour varies in different shades of grey, light to dark, and the grain size is between fine and coarse. The rock is both lineated and foliated at places (Fig. 23), but never massive and is strongly deformed and folded in many outcrops. The tonalite to granodiorite has similar patterns in the REE-spidergram and the N-MORB normalised spidergram as most of the sampled intrusive rocks (Fig. 30).

The tonalite to granodiorite has a density of 2 712 kg/m^3, a magnetic susceptibility of 1 810 × 10^{-5} SI, and a natural remanent magnetisation of 25.4 mA/m (Fig. 23C).



Figure 23. A. Tonalite to granodiorite, lineated and foliated. **B.** Sampled grey to dark grey tonalite to granodiorite, (6448470/580250). Photos: Dick Claeson. **C.** Sample used for petrophysical lab measurements. Photo: Peter Hedin.

Granite and granodiorite of the older generation are ductilely deformed and metamorphosed (Fig. 24). The granite is red to grey, often with mafic bands and pegmatite dykes, all deformed and metamorphosed. The granodiorite is predominantly grey with some reddish grey parts, deformed and veined. The granite and granodiorite have similar patterns in the REE-spidergram and N-MORB normalised spidergram as most of the sampled intrusive rocks (fig. 30). However, in the latter spidergram granite has much more pronounced troughs for P and Ti than granodiorite, due to fractionation.

The sampled granite and granodiorite have densities of 2 635 and 2 709 kg/m^3, magnetic susceptibilities of 2 710 and 3 240 × 10^{-5} SI, natural remanent magnetisations of 746 and 1 520 mA/m, and Q-values of 0.68 and 1.16, respectively (fig. 24C–D).

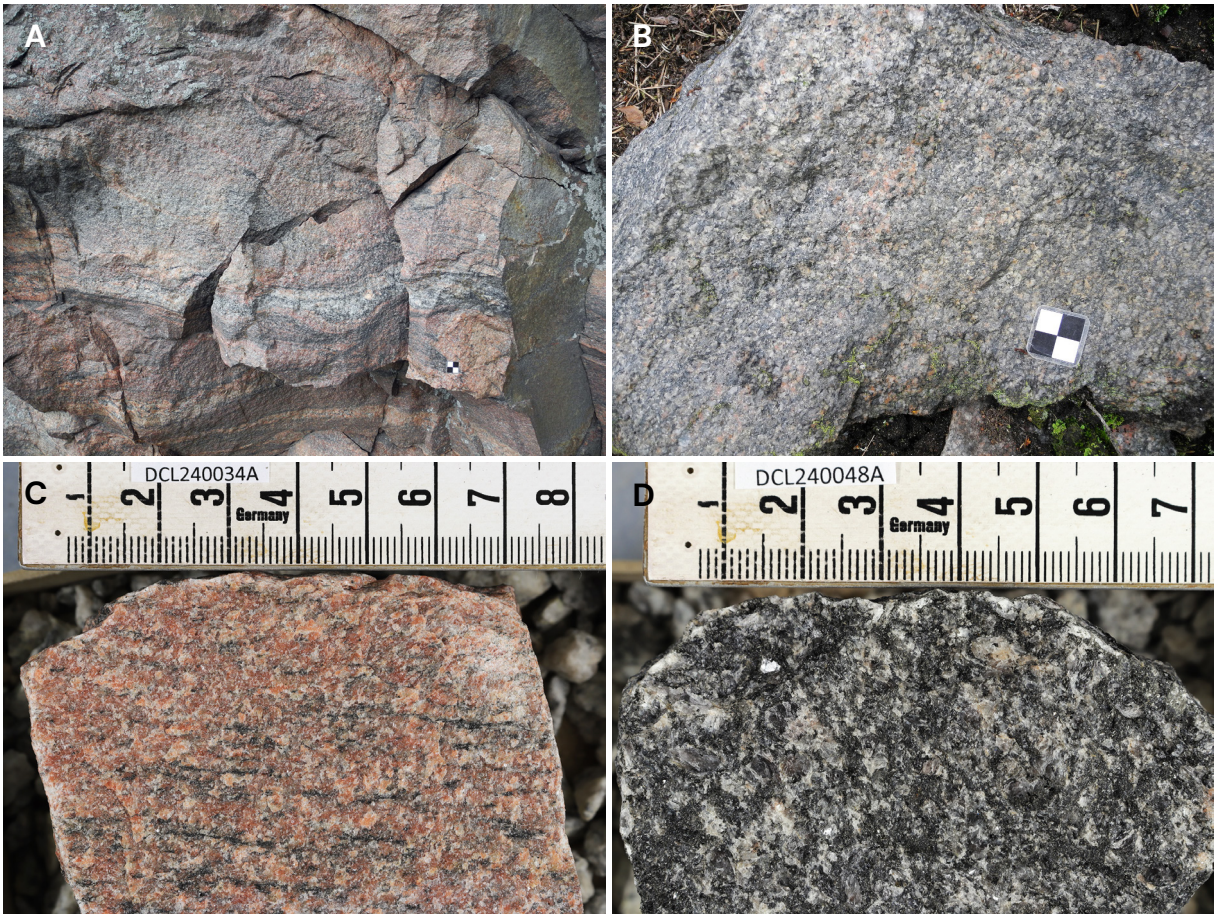

Figure 24. A. Strongly deformed, red granite with thin mafic bands and deformed pegmatite dykes, (6451234/586868). **B.** Foliated, veined reddish grey to grey granodiorite, (6455371/578428). Photos: Dick Claeson. **C.** and **D.** Samples of granite in A. and granodiorite in B. respectively, used for petrophysical lab measurements. Photos: Peter Hedin.

Younger generation of acid intrusive rocks

Granite of a presumed TIB1 age, around 1 800 Ma old, is present in the Skrickerum project area at several places but in the whole relatively scarce. The granite is even- to unevenly grained, medium- to coarse grained, greyish red to reddish grey, and most often massive or slightly deformed close to xenoliths and contacts. Occasionally lots of xenoliths of the older metavolcanic rocks are present in this granite (fig. 25). One such outcrop is approximately 20 metres north of a contact with volcanic rocks. The further away from the contact between the two rock types, the less frequent xenoliths occur in the younger granite and in the closest part xenoliths are abundant.

Massive to weakly foliated granite, mostly where xenoliths occur, has the appearance of an anatectic granite (fig. 26). This granite is seen with a massive, grey, potassium feldspar megacrystic granite that is interpreted as contemporaneous and possibly intrudes part of the anatectic granite. Dykes of massive, red pegmatite appear to be generated from the anatectic granite. Rarer are aplite dykes, also regarded to have formed from the anatectic granite where due to sudden loss of volatiles a much more fine-grained and aplitic textured rock formed (fig. 26). All these granitic rocks have euhedral to subhedral megacrysts, varying in size and abundance among them (fig. 26). All are thought to be of a similar age, if not derived from the same magma. The granites are significantly younger than the basaltoid to andesitoid that occur as xenoliths. The xenoliths have up to five mm large brownish garnets, and their magnetic susceptibility varies a lot. The anatectic granite is at places relatively heterogeneous, possibly because of partially dissolved and assimilated small xenoliths. In these partially dissolved small xenoliths garnets are present but are more reddish in colour than brownish.

The anatectic granite stands out in the magnetic anomaly map as a low magnetic area, which is used for delimiting its occurrence in the digital map database, and it often has highly anomalous U and Th contents as seen in the airborne spectrometry data, which was also used to determine its extent (Figs. 6, 12, and 13).

The massive to weakly foliated anatectic granite has a density of 2 649 kg/m^3, a magnetic susceptibility of 23 × 10^{-5} SI, and a natural remanent magnetisation of 18.7 mA/m (Fig. 27F).



Figure 25. Xenoliths of metavolcanic rocks in probable TIB1 granite, greyish red to reddish grey and mostly massive, **A.** basaltoid and **B.** andesitoid xenoliths (6448343/584856). Photo: Dick Claeson.



Figure 26. A. Massive to weakly foliated granite with pegmatite dykes. **B.** Close-up of interfingering contact between granite and pegmatite in A. **C.** Same granite as in A. and B. with aplitic dykes. **D.** Aplite and pegmatite dyke in contact with a massive, coarse-grained, grey granite. **E.** Xenoliths of basaltoid in grey granite. **F.** Close-up of grey, potassium feldspar megacrystic granite (6446041/590112). Photo: Dick Claeson.

A relatively homogenous, massive, young anatectic granite has parts with larger grain size, light greyish colour, and more abundant quartz than in the main rock (Fig. 27). An explanation of this is that the melting temperature of granite is strongly reduced in the presence of H_2O and affects the stability of quartz within the granite melt (e.g., Johannes & Holtz 1996). H_2O interacts with the quartz structure, weakening the Si-O bonds and allowing for a greater proportion of quartz to remain in the melt at a given temperature. Thus, the pockets and network of the light-grey

quartz-rich granite are the last portions to crystallise in this magmatic system. There are synmagmatic pegmatite dykes at the outcrop. Rare, partly digested older garnet-bearing gneiss xenoliths occur in the granite, where garnets are mm-sized and have a brownish red colour (Fig. 27D).

This anatectic granite has a density of 2 623 kg/m^3, a magnetic susceptibility of 178 × 10^{-5} SI, and a natural remanent magnetisation of 19.6 mA/m (Fig. 27E).

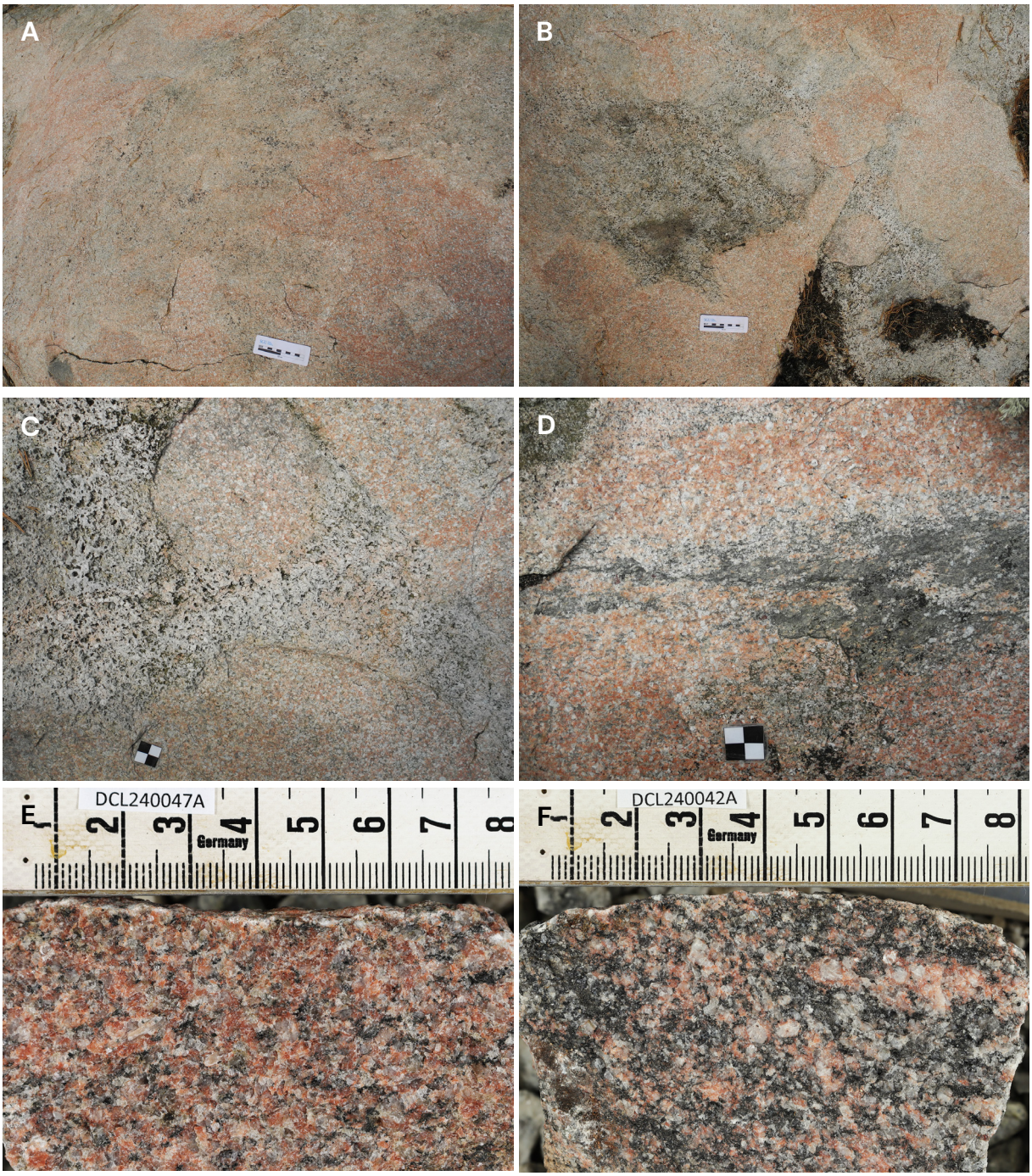

Figure 27. A. Relatively homogenous, red to reddish grey granite. **B.** Relatively homogenous, red to reddish grey granite with coarse-grained, light-grey, and quartz-rich network. **C.** Close-up of quartz-rich network in A. **D.** Rare, partly digested older garnet-bearing gneiss xenolith (6453594/578990). Photos: Dick Claeson. Samples of anatectic granite used for petrophysical lab measurements, **E.** red to reddish grey granite (6453594/578990) and **F.** grey to reddish grey granite (6446041/590112). Photos: Peter Hedin.

Basic to intermediate intrusive rocks

The gabbro rocks in the project area have different amounts of tectonic and metamorphic overprinting (Fig. 28). Some have light-coloured metamorphic veins and are strongly deformed, others are almost massive with only faint foliation and display igneous layering. Since no age determinations exist in this area of gabbroic rocks, these differences can only speculatively indicate that there are several generations of gabbroic intrusions. The oldest being the ones that are veined and have strong metamorphic overprinting, while a possible TIB generation are those with only minor signs of alteration, but the former is by far the most abundant generation in the project area. An example of a less altered, possibly TIB-related gabbro intrusion displays igneous layering, with layers of magnetite-rich, almost black and rare chalcopyrite-bearing gabbro, layers of light grey, magnetite- and plagioclase-rich, and weakly sulphide-bearing gabbro, and layers of dark grey, weakly magnetic gabbro (Fig. 28D). A strong variation of the magnetic susceptibility between different layers was measured at the outcrop.

As mentioned above in the section *Volcanic rocks* basalt and gabbro coexist at places and the latter was interpreted to be conformable dykes, a few tens of meters wide at the outcrops. These are possibly related to the generation of the basalt and being consanguineous. Both rocks have the same metamorphic overprinting and deformation (Fig. 20C).

Dark, massive to weakly foliated layered gabbro has a density of 3 059 kg/m^3, a magnetic susceptibility of 7 150 × 10^{-5} SI, a natural remanent magnetisation of 360 mA/m, and a Q-value of 0.12 (Fig. 28E).

Coarse grained, strongly deformed and veined metagabbro (Fig. 20C), has a density of 3 020 kg/m^3, a magnetic susceptibility of 580 × 10^{-5} SI, a natural remanent magnetisation of 198 mA/m, and a Q-value of 0.84 (Fig. 28F).

Ultramafic rocks were found in proximity of the lake Storsjön, Kvarnvik (Fig. 29). Two samples, 1 300 metres apart, have almost identical lithogeochemical compositions (Fig. 30). The ultramafic rock is high in MgO 26.1-25.6%, Cr 2 200-2 100 ppm, and Ni 1 025-1 040 ppm, respectively. The samples exhibit strong enrichment in Cs and Rb, possibly due to serpentinisation (Fig. 30B). The gravity map shows a very distinct positive anomaly located mostly beneath the lake Storsjön (Fig. 5), which suggests that a larger body of ultramafic and mafic rocks make up a potential layered intrusion.

The petrophysical properties of the two ultramafic samples are also almost identical, with a density of 2 796-2 800 kg/m^3, a magnetic susceptibility of 1 076-1 181 × 10^{-5} SI, a natural remanent magnetisation of 189-722 mA/m, and a Q-value of 0.43-1.51, respectively (Fig. 29C).



Figure 28. A. Gabbroid with veins and dykes of granite, both strongly deformed, (6444707/587271). **B.** Foliated gabbro, relatively plagioclase-rich, (6451475/580204). **C.** Gabbroid with granite, both deformed but may look massive perpendicular to lineation, (6447636/592547). **D.** Close-up of layered gabbro with light grey plagioclase-rich and black layers, both sulphide-bearing, weak foliation to massive, (6446100/578534). Photos: Dick Claeson. **E.** Sample of dark layered gabbro in D. used for petrophysical lab measurements. **F.** Sample of coarse-grained gabbro in Fig. 20C used for petrophysical lab measurements. Photos: Peter Hedin.

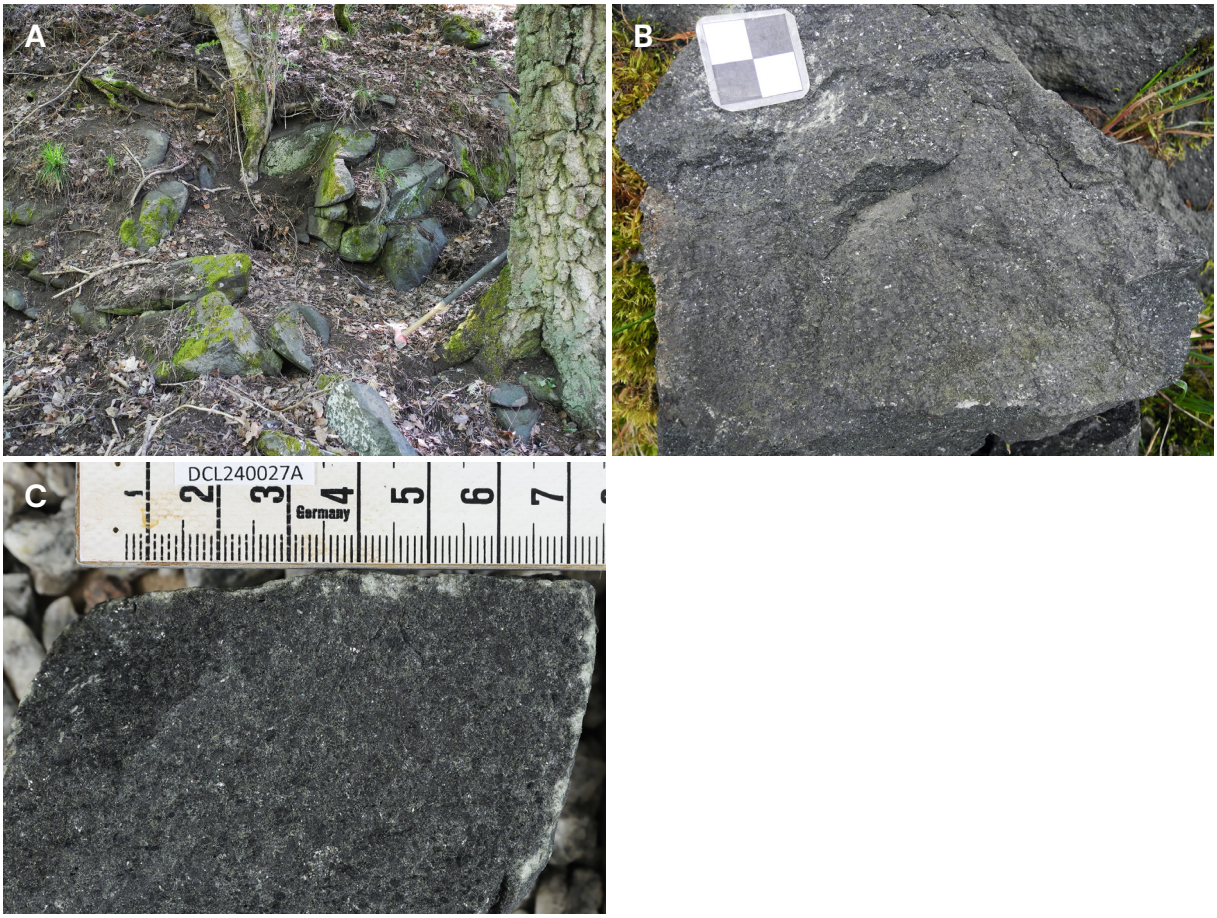

Figure 29. A. Ultramafic intrusive rock with mm-wide fissure fillings of carbonate mineral. Relatively prone to weathering (6450644/578846). **B.** Close-up of ultramafic intrusive rock from road cut (6451133/580041). Photos: Dick Claeson. **C.** Sample of ultramafic intrusive rock used for petrophysical lab measurements. Photo: Peter Hedin.

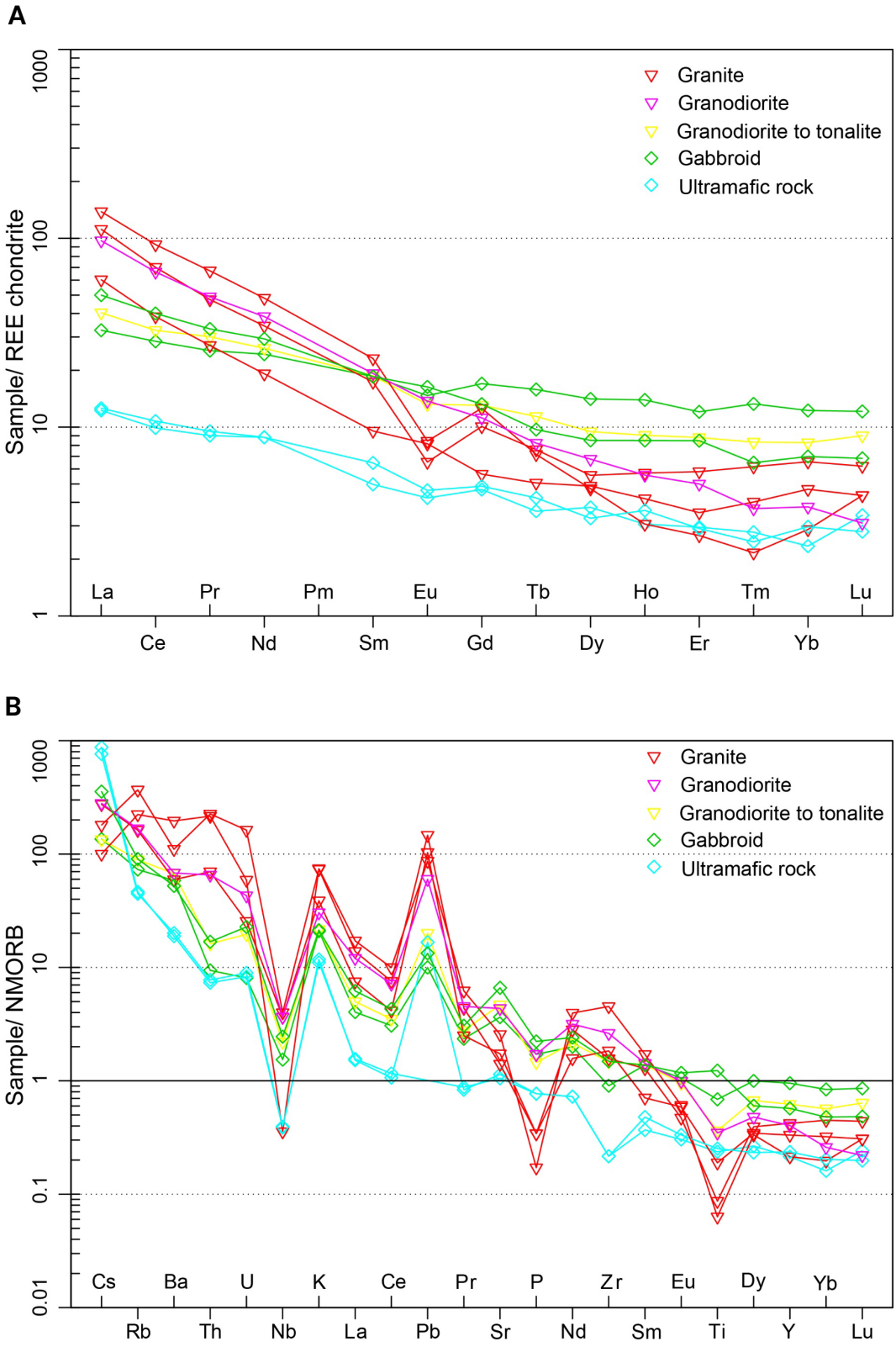

Figure 30. A. REE-spidergram of intrusive rocks from the Skrickerum project area. Normalisation values for chondrite Boynton (1984). **B.** N-MORB normalised spidergram of the same rocks, values Sun & McDonough (1989).

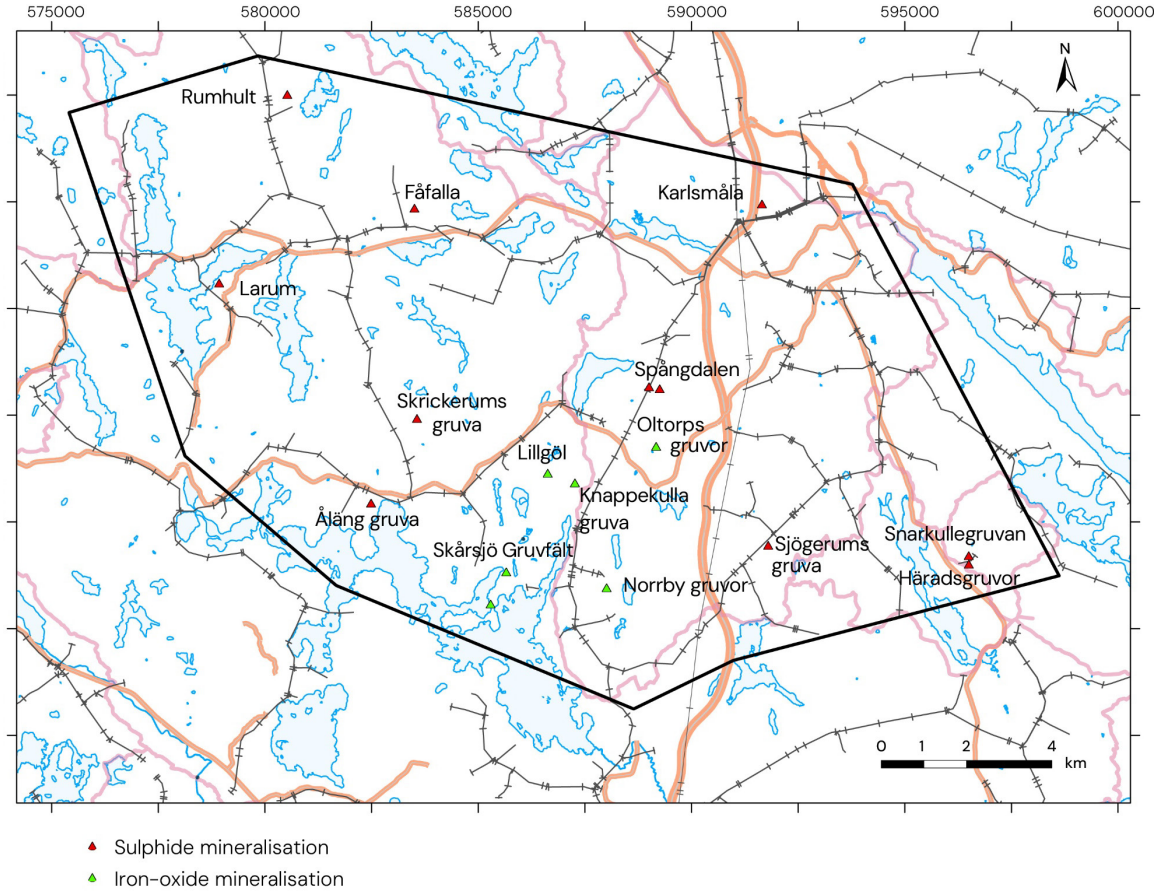

Figure 31. A. Locations of old mines and prospects mentioned in this publication.

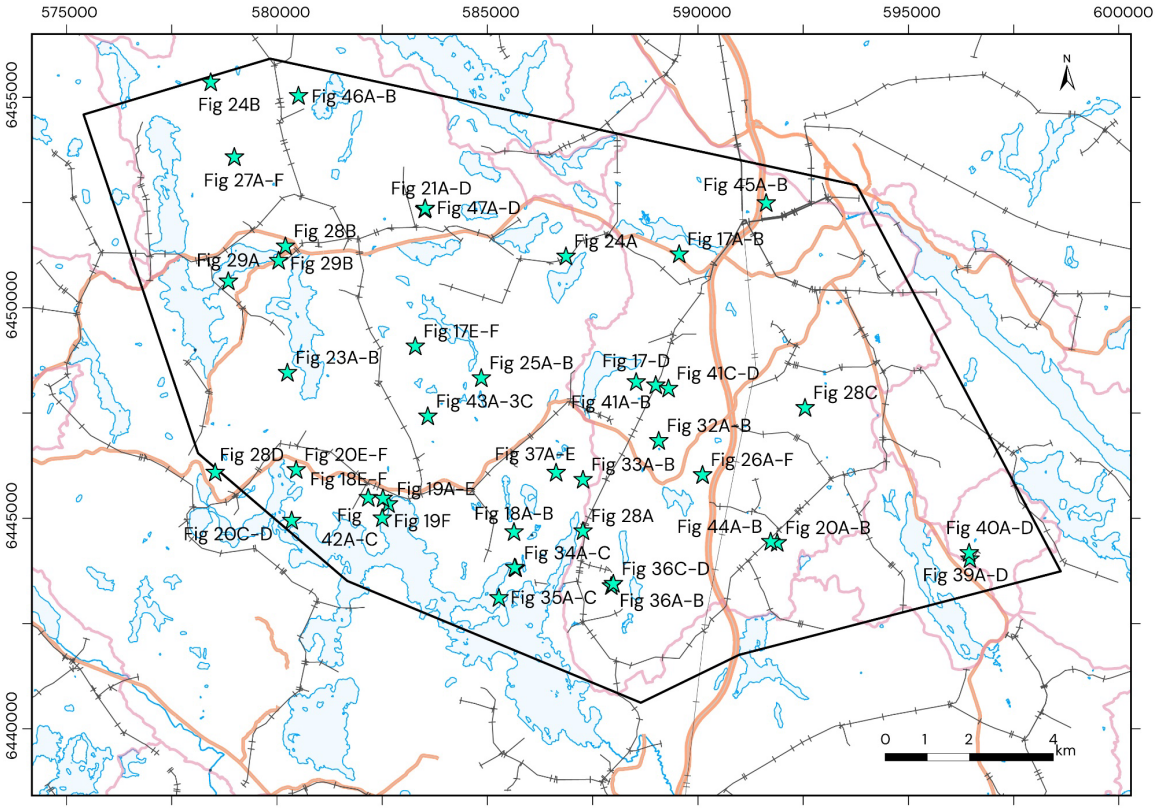

Figure 31. B. Locations of photos of rocks and mineralisations mentioned in this publication.

Iron mineralisations

Oltorps gruvor

The iron mines at Oltorp produced during the years 1843 to 1853 1 275 tonnes of iron ore (Bruun *et al.* 1995). There are five pits of different sizes, from west to east: 20 × 5 metres and 5 metres to water surface, 7 × 5 metres and 8 metres to water surface, 5 × 2 metres and water filled, 20 × 3 metres and 7 metres to water surface, and 2 × 2 metres and water filled (Fig. 32). Three more pits at a more southern location existed but are filled and buildings were built on top of them (Bruun *et al.* 1995). In outcrops decimetre wide layers of magnetite mineralised rock have the same orientation as the pits. The host rock is mainly a grey to reddish grey, fine-grained to finely medium-grained metavolcanic rock of intermediate to acid composition, which is intruded by a red granite. Note that the strike directions are uncertain due to the strong impact from the magnetite mineralised rocks on the compass in the mining area. The waste rock piles are mainly to the west of the pits and mostly consist of non-mineralised rocks but there are some strongly mineralised rocks as well that were sampled. The iron ore is magnetite and has minor garnet as skarn mineral. The rocks are foliated at 075/70.

The measured petrophysical properties of an iron oxide mineralised sample are a density of 3 514 kg/m^3, a magnetic susceptibility of 2.41 SI, a natural remanent magnetisation of 53 200 mA/m, a Q-value of 0.54, and a resistivity of 7.08 Ωm.

A lithogeochemical analysis of an iron oxide mineralised sample from the Oltorp gruvor reports 53.4% Fe_2O_3.

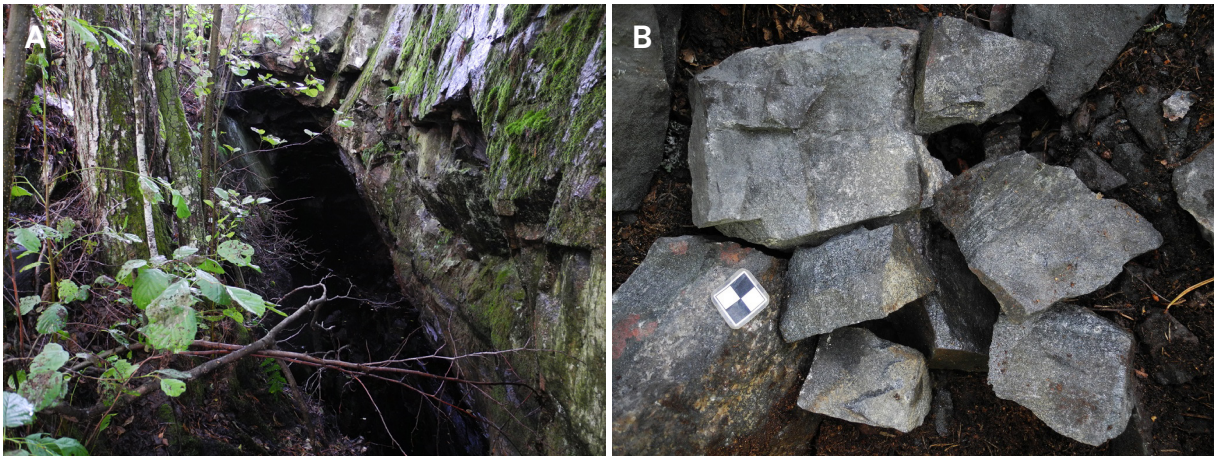

Figure 32. Oltorp gruvor. **A.** One of several pits, 20 × 3 m, oriented in the direction E–W. **B.** Sampled magnetite mineralisation (6446852/589071). Photo: Dick Claeson.

Knappekulla gruva

The mine Knappekulla gruva is 5 × 8 metres and has 4 to 5 metres to the water surface (Fig. 33). The iron oxide mineralisation is hosted in a basaltoid rock with skarn, mostly garnet and quartz. The layers of iron oxide rock are conformable with the basaltoid layering and foliation (Fig. 33). Pegmatite to granite occurs as veins and dykes, and all are foliated.

The measured petrophysical properties of an iron oxide mineralised sample are density 3 661 kg/m^3, magnetic susceptibility 6.17 SI, a natural remanent magnetisation of 52 000 mA/m, a Q-value of 0.21, and a resistivity of 7.34 Ωm (Fig. 32C).

A lithogeochemical analysis of an iron oxide mineralised sample from the Knappekullagruva reports 44.0% Fe_2O_3.

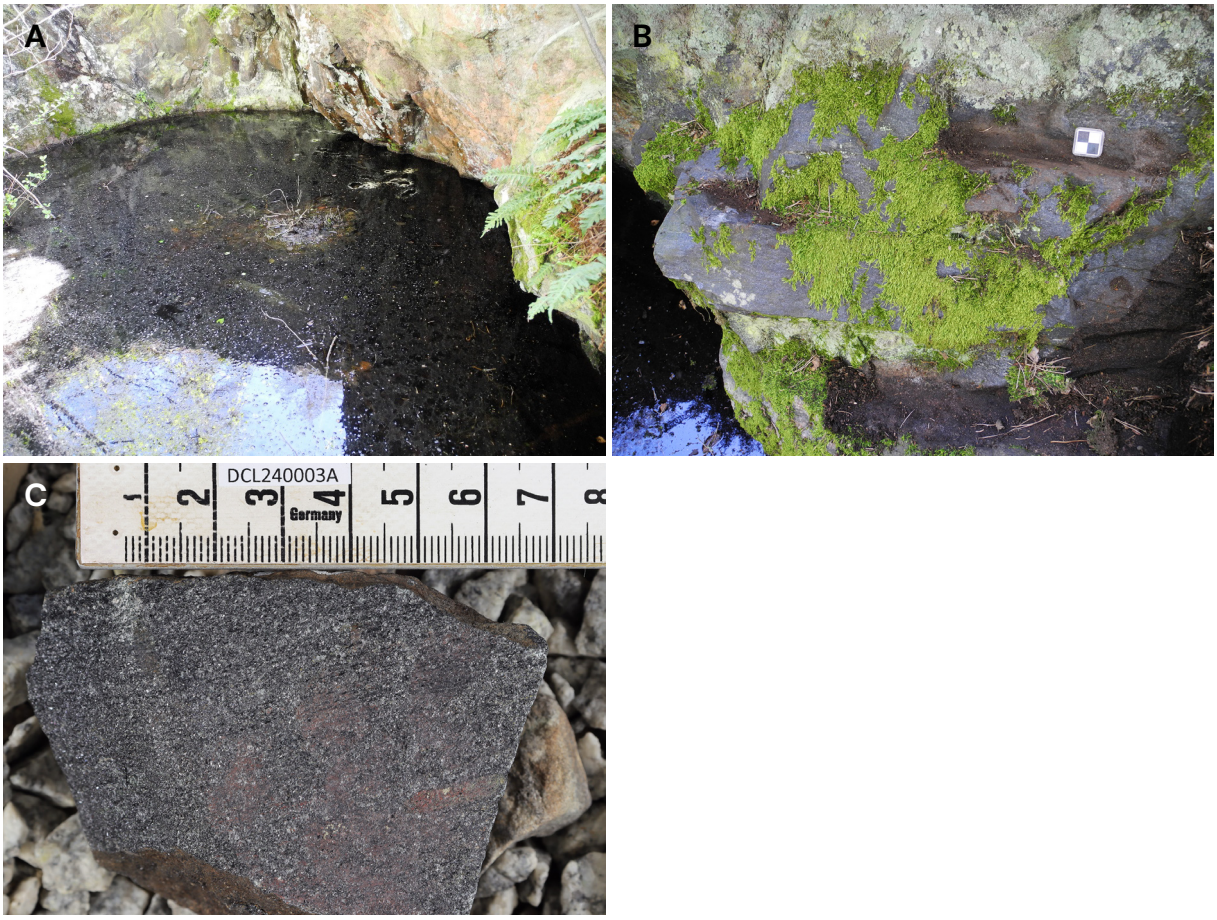

Figure 33. A. Knappekulla gruva pit, 5 × 8 and 4–5 metres to the water surface. **B.** Layers of iron-oxide mineralisation are conformable with basaltoid layers (6445928/587273). Photos: Dick Claeson. **C.** Sample of iron-oxide mineralised rock used for petrophysical lab measurements. Photo: Peter Hedin.

Skårsjö Gruvfält

In the Skårsjö Gruvfält north there are three pits in an iron oxide mineralisation. From the north a pit that is 30 to 35 × 10 metres, with 7 to 10 metres to the water surface, is striking N40E (Fig. 34). Roughly in this direction follows to the south a pit that is 10 × 4 metres, with 3 metres to the water surface, and a pit of 25 × 8 metres, with 5 metres to the water surface. A fourth pit is present north of these and strikes at N20W, has a size of 12 × 5 metres, with an outcrop of a couple of metres, that narrows to a width of 6 to 7 × 4 metres. The ordinary compass is seriously compromised by the magnetic properties of the iron oxide mineralisation in the area, so the built-in compass of the telephone was used instead and controlled by using the sun and time of day. Large amounts of waste rock are dumped to the west, but relatively few pieces from the proper iron mineralisation were found among them. Layers of iron mineralised rock with undulating contacts occur in the volcanic host rock in outcrops at the northernmost pit (Fig. 34). Skarn, garnet, and coarse-grained pyroxene is present in the host basaltoid to andesitoid rock. An undeformed, massive, young granite with fresh megacrysts of potassium feldspar occurs as dykes in the volcanic rocks.

The measured petrophysical properties of an iron oxide mineralised sample are a density of 3 664 kg/m^3, a magnetic susceptibility of 4.82 SI, a natural remanent magnetisation of 7 847 mA/m, a Q-value of 0.04, and a resistivity of 7.57 Ωm (Fig. 34C).

A lithogeochemical analysis of an iron oxide mineralised sample from the Skårsjögruvan norr 1 reports 47.3% Fe_2O_3.



Figure 34. Skårsjö Gruvfält, north. **A.** Pit is 30–35 × 10 m, 7 to 10 m to water surface, striking N40E (6443825/585672). **B.** Undulating contact between layers of basaltoid-andesitoid and iron-oxide mineralisation in outcrop (6443840/585648). Photos: Dick Claeson. **C.** Sample of iron-oxide mineralised rock used for petrophysical lab measurements. Photo: Peter Hedin.

At Skårsjö Gruvfält south, also known as Skårsjöviksgruvorna, there are three pits: from north a 25 × 15 metres pit, with 10 to 12 m to the water surface, striking 035/60, followed by a shallow 7 × 3 metres, 1-1½ metre deep pit, and further to the south an 8 × 5 metres pit, with 3 to 4 m to the water surface. The waste rock has been dumped to the west. The waste rock is mostly basaltoid-andesitoid with varying degrees of magnetite and few iron-oxide mineralised rocks occur (Fig. 35). Skarn, garnet, quartz, and calcite, where some portions have euhedral calcite crystals, are present (Fig. 35). The garnet is reddish brown and up to 20 mm in diameter. The outcrops are dominated by basaltoid-andesitoid with minor pegmatite.

The measured petrophysical properties of an iron-oxide mineralised sample are a density of 3 603 kg/m^3, a magnetic susceptibility of 4.02 SI, a natural remanent magnetisation of 334 000 mA/m, a Q-value of 2.04, and a resistivity of 10.3 Ωm (Fig. 35C).

A lithogeochemical analysis of an iron-oxide mineralised sample from the Skårsjö Gruvfält south reports 49.0% Fe_2O_3 and another analysis of parts dominated by skarn, garnet, and magnetite reports 466 ppm (186+280) REE+Y, 92 ppm HREE (Er-Lu). The skarn-garnet sample stands out in the REE spidergram for the MREE and HREE compared to the iron-oxide mineralised samples but not so much in the pattern of the N-MORB normalised spidergram (Fig. 38).

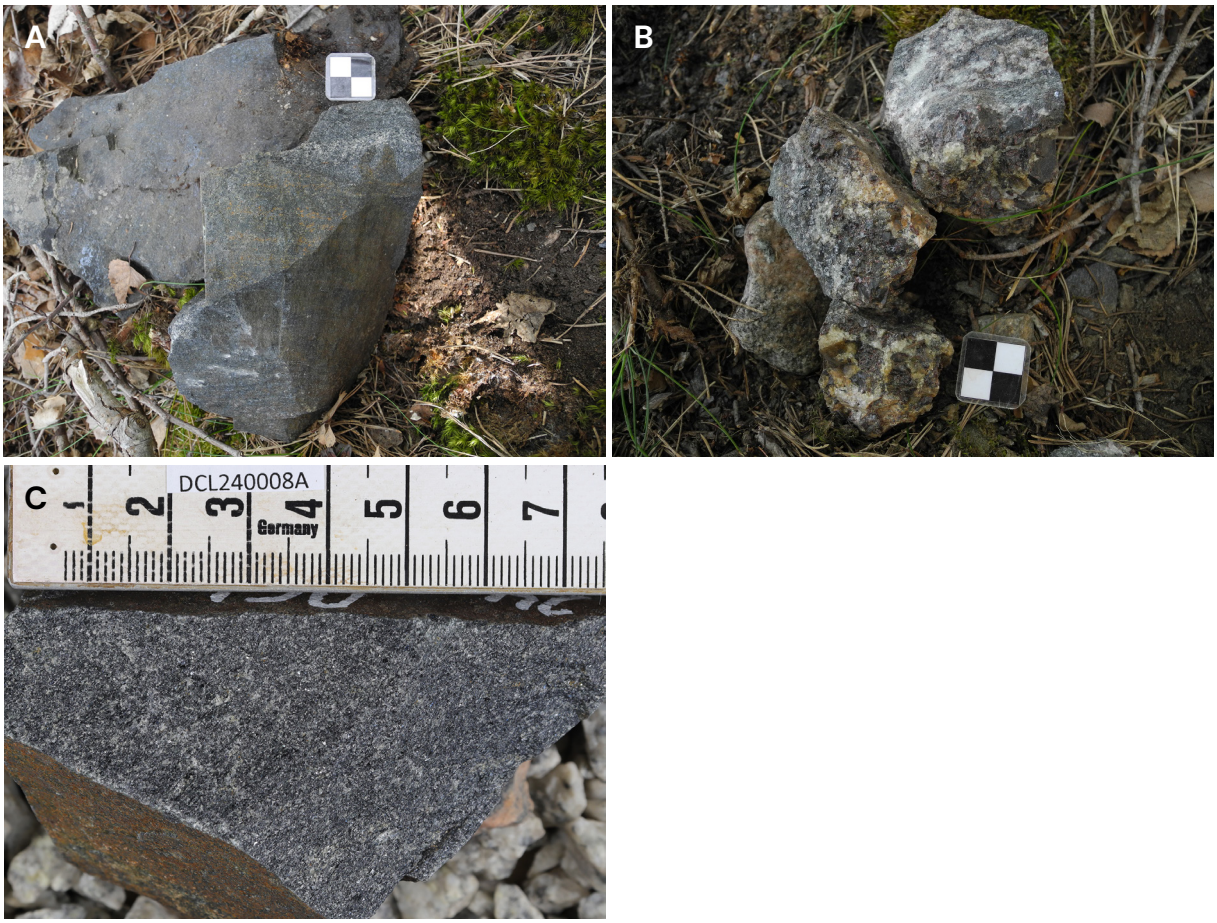

Figure 35. Skårsjö Gruvfält, south. **A.** Close-up of magnetite-rich rock. **B.** Skarn with garnet and magnetite, rich in HREE (6443120/585275). Photos: Dick Claeson. **C.** Sample of iron oxide mineralised rock used for petrophysical lab measurements. Photo: Peter Hedin.

Norrby gruvor

The western pit at Norrby gruvor, also known as Gölsveden or Gruvberget, is 15 × 4 metres, has 4 to 7 metres to the water surface and a NE-SW strike (Fig. 36A). Waste rock piles to the west of the pit contain some iron-oxide-rich rocks (Fig. 36B). Magnetite mineralised layers, several decimetres wide and steeply dipping, are observed at outcrops. Magnetite layers at outcrops outside of the pit area have a different strike than at the pit, layering at 350/75 and 045/45 respectively, possibly indicating a fold or even its hinge. The iron oxide mineralisation is hosted by an acid to intermediate metavolcanic rock, which is intruded by granite dykes. Skarn with dominance of magnetite, garnet, calcsilicate minerals, and amphibole was observed.

The measured petrophysical properties of an iron oxide mineralised sample are a density of 3 547 kg/m^3, a magnetic susceptibility of 1.12 SI, a natural remanent magnetisation of 85 000 mA/m, a Q-value of 1.88, and a resistivity of 21.8 Ωm.

A lithogeochemical analysis of an iron-oxide mineralised sample from the Norrby gruvor, western pit reports 54.4% Fe_2O_3.



Figure 36. A. Norrby gruvor, western pit. **B.** Iron-oxide mineralised sample for analysis (6443403/587944). **C.** Norrby gruvor, eastern pit. **D.** Layers of iron-oxide mineralisation in basic to intermediate volcanic rocks with foliated granite dykes (6443457/587993). Photo: Dick Claeson.

The eastern pit at Norrby gruvor is 20 × 5 metres, has a few decimetres to 2 metres to the water surface and a NW–SE strike (Fig. 36C). At the surface the pit appears to have been more or less vertically mined. Large amounts of waste rock, c. 30 × 15 × 5 metres, are dumped to the SW of the pit. Layers of magnetite in the outcrop to the west of the pit are oriented 040/62 with possible minor misreading of the compass due to magnetite-rich rocks (Fig. 36D). Around the pit are outcrops of andesitoid to basaltoid, probably the host rock, with dykes of foliated granite. Skarn with dominance of magnetite, garnet, calcsilicate minerals, and amphibole was observed.

The measured petrophysical properties of an iron oxide mineralised sample are a density of 3 558 kg/m^3, a magnetic susceptibility of 1.93 SI, a natural remanent magnetisation of 236 000 mA/m, a Q-value of 3.02, and a resistivity of 7.9 Ωm.

A lithogeochemical analysis of an iron oxide mineralised sample from the Norrby gruvor, eastern pit reports 55.9% Fe_2O_3.

Lillgöl prospect

An 8 × 8 metres pit, with 1 to 3 metres to the water surface, occurs c. 350 metres south of Lillgöl. The mineralisation has a strike of 60 and dip of 80 degrees. The iron mineralisation consists of magnetite and relatively large amounts of skarn, mostly garnet, up to 50% in parts (Fig. 37). The garnet is reddish brown to brownish red, with mm-sized to several cm large aggregates. Amphibole and quartz are common among the skarn minerals, quartz is often found as large masses and amphibole as stripes. The host rock is a granitic gneiss with foliation at 060/80.

The Lillgöl occurrence is the only analysed iron oxide mineralisation with high manganese content in the Skrickerum project area. The sample had 39.8% Fe_2O_3 and 5.98% MnO. The elements Cs, Rb, Th, U, and Zr are enriched in the Mn-rich Lillgöl sample compared to the other iron-oxide mineralisations in the area (Fig. 38). The high manganese content indicates that the garnet could be of spessartine-rich composition. Even though the Knappekulla gruva is located only c. 600 m to the east, it has negligible manganese content and only minor skarn in the form of garnet and quartz was observed there. The measured petrophysical properties of an iron oxide mineralised sample with minor skarn are a density of 3 702 kg/m^3, a magnetic susceptibility 0.781 SI, a natural remanent magnetisation of 4 980 mA/m, and a Q-value of 0.16 (Fig. 37E).



Figure 37. Lillgöl pit. **A.** Magnetite mineralisation with stripes of amphibole. **B.** Magnetite mineralisation with bands of garnet. **C.** Magnetite mineralisation with around 50% garnet disseminated throughout. **D.** Skarn with garnet, quartz, and magnetite (6446096/586633). Photos: Dick Claeson. **E.** Sample used for petrophysical lab measurements. Photo: Peter Hedin.

To sum up, the lithogeochemical analyses of iron mineralisations in the Skrickerum project area suggest that all are mainly iron oxide, part from Lillgöl with anomalous manganese, and for the most part have very low abundance of sulphide minerals. Skarn parts have elevated HREE+Y concentrations, probably due to garnet in the skarn (Fig. 38).

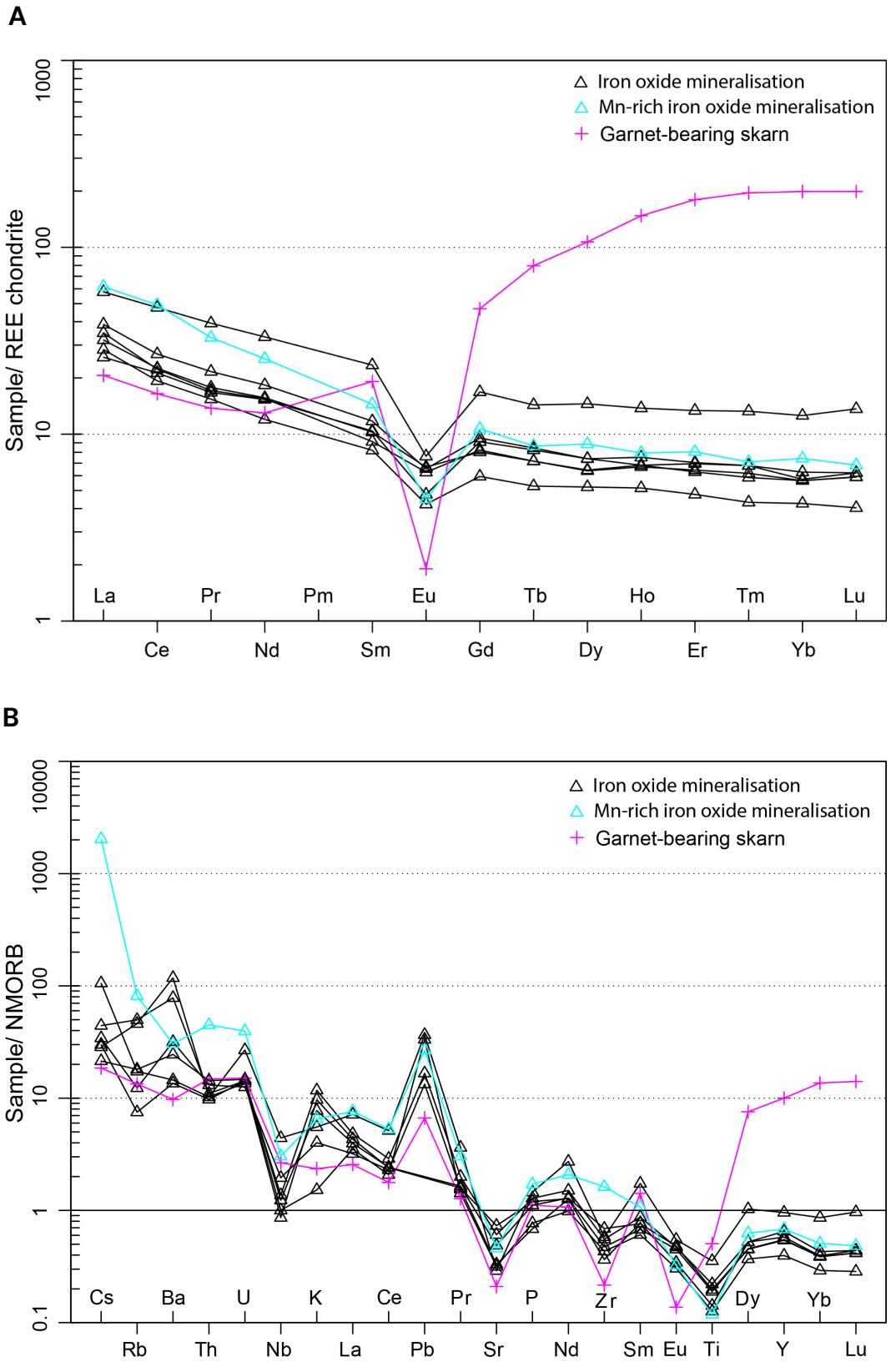

Figure 38. A. REE-spidergram of iron-oxide mineralisations and an associated garnet-bearing skarn from the Skrickerum project area. Normalisation values for chondrite Boynton (1984). **B.** N-MORB normalised spidergram of the same rocks, values Sun & McDonough (1989).

Sulphide mineralisations

Häradsgruvor and Snarkullegruvan

Earlier work state that the Häradsgruvor and Snarkullegruvan were mainly processed during the 1870s and some mine profiles and mine maps are reported (Tegengren 1924, Bruun *et al.* 1995). According to the mine maps, the Häradsgruvorna is 68 metres deep and the Snarkullegruvan only 7 metres (Tegengren 1924). The combined ore production is reported at 5 340 tonnes (Tegengren 1924). The original waste rock pile was much larger according to the information sign at the location and it states that most was used for road construction during the 1930s and infilling of the harbour of Valdemarsvik in the 1980s (Fig. 39A). In the mineralised waste rock chalcopyrite, pyrrhotite, and galena were identified (Fig. 39). The host rock is a basic metavolcanic rock with calciferous skarn. The rocks are foliated at 060/72.

The measured petrophysical properties of a sulphide mineralised sample from Häradsgruvorna are a density of 2 984 kg/m^3, a magnetic susceptibility of 314 × 10^{-5} SI, a natural remanent magnetisation of 2 070 mA/m, a Q-value of 16.3, and a resistivity of 264 Ωm.

A lithogeochemical analysis of a sulphide mineralised sample from Häradsgruvorna reports Cu 1.15%, S 2.66%, Au 0.16 ppm, Ag 4.5 ppm, Bi 11 ppm, Se 16 ppm, and Te 2.6 ppm.



Figure 39. Häradsgruvor. **A.** Information sign about copper mine Häradsgruvor. **B.** One of three shafts. **C.** What is left of the waste rock pile. **D.** Typical piece of sampled sulphide mineralised rock with chalcopyrite, pyrrhotite, and rare galena present (6444044/596463). Photo: Dick Claeson.

The Snarkullegruvan measures 6 × 4 metres, with c. 7 metres to the water surface (Fig. 40). The waste rock is west of the pit. The sulphide mineralised rocks have chalcopyrite, pyrrhotite, and malachite. The host rock is a basaltoid with minor amphibole porphyroblasts and some calciferous skarn. The basaltoid is folded, with a fold axis oriented 170/50 and foliated in the direction 310/60. To the east, thick layers of intermediate metavolcanic rock appear and has decimetre wide layers of basaltoid. The intermediate metavolcanic rock is severely partially melted and veined, with a migmatitic structure, and is deformed displaying both S- and Z-folds (Fig. 40). A foliation in the intermediate metavolcanic rock is oriented 345/73.

The measured petrophysical properties of a sulphide mineralised sample from the Snarkullegruvan are a density of 3 021 kg/m^3, a magnetic susceptibility of 62 × 10^{-5} SI, a natural remanent magnetisation of 38.2 mA/m, and a Q-value of 1.52.

A lithogeochemical analysis of a sulphide mineralised sample from the Snarkullegruvan reports Cu 2.65%, S 3.64%, Au 0.23 ppm, Ag 15.5 ppm, Bi 21 ppm, Se 22 ppm, and Te 2.6 ppm.

The measured petrophysical properties of a basaltoid host rock at the Snarkullegruvan are a density of 2 943 kg/m^3, a magnetic susceptibility of 50 × 10^{-5} SI, a natural remanent magnetisation of 23.9 mA/m, and a Q-value of 1.52.



Figure 40. A. Snarkullegruvan 6 × 4 metres, c. 7 m to water surface. **B.** Sampled sulphide mineralised rock with chalcopyrite, pyrrhotite, and malachite. **C.** Basaltoid host rock and andesitoid strongly deformed and veined. **D.** Close-up of skarn-bearing basaltoid host rock (6444191/596445). Photo: Dick Claeson.

Spångdalen

The Spångdalen western pit strikes NE-SW and is 35 to 40 metres by 2 to 10 metres wide, with at most 5 metres to the water surface (Fig. 41A). The depth is more than 11 metres according to earlier measurements done by SGU (Bruun *et al.* 1995). Waste rock is scattered around in the terrain with some rock piles indicating hand-dressing at the site. Ore minerals are chalcopyrite and pyrrhotite (Fig. 41B). The copper mineralisation is hosted in a andesitoid to basaltoid, where the mineralised parts are severely altered with both garnet and quartz along with the ore minerals. All rocks within the outcrop area contain garnet to varying extents. A foliation observed in the area is oriented 055/78.

A lithogeochemical analysis of a sulphide mineralised sample from the Spångdalen western pit reports Cu 4.26%, S 5.05%, Au 0.229 ppm, Ag 21 ppm, Bi 14.2 ppm, Te 2.1 ppm, Se 45.7 ppm, REE+Y 547 (512+35) ppm, probably not from apatite since only 0.11% P_2O_5 was reported. The anomalous gold, silver, and REE has not been noted before.

The measured petrophysical properties of a sulphide mineralised sample are a density of 2 918 kg/m^3, a magnetic susceptibility of 48 × 10^{-5} SI, a natural remanent magnetisation of 20.4 mA/m, and a resistivity of 75 000 Ωm.

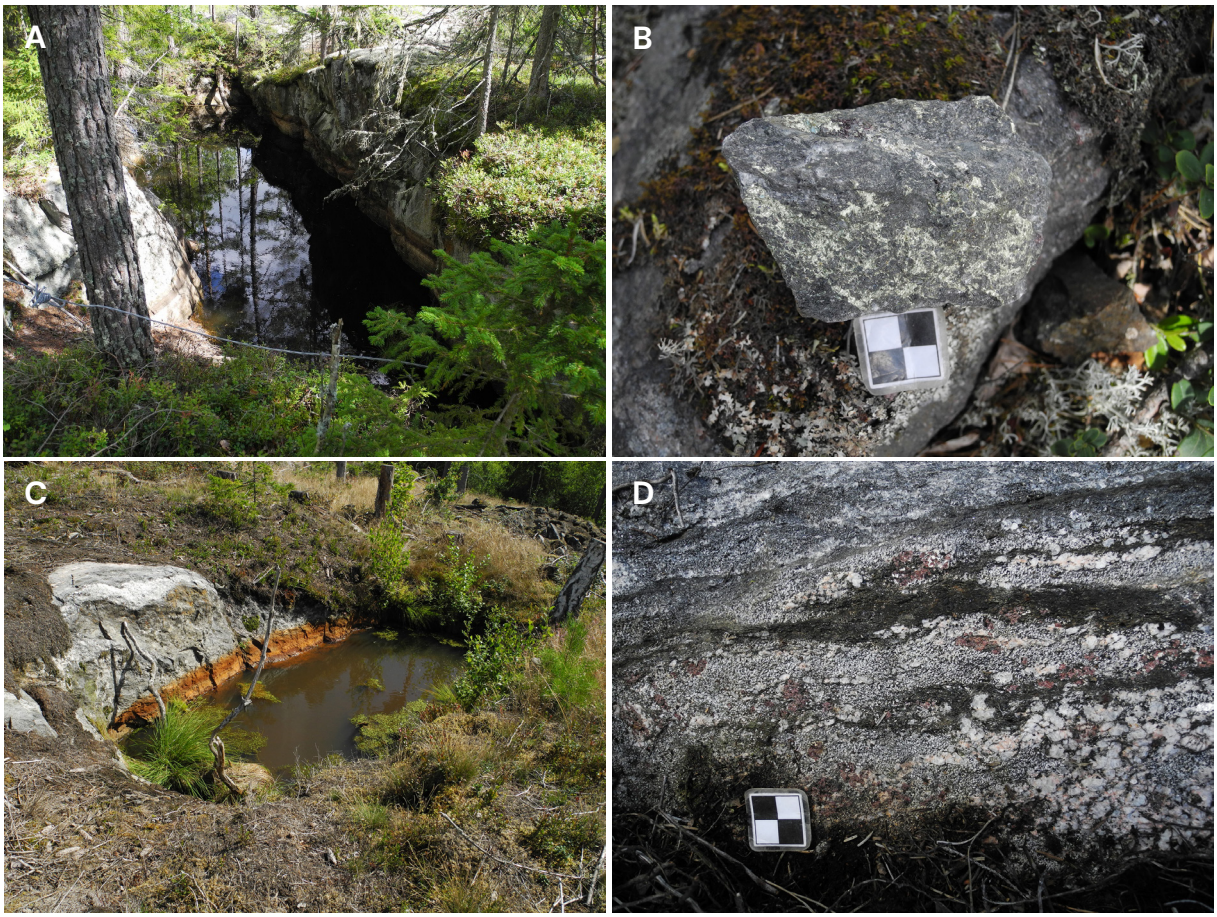

Figure 41. A. Spångdalen western pit, part of pit in NE-SW direction, 35–40 m × 2 to 10 m wide. **B.** Andesitoid to basaltoid with rich impregnation of chalcopyrite (6448174/589000). **C.** Spångdalen eastern pit 6 × 2.5 metre. **D.** Close-up of bedrock surface in C. with basaltoid to andesitoid metavolcanic rock and light grey, medium-grained to pegmatitic metagranite, all rocks garnet-bearing (6448095/589304). Photo: Dick Claeson.

The Spångdalen eastern pit is 6 × 2.5 metres and earlier measured by SGU to 3 m depth (Bruun *et al.* 1995, Fig. 41C). The waste rock is very poor in mineralised rocks so no effort to a lithogeochemical sampling was performed. The copper mineralisation consists of chalcopyrite, pyrrhotite, and pyrite and is hosted in a basic to intermediate metavolcanic rock (Fig. 41D). A light grey, medium-grained to pegmatitic metagranite occurs as dykes and veins. All rocks at the outcrop are garnet-bearing and severely deformed, with a foliation oriented 130/80.

An earlier lithogeochemical analysis indicated that the mineralised rock was gold and silver anomalous (Bruun *et al.* 1995).

Åläng gruva

The Åläng gruva was first claimed by Åtvidabergs kopparverk in the year 1776 (Tegengren 1924). The pit is water filled and is asymmetric at the surface with dimensions 20 to 25 by 15 to 20 metres, one could possibly call it semi-circular (Fig. 42A). A small exploration pit 2 × 2 metres and 1 metre deep occurs c. 20 metres west of the pit. Most of the waste rock from the mine is dumped to the south and southwest of the pit and consists of large cobbles and boulders that lack mineralised portions. Some of them had relatively well mineralised parts and were used for sampling. Disseminations of sulphide minerals and fracture fillings consist mostly of chalcopyrite and pyrite. The host rock is a garnet-bearing basaltoid to andesitoid metavolcanic rock (Fig. 42B).



Figure 42. Åläng gruva. **A.** Asymmetrical pit 20–25 × 15–20 metres. **B.** Dissemination of chalcopyrite and pyrite in garnet-bearing basaltoid metavolcanic rock (6445485/582520). Photos: Dick Claeson. **C.** Sample used for petrophysical lab measurements. Photo: Peter Hedin.

A lithogeochemical analysis of a sulphide mineralised sample from the Åläng gruva reports Cu 0.98%, Au 0.07 ppm, Ag 7.64 ppm, Bi 3.28 ppm, Se 12.4 ppm, and Te 1.73 ppm. An earlier lithogeochemical analysis indicated that the mineralised rock was gold and silver anomalous (Bruun *et al.* 1995).

The measured petrophysical properties of a sulphide mineralised sample are a density of 3 185 kg/m^3, a magnetic susceptibility of 800 × 10^{-5} SI, a natural remanent magnetisation of 1 530 mA/m, a Q-value of 4.70, and a resistivity of 23.2 Ωm (Fig. 42C).

Skrickerums gruva

The Skrickerums gruva was mined for copper from 1779 to 1784 and 1826 to 1835 (Bruun *et al.* 1995). The copper ore was around a metre wide and consisted of chalcopyrite and bornite, and the mine pit is 5 × 4 metres and 28 metres deep (Bruun *et al.* 1995, Fig. 43A). In the year 1818 interest in the mine was renewed due to Berzelius discovery of the element selenium at Falu gruva (Bruun *et al.* 1995). In 1873 the electrical engineer Willoughby Smith found that the electrical conductivity of grey selenium was affected by light, which led to its use as a cell for sensing light (Smith 1873). The first commercial products using selenium were developed by Werner Siemens in the mid-1870s. The selenium cell was used in the photophone developed by Alexander Graham Bell in 1879. Selenium transmits an electric current proportional to the amount of light falling on its surface. This phenomenon was used in the design of light meters and similar devices. The new technical achievements meant that the carbonate vein deposit, dyke-formed and runs through the copper ore, was mined for selenium from 1898 to 1899 and from 120 tonnes of rock, 12 tonnes of selenium ore with a Se-grade of 1% was achieved (Bruun *et al.* 1995). In particular, three selenium ore minerals were recovered at Skrickerum, eucairite CuAgSe, berzelianite Cu_2Se, and crookesite $(Cu,Tl,Ag)_2Se$ (Bruun *et al.* 1995). Several other rare minerals have been reported from Skrickerum, e.g., selenojalpaite Ag_3CuSe_2 and Te-Cu-rich sudburyite (Pd,Cu)(Sb,Te,Se,S) by Bindi & Pratesi (2005) and Jonsson *et al.* (2014), respectively.

In the mining area and in the waste rock pile basaltoid to andesitoid and granitic gneiss is commonly observed. A lithogeochemical analysis of waste rock had 3.92% S but weak concentrations of Cu, Pb, and Zn, consistent with predominantly pyrrhotite and pyrite in the sampled andesitoid (Fig. 43B).

The measured petrophysical properties of a sulphide mineralised andesitoid sample are a density of 2 931 kg/m^3, a magnetic susceptibility of 2 080 × 10^{-5} SI, a natural remanent magnetisation of 75.6 mA/m, a Q-value of 0.90, and a resistivity of 683 Ωm (Fig. 43C).



Figure 43. Skrickerum gruva. **A.** Vertical entrance to pit. **B.** Mostly pyrrhotite and pyrite in the sampled andesitoid (6447436/583585). Photos: Dick Claeson. **C.** Sample used for petrophysical lab measurements. Photo: Peter Hedin.

Sjögerums gruva, Silvermossens gruva

The Sjögerums gruva, also known as Silvermossens gruva, is 10 × 5 metres and 3 metres deep (Fig. 44A). The pit strikes NNW-SSE. The Zn-Cu mineralisation is hosted in a grey to dark grey gneiss, probably of an andesitoid origin (Fig. 44B). In several of the rock pieces in the waste pile south of the pit, chalcopyrite, sphalerite, and pyrrhotite is commonly observed. The lithogeochemical analysis indicates that a lot of the sulphur is in pyrrhotite. A definitely greenish feldspar is present as megacrysts in most rock pieces and since the calcium content of the rock is low at 0.58% and potassium at 2.83%, a potassium feldspar is probable. The host rocks are foliated at 335/68.

A lithogeochemical analysis of a sulphide mineralised sample from the Sjögerum gruva reports Zn 1.28%, Fe_2O_3 22.6%, S 10.1%, Au 0.10 ppm, Cu 884 ppm, Ag 12.3 ppm, Cd 46 ppm, Se 28 ppm, and Tl 3.55 ppm.

The measured petrophysical properties of a sulphide mineralised gneiss-andesitoid sample are a density of 2 971 kg/m^3, a magnetic susceptibility of 2 063 × 10^{-5} SI, a natural remanent magnetisation of 3 370 mA/m, a Q-value of 4.03, and a resistivity of 87.5 Ωm.

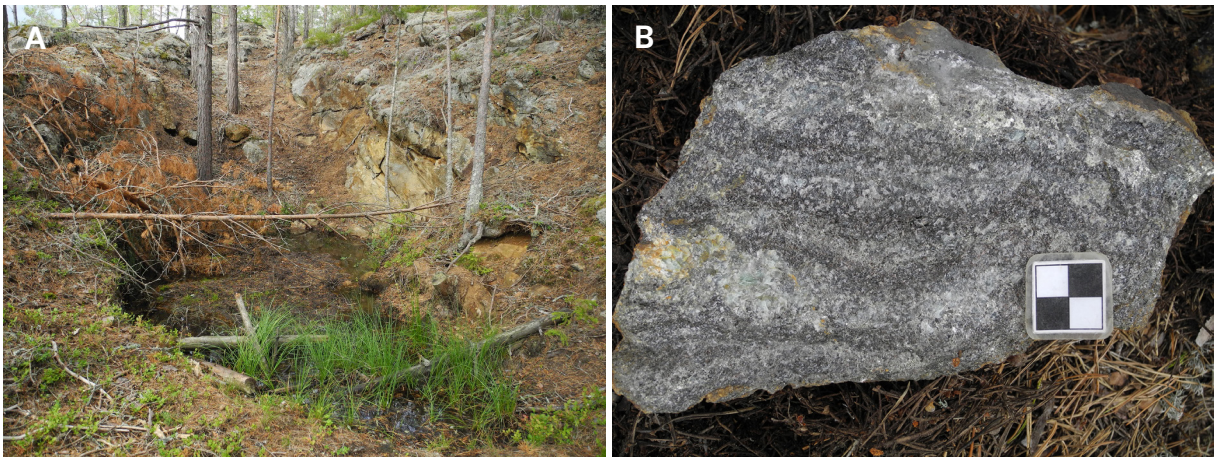

Figure 44. Sjögerum, Silvermossens gruva. **A.** Pit in andesitoid with Zn–Cu sulphide mineralisation. **B.** Andesitoid with sphalerite, pyrrhotite, and chalcopyrite. Megacrysts of feldspar (6444456/591731). Photo: Dick Claeson.

Karlsmåla prospect

A 10 × 3 metres large pit with an estimated depth of 6 metres is present c. 400 metres northeast of Karlsmåla. The waste rock is distributed west of the pit. The host is a strongly altered basaltoid volcanic rock that contains sulphide and magnetite mineralised portions. Among the waste rock are large lumps of pyrrhotite and magnetite (Fig. 45A). Chalcopyrite occurs both as dissemination and smaller lumps or aggregates (Fig. 45B). Most of the outcrop surrounding the pit consists of a metamorphosed, foliated reddish grey to greyish red, even-grained, medium- to coarse-grained granite. Several types of basic and intermediate metavolcanic rocks are present some tens of metres from the pit. The prospect has the characteristics of a Ni-Cu-Au deposit with elevated content of Co, Pd, Re, Se, and Te.

The analysed lithogeochemical sample consisted of a mix of pyrrhotite lumps, magnetite lumps, and more ordinary sulphide-mineralised basaltoid and the analysis reported Cu 1.56%, Ni 1 650 ppm, Au 0.157 ppm, Co 599 ppm, Pd 0.063 ppm, Re 0.038 ppm, Se 32.7 ppm, and Te 3.96 ppm.

The measured petrophysical properties of a sulphide and magnetite mineralised basaltoid sample are a density of 3 497 kg/m^3, a magnetic susceptibility of 25 000 × 10^{-5} SI, a natural remanent magnetisation of 701 000 mA/m, a Q-value of 68.9, and a resistivity of 9.21 Ωm (Fig. 45C).

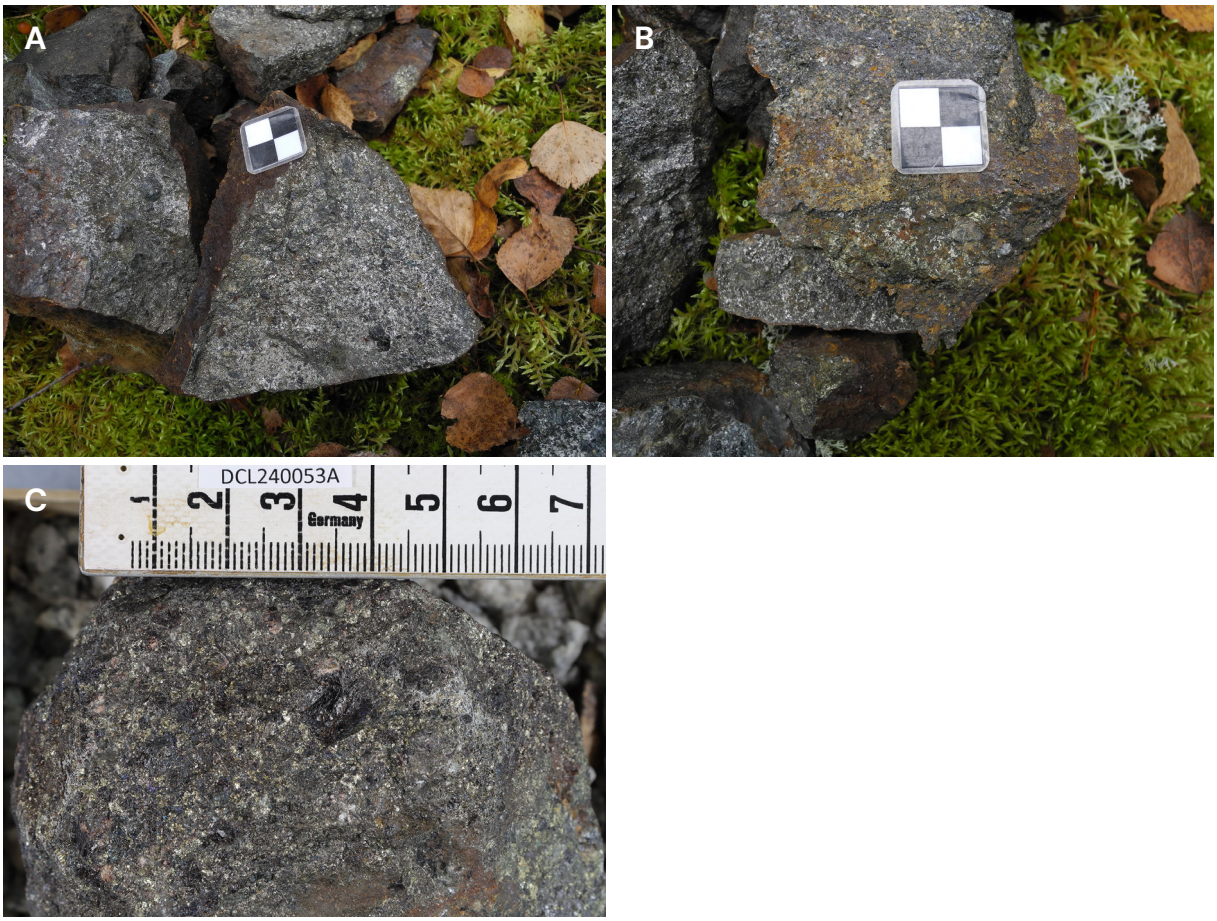

Figure 45. A. Lumps of mostly pyrrhotite in basaltoid. **B.** Chalcopyrite as lumps and dissemination in pyrrhotite- and magnetite-rich basaltoid (6452503/591624). Photos: Dick Claeson. **C.** Sample used for petrophysical lab measurements. Photo: Peter Hedin.

Rumhult prospect

The Rumhult prospect is 6 × 3 metres large and had 3 metres to the water surface when visited (Fig. 46A). The pit and contact of the basaltoid strike 190 and the dip of the basaltoid is almost vertical at 88 degrees. The waste rock is towards the east, next to a cultivated field. Rare granite dykes occur. The sulphide mineralised parts of the altered basaltoid have pyrrhotite, chalcopyrite, and pyrite (Fig. 46B). The basaltoid waste rock with sulphide present was collected for lithogeochemical analysis, which resulted in Cu 0.33%, Fe_2O_3 25.7%, S 8.32%, and elevated Co 183 ppm.

The measured petrophysical properties of a sulphide mineralised basaltoid sample are a density of 3 064 kg/m^3, a magnetic susceptibility of 4 544 × 10^{-5} SI, a natural remanent magnetisation of 17 700 mA/m, a Q-value of 9.59, and a resistivity of 36.5 Ωm (Fig. 46C).

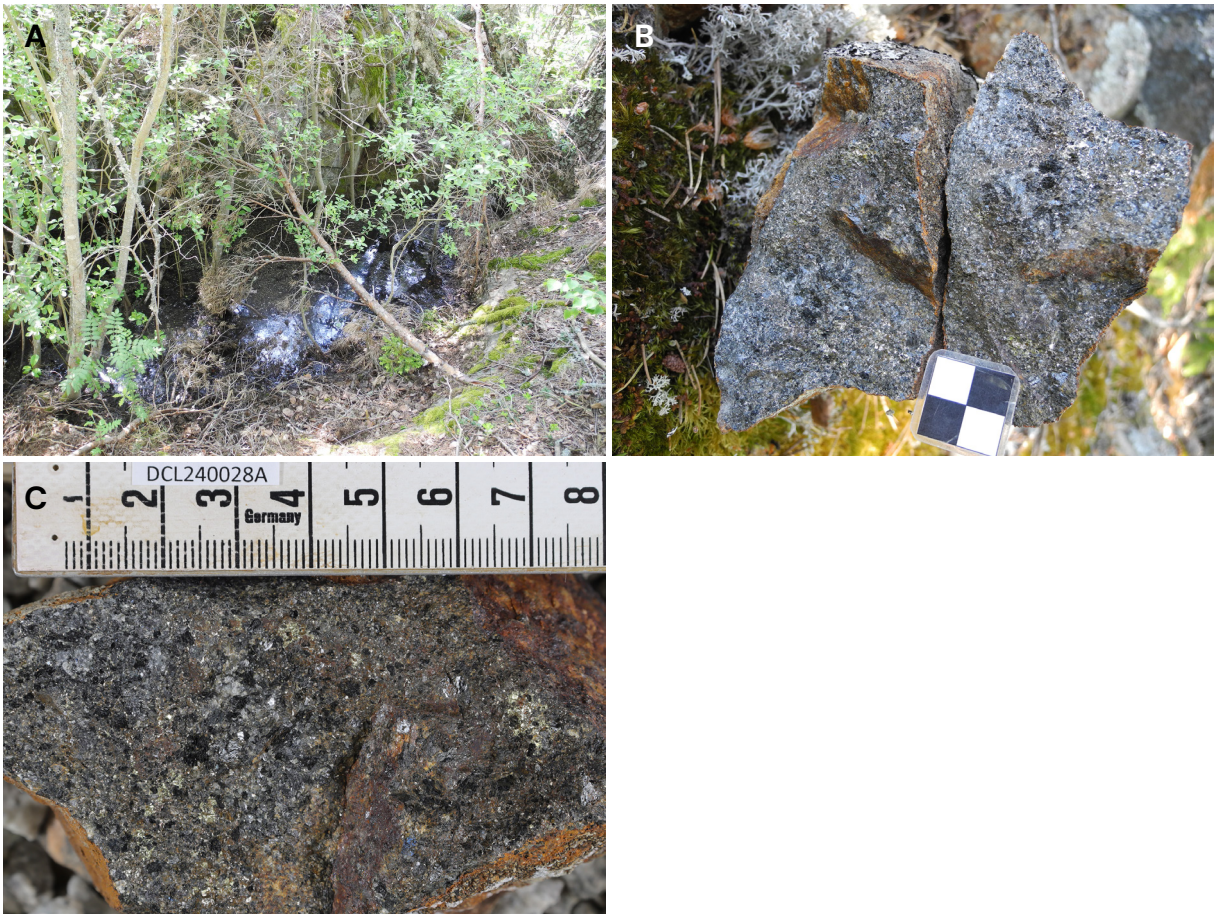

Figure 46. A. Rumhult pit, 6 × 3 metres large and 3 metres to the water surface. **B.** Sampled sulphide mineralised basaltoid (6455050/580513). Photos: Dick Claeson. **C.** Sample used for petrophysical lab measurements. Photo: Peter Hedin.

Fåfalla prospect

The prospect pit at Fåfalla is 3 × 3 metres and 2 metres deep at its deepest end, and there is no knowledge if it has been filled with waste rock. Drilling marks were observed in the walls, short and closely spaced. A fine-grained, dark coloured basaltoid has dissemination of mainly chalcopyrite and pyrite (Fig. 47A). There are also sulphide mineralised portions that occur with

quartz-rich bands or fracture fillings, which have mostly dissemination of Fe-sulphides pyrrhotite and pyrite, and chalcopyrite (Fig. 47B). The quartz-rich bands were sampled for lithogeochemical analysis and had SiO_2 72.4%, Fe_2O_3 9.32%, S 4.52%, Cu 0.129%, and Au only 0.003 ppm. In the REE-spidergram it has a similar pattern as the other Cu-mineralisations, apart from a more pronounced positive Eu anomaly and the lowest REE concentrations of all, which is most obvious for the HREE (Fig. 48A). In the NMORB-spidergram the quartz-rich sample has a similar pattern as most sulphide mineralised samples but mostly at lower concentrations, e.g., P and Zr, and the highest concentration for Cs (Fig. 48B). This is probably due to a hydrothermal origin of the bands, and the fact that quartz, which is abundant in the sampled rock, has low concentrations of most elements.

The measured petrophysical properties of the sulphide mineralised basaltoid sample are a density of 3 119 kg/m^3, a magnetic susceptibility of 6 640 × 10^{-5} SI, a natural remanent magnetisation of 4 570 mA/m, a Q-value of 1.69, and a resistivity of 577 Ωm (Fig. 47C). The measured petrophysical properties of the sample with quartz-rich bands are a density of 2 743 kg/m^3, a magnetic susceptibility of 27 × 10^{-5} SI, a natural remanent magnetisation of 121 mA/m, a Q-value of 11.1, and a resistivity of 23 700 Ωm (Fig. 47D).

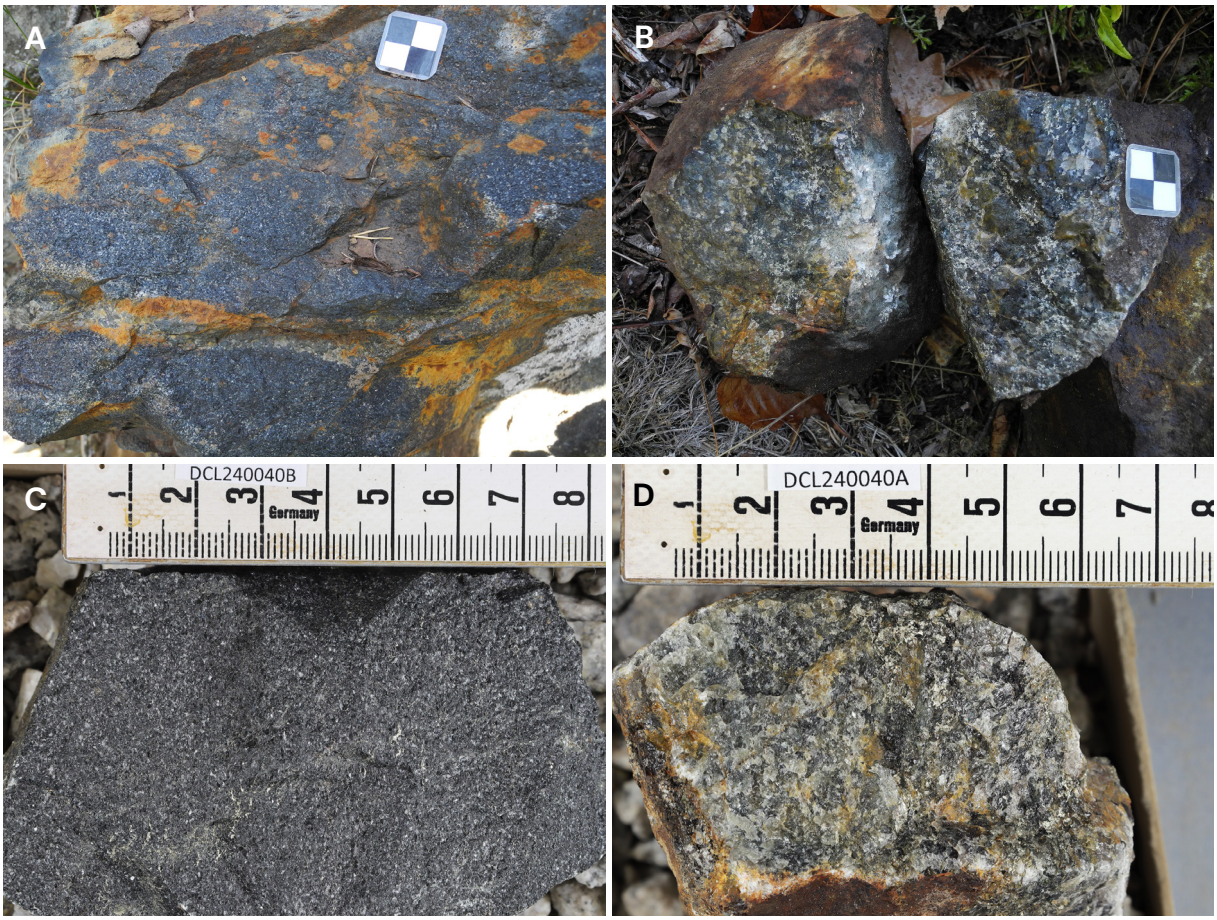

Figure 47. Ore prospect at Fåfalla. **A.** Basaltoid with minor dissemination of pyrite and chalcopyrite. **B.** Sampled rock rich in pyrrhotite, pyrite, and quartz, some chalcopyrite is present (6452376/583524). Photos: Dick Claeson. **C.** and **D.** Samples used for petrophysical lab measurements, basaltoid with sulphides and sulphide–quartz-rich rock, respectively. Photos: Peter Hedin.

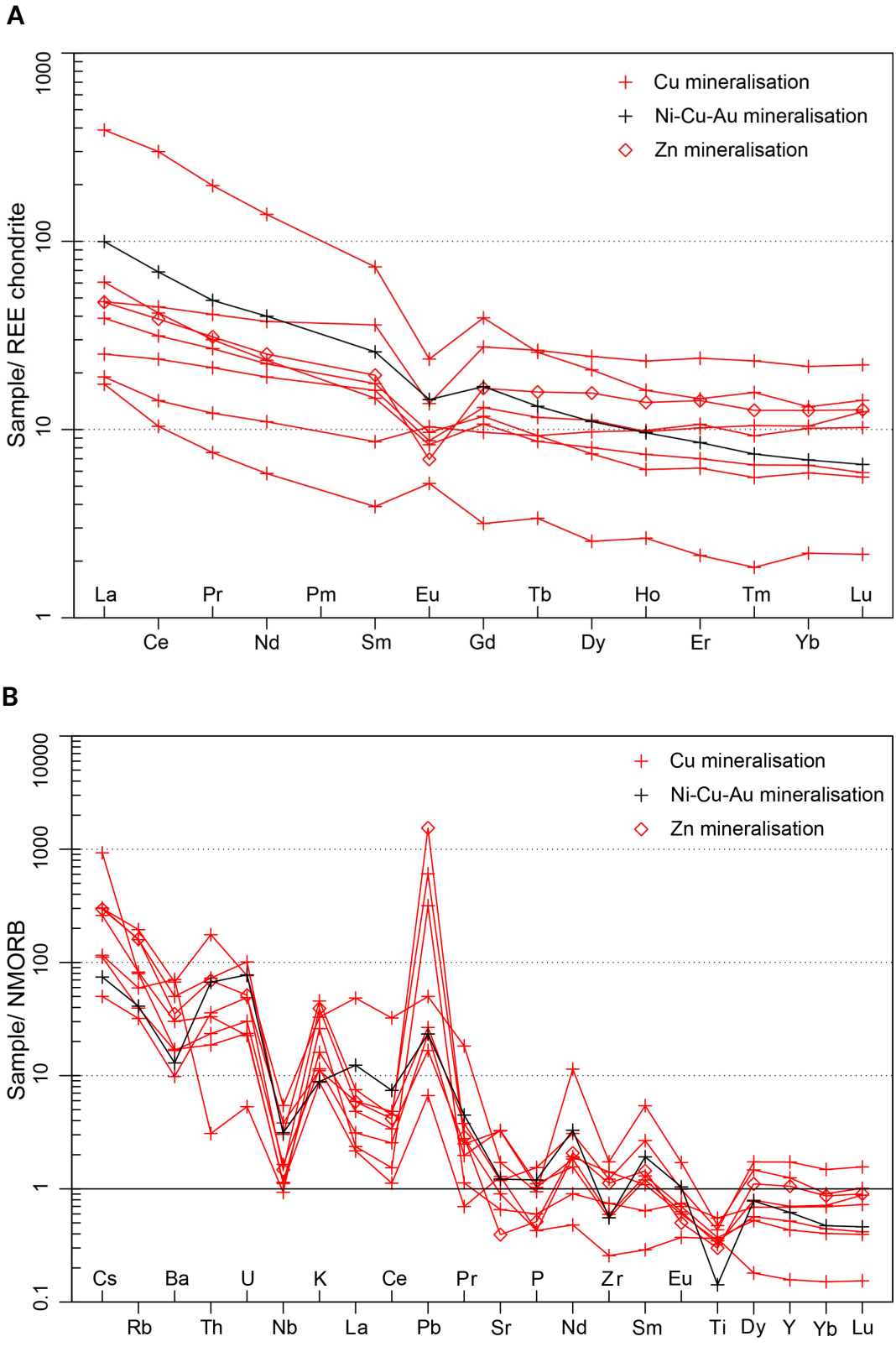

Figure 48. A. REE-spidergram of sulphide mineralisations from the Skrickerum project area. Normalisation values for chondrite Boynton (1984). **B.** N-MORB normalised spidergram of the same rocks, values Sun & McDonough (1989).

Structural measurements

Apart from the younger rocks that formed after major deformation and metamorphism occurred, almost every older rock has some form of deformation recorded in the project area Skrickerum. Foliation is by far the most common structural element, fold axes relatively common whereas lineation is the most seldom appearing. In the most deformed rocks, all directions of foliation can be obtained on the outcrops and folding and possible refolding have made measurements there challenging to interpret, even the fold axes may point in any direction. The new structural measurements were plotted using the program Stereonet (Allmendinger *et al.* 2012, Cardozo & Allmendinger 2013). Even though there are not that many measurements, they give an indication of prevailing trend and plunge of the different structural elements (Fig. 49).

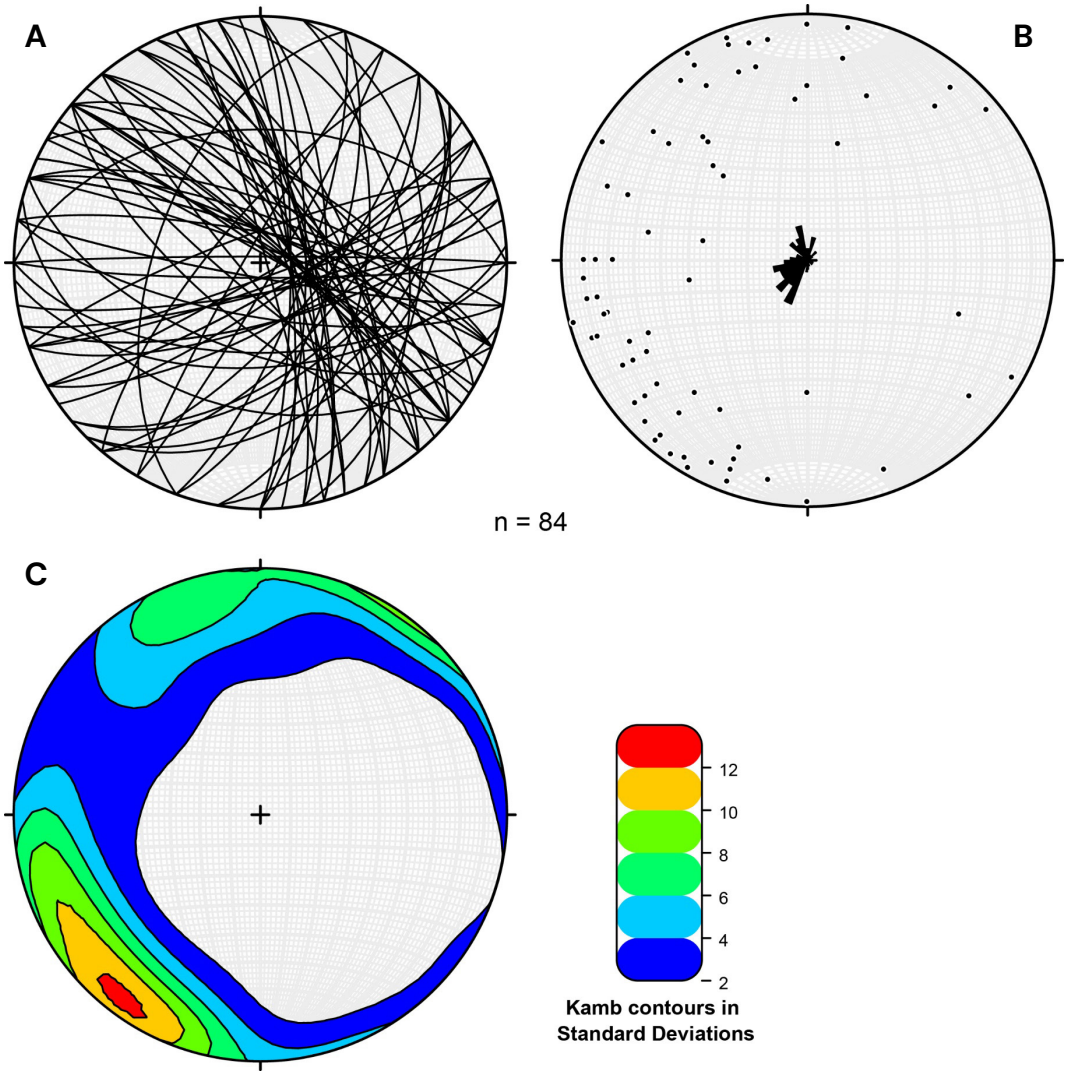

Figure 49. A. Planes of foliation. **B.** Poles of foliation planes and a rose diagram of these. **C.** Kamb contouring of the poles to foliation planes. The number of measurements of foliations are 84.

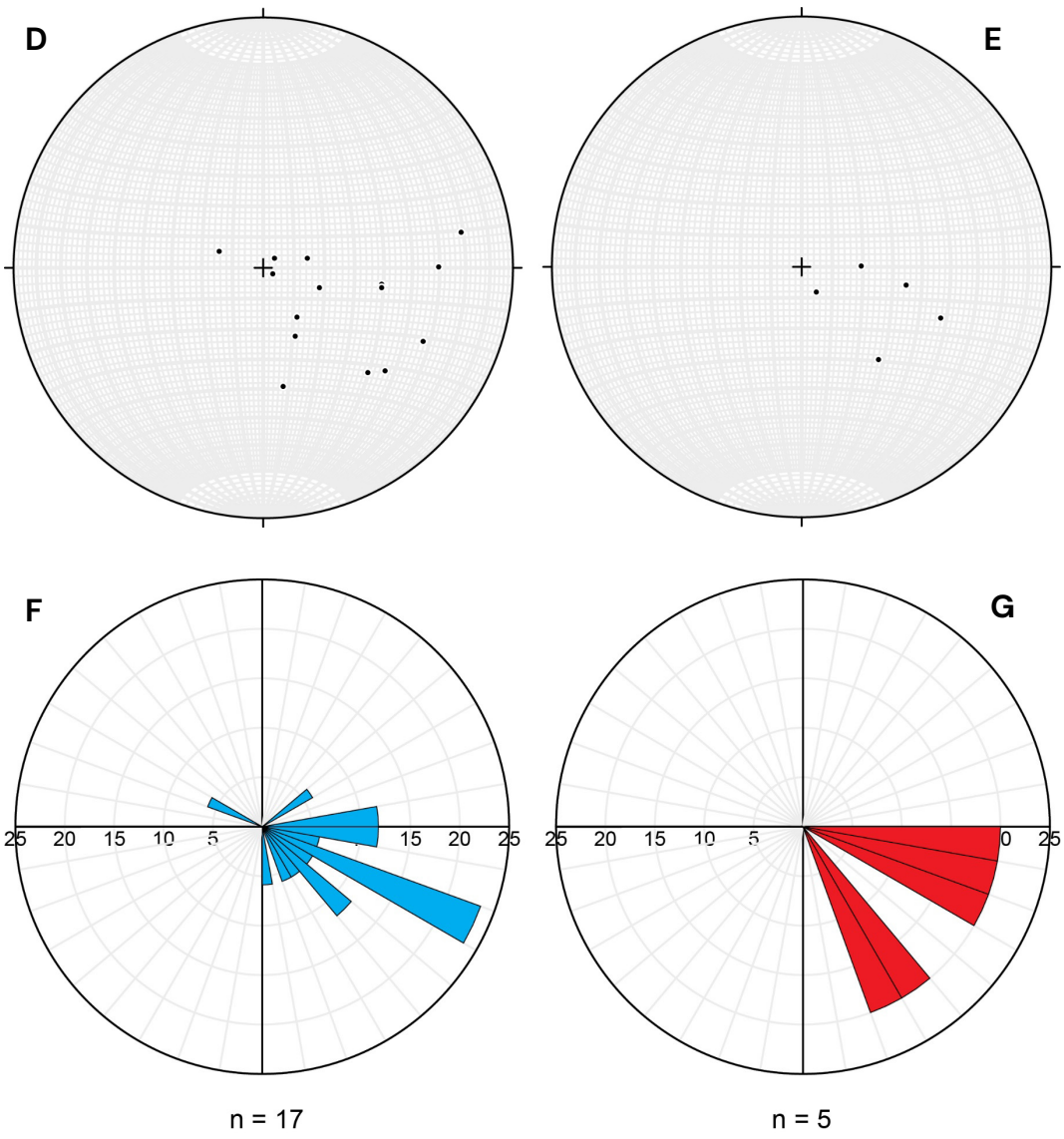

Figure 49 continued. D. Fold axis measurements in a stereonet. **E.** Lineation measurements in a stereonet. **F.** Fold axis measurements in a rose diagram. **G.** Lineation measurements in a rose diagram.

References

Allmendinger, R.W., Cardozo, N. & Fisher, D., 2012: Structural geology algorithms: Vectors and tensors in structural geology. *Cambridge University Press*, 1–289.

ALS 2023: ALS Geochemistry Fee Schedule EUR 2023.

Bindi, L. & Pratesi, G., 2005: Selenojalpaite, Ag_3CuSe_2, a new mineral species from the Skrikerum Cu–Ag–Tl selenide deposit, Småland, southeastern Sweden. *The Canadian Mineralogist 43*, 1373–1377.

Boynton, W.V., 1984: Cosmochemistry of the Rare Earth Elements: Meteorite studies. *In* P. Henderson (ed.): *Rare earth element geochemistry*. Elsevier Science B.V., 63–114.

Bruun, Å., Nilsson, C.-A., Sundberg, A., Wik, N.-G. & Wikström, A., 1995: Malmer, industriella mineral och bergarter i Östergötlands län. *Rapporter och meddelanden 80*, 1–353, Sveriges geologiska undersökning.

Cardozo, N. & Allmendinger, R.W., 2013: Spherical projections with OSXStereonet. *Computers & Geosciences 51*, 193–205.

Dentith M., Mudge S. T., 2014: Geophysics for the Mineral Exploration Geoscientist. *Cambridge University Press*, 1–438.

Henkel H. 1994: Standard diagrams of magnetic properties and density – a tool for understanding magnetic petrology. *Journal of Applied Geophysics 32*, 43–53.

Janoušek, V., Farrow, C. M. & Erban, V., 2006: Interpretation of whole-rock geochemical data in igneous geochemistry: introducing Geochemical Data Toolkit (GCDkit). *Journal of Petrology 47(6)*, 1255–1259.

Jelinek C. & Eliassson T., 2015: Strålning från bergmaterial. *SGU-rapport 2015:34*. Sveriges geologiska undersökning, 1–26.

Johannes, W. & Holtz, F., 1996: *Petrogenesis and experimental petrology of granitic rocks*. Springer-Verlag Berlin Heidelberg, 1–335.

Jonsson, E., Högdahl, K., Majka, J. & Murashko, M., 2014: Te-Cu-rich sudburyite – the first platinum-group-element mineral from the selenide mineralisation at Skrikerum, Sweden. *Neues Jahrbuch für Mineralogie – Abhandlungen 191/2*, 137–144.

Lundqvist, J., Lundqvist, T., Lindström, M., Calner, M. & Sivhed, U., 2011: *Sveriges Geologi: Från urtid till nutid* (in Swedish) (3rd ed.). Studentlitteratur, 1–628.

Smith, W., 1873. Effect of light on selenium during the passage of an electric current. *Nature 7*, 303.

Stephens, M.B. & Bergman, S., 2020: Regional context and lithotectonic framework of the 2.0–1.8 Ga Svecokarelian orogen, eastern Sweden. *In* M.B. Stephens, J. Bergman Weihed (eds.): *Sweden: Lithotectonic Framework, Tectonic Evolution and Mineral Resources*. Geological Society, London, Memoirs 50, 9–26.

Sun, S.-S. & McDonough, W.F., 1989: Chemical and isotopic systematics of oceanic basalts: implications for mantle composition and processes. *In* A.D Saunders & M. J. Norry (eds.): *Magmatism in the Ocean Basins*. Geological Society Special Publication No. 42, 313–345.

Tegengren, F.R., m.fl., 1924: Sveriges ädlare malmer och bergverk. *Sveriges geologiska undersökning Ca 17*, 1–406.

Wik N.-G., Bergström U., Bruun Å., Claeson D., Jelinek C., Juhojuntti N., Kero L., Lundqvist L., Stephens M. B., Sukotjo S. & Wikman H., 2005: Beskrivning till regional berggrundskarta över Kalmar län, *Sveriges geologiska undersökning Ba 66*, 1–54.